

**The active contribution of oligodendrocyte progenitor cells to
neuroinflammation is mediated by LRP1**

Anthony Fernández-Castañeda
Pico Rivera, California

B.S. Molecular Biology, University of California San Diego, 2010

A Dissertation presented to the Graduate Faculty of the University of Virginia in
Candidacy for the Degree of Doctor of Philosophy

Neuroscience Graduate Program

University of Virginia
December, 2019

Acknowledgements

My Mom, Priscilla, and Ezra. We may have started in the garage but we all knew it would not end there.

Come with me, Hail Marin... You hit me with that southpaw and introduced me to more than pasta, salami, and cheese.

DoRo, those context clues never fail you and I am here because of it.

Plays the 5 and shoots the 3... Shout-out

The Gaultier Lab science family, I may have a condition but I doubt I will forget our time together.

Dearest familia and Latina Manor, your support was invaluable. Y yo le llego.

ThunderCats, those were character building years.

The faculty and staff that made the training environment a success, your work is deeply appreciated and shall not be overlooked.

My mentor and friend, thank you for taking a chance on me. One more rep.

Table of Contents

Chapter 1: Remyelination Failure in Multiple Sclerosis.....1

- A. Introduction to multiple sclerosis
- B. Risk factors
- C. Pathological hallmarks
- D. Animal models of demyelination and remyelination
- E. Remyelination failure

Chapter 2: Oligodendrocyte progenitor cells – myelination and beyond.....16

- A. Abstract
- B. Introduction
- C. OPCs in the adult CNS
- D. CNS myelination in adulthood
- E. Neuron-OPC bidirectional crosstalk
- F. OPC heterogeneity
- G. OPCs respond to CNS injury
- H. OPCs contribute to glial scar formation
- I. OPCs as active participants in neuroinflammation
- J. Conclusion

Chapter 3: The multifunctional receptor low-density lipoprotein receptor-related protein 1 (LRP1).....35

- A. LRP1 overview
- B. Neuronal LRP1 in the central nervous system
- C. LRP1 functions as a phagocytic receptor for myelin

D. LRP1, microglia, and neuroinflammation

E. Rationale for studying the role of LRP1 in OPCs during CNS demyelination

Chapter 4: The active contribution of OPCs to neuroinflammation is mediated by

LRP1.....44

A. Abstract

B. Introduction

C. Results

D. Discussion

E. Methods

F. Supplementary material

Chapter 5: Unanswered questions and future directions.....90

A. Overview

B. Future directions

Appendix A.....96

References.....107

Chapter 1: Remyelination Failure in Multiple Sclerosis

A. Introduction to multiple sclerosis

Multiple sclerosis (MS) is an inflammatory disease of the central nervous system (CNS) that is largely characterized by myeloid and lymphocyte infiltrating cells, destruction of oligodendrocytes and their myelin sheath, and neurodegeneration (Compston and Coles, 2008). Although the cause of MS is unknown, MS has traditionally been categorized as an autoimmune disorder (Weiner, 2004), where the adaptive immune system incorrectly recognizes CNS myelin and orchestrates its destruction. The categorization of MS as an autoimmune disease has consistently been disputed (Gulcher et al., 1994, Chaudhuri and Behan, 2004), in part because of the lack of a known myelin or neuronal autoantigen specific to MS patients. However, it is clear that effector T cells participate in MS disease progression, which can be further exacerbated by CNS-resident glial cells and peripheral myeloid cells (Baecher-Allan et al., 2018, Ajami et al., 2011). It is estimated that 2.5 million people worldwide suffer from MS, which is predominantly diagnosed in young adults, and is twice as common in females than males (Milo and Kahana, 2010). Average life expectancy in MS patients is reduced by five to ten years (Bronnum-Hansen et al., 2004), but the heavy burden of this disease is attributed to the irreversible physical and cognitive disabilities in its advanced stages (Kurtzke, 1983).

Further complicating our understanding of MS is the fact that this disease is heterogeneous. The majority of patients (~85%) present with relapsing-remitting MS (RRMS), characterized by bouts of inflammatory demyelination that result in worsening neurological function, and followed by recovery (Mallucci et al., 2015). Active episodes

of CNS inflammation and demyelination, commonly referred to as flares, are unpredictable but can occur up to 1.5 times per year, and are accompanied with neurological dysfunction specific to lesion location (Compston and Coles, 2008). Symptoms can include, but are not limited to, loss of vision, motor deficits, and cognitive impairment (Compston and Coles, 2002). Within 15 years of a RRMS diagnosis, ~75% of RRMS patients will develop secondary progressive MS (SPMS), characterized by a steady worsening of neurological deficits (Mallucci et al., 2015). In 15% of patients, MS is progressive from the start, a disease course known as primary progressive MS (PPMS) (Mallucci et al., 2015). It is unclear what factors govern susceptibility to different MS disease types, or if progressive forms of MS are an entirely different disease.

Over the past few decades, approved MS therapies have had limited success with controlling relapses in RRMS patients, and these therapeutics are ineffective in progressive forms of the disease (Baecher-Allan et al., 2018). Unfortunately, disease-modifying treatments are exclusively immunomodulatory or immunosuppressive, and no intervention promotes CNS repair. Remyelination, the endogenous process of myelin regeneration by CNS-resident oligodendrocyte progenitor cells (OPCs), has long been considered a worthy therapeutic target (Franklin, 2002, Chang et al., 2012, Stangel et al., 2017). Indeed, demyelinated axons have impaired saltatory conduction, lack trophic support, and are more susceptible to death (Smith et al., 1979, Griffiths et al., 1998, Lee et al., 2012). Driving OPC differentiation into newly-myelinating oligodendrocytes could theoretically prevent neuronal death, halt further clinical disability, and induce functional recovery (Stangel et al., 2017). However, despite the elucidation of several signaling mechanisms that govern remyelination, early clinical trials have had lackluster results

(Cunniffe and Coles, 2019), highlighting the importance of a better understanding of the factors that control myelin repair in the CNS.

B. Risk factors

While the etiology of MS remains unknown, it is clear that a combination of genetic and environmental factors play a role in MS susceptibility (Baecher-Allan et al., 2018). The most dominant MS risk allele, *HLA-DRB1*15:01*, can be found in the major histocompatibility complex 2 locus, and has an estimated odds ratio of 3.08 (Sawcer et al., 2005, Hollenbach and Oksenberg, 2015). Previous genome-wide association studies have also found interleukin receptor 2A (*IL2RA*) and interleukin receptor 7 (*IL7R*) genes to be inheritable risk factors (International Multiple Sclerosis Genetics et al., 2007). The most recent genome-wide association studies have now discovered over 200 immune-related loci associated with MS susceptibility, which explains about 48% of total MS risk (International Multiple Sclerosis Genetics, 2019).

It has long been recognized that environmental factors also play a role in MS risk, and these stimuli are thought to act as triggers in genetically susceptible patients. Three well documented environmental risk factors for MS are Vitamin D deficiency, smoking, and Epstein-Barr virus infection (Ascherio et al., 2014, Wingerchuk, 2012, Levin et al., 2005, Belbasis et al., 2015). Vitamin D has been shown to suppress T cell proliferation and can skew T cells into anti-inflammatory states (Aranow, 2011). Smoking is thought to affect MS risk by increasing the number of a specific subset of inflammatory lymphocytes, T-helper 17 (Th17) cells, in the lung (Ramanujam et al., 2015). Finally, elevated levels of Epstein-Barr virus (EBV) antibodies have been strongly associated with MS susceptibility

(Belbasis et al., 2015). The mechanisms by which EBV infection increase MS risk are still unknown. A common hypothesis is that viral antigens resemble myelin proteins and the immune system cannot distinguish between self and non-self, resulting in an autoimmune response (Geginat et al., 2017). However, the existence of EBV protein or RNA in the CNS of MS patients continues to be debated (Sargsyan et al., 2010, Lossius et al., 2014).

C. Pathological hallmarks

Magnetic resonance imaging (MRI) has been instrumental in diagnosing and tracking MS disease progression due to its ability to visualize white matter lesions in live patients (Wattjes et al., 2015). However, our understanding of MS has mainly come from careful examination of MS lesions, from either biopsies or autopsies, using histochemistry and immunohistochemistry to visualize pathology. These thorough analyses have revealed the presence of peripheral immune cells in MS lesions, like CD8 T cells and B cells, cells that are not normally found in the CNS (Machado-Santos et al., 2018). In addition, histological studies have revealed the heterogeneity of MS lesions and have shined light onto potential pathogenic mechanisms driving disease, such as mitochondrial dysfunction in oligodendrocytes. Interestingly, neuropathological heterogeneity exists between patients, but not within lesions of the same individual. The seminal work by Lucchinetti et al. characterized active MS lesions, from acute and RRMS, into four distinct patterns of white matter demyelination, which will be discussed herein (Lucchinetti et al., 2000).

Pattern I lesions are present in 15% of MS patients who have been biopsied and are characterized by distinct perivascular lesions containing T lymphocytes and myelin-

laden macrophages, but lack both immunoglobulin reactivity and complement activation (Popescu et al., 2013). For this reason, it is hypothesized that oligodendrocyte death in pattern I lesions is a result of the inflammatory factors produced by reactive macrophages. The demyelinated lesion is devoid of canonical myelin proteins like CNP, MAG, PLP, and MBP. This non-selective loss of myelin protein suggests active demyelination since CNP and MAG are preferentially lost in early active lesions, while PLP and MBP are lost in late active lesions (Popescu et al., 2013).

Pattern II active lesions are present in 58% of MS biopsies, and are defined by the presence of immunoglobulin and complement deposition (Popescu et al., 2013). T lymphocytes are also present, and macrophages can be found phagocytosing complement-opsonized myelin debris. It is thought that this type of demyelination is a result of antibody- and complement-mediated oligodendrocyte death. Similar to pattern I lesions, pattern II plaques are clearly defined and usually found centered around veins or venules (Lucchinetti et al., 2000).

Pattern III lesions are present in 26% of MS biopsies, and are characterized by their poorly defined boundaries, the presence of T cells and macrophages, visualization of apoptotic oligodendrocytes, and the lack of both immunoglobulin and complement activation (Popescu et al., 2013). There is a preferential loss of MAG and CNP in periaxonal myelin (the myelin sheath wrapped closest to the neuron), but not PLP, MBP, or MOG. The morphological changes in oligodendrocytes are characteristic of oligodendrogliopathy, similar to that seen in viral, toxin, and ischemic/hypoxic settings. This suggests oligodendrocyte death might be driven by reactive oxygen species and mitochondrial dysfunction (Aboul-Enein and Lassmann, 2005).

Pattern IV lesions are present in 1% of MS biopsies, and are defined by the non-apoptotic death of oligodendrocytes in the presence of T lymphocytes and macrophages. These lesions do not display preferential myelin protein loss, and do not contain immunoglobulin or complement deposition (Lucchinetti et al., 2000). It is hypothesized that these lesions might be the result of metabolic defects in oligodendrocytes, rendering them susceptible to the inflammatory milieu (Popescu et al., 2013).

In addition to these four patterns of active demyelination, chronic active and chronic inactive lesions have also been described (Popescu et al., 2013). Chronic plaques are mostly seen in patients with progressive MS and consist of sharply defined demyelinated area with the presence of few myelin-laden macrophages at the lesion rim. In contrast, chronic inactive lesions are extensively demyelinated, contain few T cells and macrophages, but have robust astrogliosis and axonal damage. Although active lesions do contain axonal injury markers, like axonal swelling and amyloid- β precursor deposition, extensive axonal loss is observed, mainly in chronic MS lesions (Popescu et al., 2013).

This careful characterization of MS pathology has highlighted the fact that MS is a heterogeneous disease and might have multiple pathogenic mechanisms. Still, the loss of oligodendrocytes and the extensive demyelination in these lesions remains a common factor. Remyelination, the process of generating new myelin sheath, can occur in pattern I and II lesions, but is often incomplete and insufficient to reverse neurological symptoms. There is an unmet need for remyelination therapeutics to prevent future axonal damage and improve the quality of life in MS patients.

D. Animal models of demyelination and remyelination

Our understanding of remyelination failure in MS comes from two main categories of animal models that do not faithfully mimic human disease, but have proven indispensable nonetheless (El Waly et al., 2014). The first category includes models that recapitulate MS disease pathogenesis, including a robust peripheral immune response, CNS specific demyelination, and motor disability. The second group of models isolates specific features of the disease, such as focal demyelination without neurological symptoms. Many genetic models of oligodendrocyte death have also been recently generated, but their utility in understanding MS remains unclear (Ransohoff, 2012).

The most common animal model used to study MS pathogenesis is experimental autoimmune encephalomyelitis (EAE). EAE is characterized by infiltration of myelin-specific T cells into the CNS, which further recruit peripheral immune cells, including macrophages, leading to the destruction of CNS white matter (Stromnes and Goverman, 2006). This is a model of CNS autoimmunity, and can be triggered in C57BL/6 mice either by immunization with myelin-derived peptides or transfer of activated myelin-specific T cells (Ransohoff, 2012). Inflammation and demyelination in classic EAE are restricted to the spinal cord, although there are modifications that can be made to induce pathology in the brain (Stromnes and Goverman, 2006). Mice exhibit ascending paralysis as a result of the progressive immune attack on the spinal cord. Clinical symptoms begin with a loss of tail tonicity, and can progress to complete hind limb paralysis (Stromnes and Goverman, 2006). One major caveat of the EAE model is that it cannot be used to study CNS repair, perhaps because of the irreversible damage caused by neuroinflammation (Tripathi et al., 2010). EAE is also not well suited to study remyelination because timing

of lesion formation and location are unpredictable (Ransohoff, 2012). Depending on the mouse strain and protocol used, EAE can also exhibit a relapsing-remitting or progressive disease course (El Waly et al., 2014). Despite its weaknesses, the EAE model has been valuable in our understanding of how immune and inflammatory features of MS contribute to disease progression.

Knowledge of CNS remyelination comes from studies using focal demyelination models. Rodent models of focal oligodendrocyte and myelin loss employ the use of gliotoxic compounds, either by focal or systemic administration (El Waly et al., 2014). In contrast to EAE, toxin-induced models of demyelination show robust spontaneous remyelination. One commonly used toxin is lysolecithin, a membrane-dissolving compound with preference for lipid-rich myelin (Woodruff and Franklin, 1999). Lysolecithin solution can be injected into white matter tracts of the CNS, resulting in a localized lesion with peak demyelination 7 days post injection. Lysolecithin destroys most myelinating cells but leaves oligodendrocyte progenitor cells unharmed, which can differentiate into myelin-producing cells and full remyelination is achieved by 14-21 days post injection. Lysolecithin has long been criticized for being an artificial model of demyelination that lacks a robust immune response. However, recent studies have shined light onto how the immune system participates in lysolecithin-induced demyelination and promotes repair (Psachoulia et al., 2016, Dombrowski et al., 2017). Additionally, focal lysolecithin administration in the brain or spinal cord does not result in clinical symptoms. In spite of its limitations, the lysolecithin model offers spatial and temporal control of demyelination not available in EAE (Ransohoff, 2012).

Another toxin used to induce demyelination is the copper chelator cuprizone. It is believed that cuprizone disrupts mitochondrial function in oligodendrocytes, which require high metabolic activity in order to maintain their large amounts of cell membrane (Skripuletz et al., 2011). Unlike lysolecithin, cuprizone is not a focal demyelinating agent. Administration of 0.2% cuprizone for 4-6 weeks in mouse food causes extensive demyelination across gray and white matter areas of the brain (Steelman et al., 2012, Skripuletz et al., 2011). Two weeks after withdrawal, complete remyelination of affected areas is observed. The most commonly examined CNS structure in the cuprizone model is the corpus callosum, where de- and remyelination is extremely robust (Skripuletz et al., 2011). Although widespread demyelination can occur in the brain, there are no prominent neurological deficits. Much like the lysolecithin model, it was once thought that cuprizone-induced demyelination was immune-independent. Several studies, including my own, have now better characterized the involvement of both the adaptive and innate immune responses in the cuprizone model (Liu et al., 2010, Fernandez-Castaneda et al., 2019). Still, no one model of demyelination is perfect, but together they can provide a better understanding of the remyelination process in the CNS.

E. Remyelination failure

The adult CNS has the remarkable ability to perform adaptive myelination, like generating newly-myelinating oligodendrocytes when learning a new motor skill (McKenzie et al., 2014). White matter changes have also been observed in humans who practice piano rigorously or do extensive juggling training (Bengtsson et al., 2005, Scholz et al., 2009). In the last few decades, oligodendrocyte progenitor cells (OPCs) have been

shown to carry out this *de novo* myelination process (McKenzie et al., 2014, Gibson et al., 2014). Adult OPCs are evenly distributed across the CNS and maintain the ability to differentiate into mature myelin-producing oligodendrocytes (Dawson et al., 2003, Hughes et al., Hughes et al.). However, OPC differentiation fails in MS, and many efforts have been made to understand the nature of this phenomenon.

Several hypotheses have been proposed to explain remyelination failure in MS. To better understand factors that inhibit remyelination, one must take into account the events that occur during lesion formation. In an MS plaque where immune cells are actively contributing to myelin destruction, any newly made myelin will be destroyed. Myelin debris, a feature of the demyelinating lesion, has been shown to inhibit remyelination by blocking OPC differentiation (Lau et al., 2012). Additionally, formation of the glial scar and changes in the extracellular matrix (ECM) are not permissive to remyelination, as they can also inhibit OPC differentiation (Siebert and Osterhout, 2011). Understanding the factors that inhibit remyelination can ultimately aid in generating effective therapies to promote repair in MS patients.

Role of cytokines

Oligodendrocyte death and demyelination in MS can be mediated by T cells that produce a milieu of inflammatory cytokines, including interferon- γ (IFN γ) and tumor necrosis factor-alpha (TNF α) (Patel and Balabanov, 2012). The inflammatory response is further exacerbated when these cytokines activate infiltrating macrophages and resident microglia, which also generate TNF α (Hartung et al., 1992, Mallucci et al., 2015). Both IFN γ and TNF α have been shown to inhibit OPC differentiation and induce OPC death *in vitro* (Andrews et al., 1998, Feldhaus et al., 2004, Watzlawik et al., 2010). It is

likely that these cytokines inhibit remyelination by acting on OPCs present in demyelinating lesions. Lin *et al.* analyzed the role of IFN γ *in vivo* using mice with inducible overexpression of IFN γ in the CNS and subjected them to EAE- and cuprizone-induced demyelination (Lin *et al.*, 2006). In both models, IFN γ expression inhibited CNS remyelination by limiting the number of remyelinating oligodendrocytes in demyelinated areas (Lin *et al.*, 2006). In the few oligodendrocytes that were generated, markers of endoplasmic reticulum (ER) stress were present, potentially explaining their failure to remyelinate (Lin *et al.*, 2006). This suggests IFN γ induces a detrimental ER stress response in oligodendrocytes, which, if not controlled, ultimately inhibits oligodendrocyte maturation and remyelination.

Priming the CNS with moderate doses of IFN γ before EAE onset also induces oligodendrocyte ER stress, but surprisingly it confers a protective effect (Lin *et al.*, 2007). Mice with IFN γ pretreatment showed reduced EAE disease severity, accompanied by less oligodendrocyte loss and axonal damage (Lin *et al.*, 2007). This protective role is consistent with studies showing ectopic expression of low levels of IFN γ in oligodendrocytes can prevent cuprizone-induced demyelination (Gao *et al.*, 2000). IFN γ could mediate its protective effect in part by acting on microglia. It has been shown that microglia treated with low levels of IFN γ can promote oligodendrogenesis *in vitro* (Butovsky *et al.*, 2006). Alternatively, the same study showed that high levels of IFN γ inhibit OPC differentiation by promoting TNF α secretion in microglia. Overall, it is thought that high levels of IFN γ can play a detrimental role on oligodendrocyte and OPC survival.

The role of TNF α in remyelination is equally complex. TNF α is highly expressed in demyelinating MS lesions and has been shown to potentiate IFN γ -induced cell death *in*

vitro (Andrews et al., 1998, Watzlawik et al., 2010). Arnett *et al.* showed a modest delay in cuprizone-induced oligodendrocyte death in TNF α knockout mice, implicating it as a potential harmful cytokine (Arnett et al., 2001). Unexpectedly, this study also showed that TNF α knockout mice suffered from impaired remyelination (Arnett et al., 2001). Mice lacking TNF α showed decreased OPC proliferation, which resulted in less oligodendrocyte generation and impaired remyelination (Arnett et al., 2001). Mechanistically, TNF α promoted remyelination by signaling through TNF receptor 2 (TNFR2), as no deficits were observed in TNFR1 knockout mice (Arnett et al., 2001). The importance of TNF α in MS patients has also been documented. In clinical trials, patients who received TNF-blockers suffered from more relapses with heightened severity (Ransohoff et al., 2015). This observation has been attributed to TNF α expanding regulatory T cells, which are responsible for suppressing an immune response against self-antigens (Ransohoff et al., 2015).

Myelin debris

As inflammation continues to drive demyelination, an abundance of myelin debris is generated due to oligodendrocyte loss and degradation of the myelin sheath (Huang et al., 2011). Inefficient clearance of myelin debris by macrophages from demyelinating lesions results in poor remyelination in animal models (Kotter et al., 2001). It has been postulated that the ability of macrophages to clear debris also decreases with age. Ruckh *et al.* showed inefficient myelin debris clearance was rescued when old mice were parabiotically joined with young mice, allowing young macrophages to infiltrate the CNS and clear debris generated in lysolecithin lesions (Ruckh et al., 2012). In addition, direct injection of purified myelin into sites of focal demyelination also prevented remyelination

compared to controls (Kotter et al., 2006). Kotter *et al.* demonstrated failure to remyelinate was not due to poor OPC recruitment, but that myelin debris inhibited OPC differentiation as measured by a decrease in differentiation marker Nkx2.2 (Kotter et al., 2006). The mechanisms of myelin-mediated inhibition have been further examined *in vitro*. Baer *et al.* have shown purified OPCs plated on myelin substrate fail to upregulate MBP transcript, a measure of OPC differentiation (Baer et al., 2009). Myelin also decreases activation of Fyn-1 tyrosine kinase, which is known to regulate myelin sheath formation (Baer et al., 2009). Inhibitory myelin also induces activation of RhoA-GTP, and its inactivation is necessary for proper OPC differentiation (Baer et al., 2009). Myelin-mediated inhibition of OPC differentiation was also rescued using Rho-kinase II inhibitors, which regulate downstream RhoA signaling (Baer et al., 2009). Unlike the myelin proteins that inhibit axon regeneration, the myelin components that inhibit remyelination are not known (Syed et al., 2008).

The glial scar

The formation of the glial scar and changes in the ECM in demyelinated tissue also impedes successful remyelination. Chondroitin sulfate proteoglycans (CSPGs) accumulate around the borders of active MS lesions, and have been shown to inhibit human OPC adhesion and oligodendrocyte process extension *in vitro* (Lau et al., 2012). In mouse models of focal demyelination there is an increase of CSPGs during demyelination that are cleared during the remyelination phase (Lau et al., 2012). To assess the *in vivo* role of CSPGs, Lau *et al.* induced lyssolecithin demyelination in mice and treated them with xyloside, a known CSPG synthesis inhibitor (Lau et al., 2012). Treatment with xyloside did not affect lesion formation but resulted in an increase number

of OPCs recruited to the lesion site, as well as more mature oligodendrocytes during remyelination stages (Lau et al., 2012). Although the authors reported that no CSPG accumulation is found in chronic inactive MS lesions, they propose accumulation of these proteins during active lesions might inhibit OPC recruitment into the lesion core (Lau et al., 2012).

High molecular weight (HMW) hyaluronan is another ECM component that accumulates in demyelinated MS lesions and inhibits remyelination (Back et al., 2005). In contrast to CSPGs, HMW hyaluronan accumulates in the core of older chronic MS lesions (Back et al., 2005). Back *et al.* co-injected HMW hyaluronan and lysolecithin in the mouse corpus callosum, which resulted in remyelination failure compared to controls (Back et al., 2005). A higher number of OPCs were found at the onset of remyelination in HMW hyaluronan injected lesions, suggesting hyaluronan inhibited OPC maturation (Back et al., 2005). In studies where OPCs were co-cultured with astrocytes, the primary source of HMW hyaluronan in the CNS, the differentiation block was removed with hyaluronidase treatment (Back et al., 2005).

Neuronal integrity

In the event that oligodendrocytes are generated, it is still possible that axon integrity can limit remyelination. Demyelinated axons in MS lesions re-express polysialylated-neural cell adhesion molecule (PSA-NCAM) thought to inhibit remyelination (Charles et al., 2002). Evidence to support this comes from studies in which PSA-NCAM downregulation precedes developmental myelination (Charles et al., 2000). Recently, the discovery that neuronal activity promotes adaptive myelination in the adult CNS (Gibson et al., 2014) has led to the investigation of whether remyelination is under

similar control. Indeed, several studies have now demonstrated that neuronal activity promotes myelin repair in lysolecithin models of demyelination, in part by glutamate signaling through NMDA receptors on OPCs (Gautier et al., 2015, Ortiz et al., 2019). Given the lack of neuronal damage and the absence a robust inflammatory response in the lysolecithin model, it remains to be seen whether promoting neuronal activity in MS patients would be beneficial.

Conclusions

Targeting all these confounding factors represents one of the many challenges of developing suitable therapies to promote CNS remyelination. However, as our understanding of remyelination grows, developing such therapies is becoming feasible. In the last decade, several exciting studies have shined light onto novel non-myelinating roles of OPCs in the diseased CNS. These alternate OPC functions give rise to the possibility that remyelination may not be a primary function of OPCs in the demyelinating CNS. These studies might also imply the existence of several OPC populations with distinct functions. The next chapter will explore both myelinating and non-myelinating roles of OPCs in more detail.

Chapter 2: Oligodendrocyte progenitor cells – myelination and beyond

This chapter expands on the review article authored by Anthony Fernández-Castañeda and Alban Gaultier. 2016. Adult oligodendrocyte progenitor cells - multifaceted regulators of the CNS in health and disease. Brain, Behavior, and Immunity

A. Abstract

Oligodendrocyte progenitor cells (OPCs) are the underappreciated fourth glial cell type in the central nervous system (CNS). For a long time, our vision of OPC function was limited to the generation of mature oligodendrocytes. However, new studies have highlighted the fact that OPCs are multifaceted cells. During homeostatic and pathological conditions, OPCs are the most proliferative cell type in the CNS, a property not consistent with the need to generate new oligodendrocytes. Indeed, OPCs modulate neuronal activity and OPC depletion in the brain can trigger depressive-like behavior. More importantly, OPCs are actively recruited to injury sites, where they orchestrate glial scar formation and contribute to the immune response. The following is a comprehensive analysis of the literature on OPC function beyond myelination, in the context of the healthy and diseased adult CNS.

B. Introduction

The CNS is home to three major classes of glia: Astrocytes, microglia, and oligodendrocytes. In the last two decades, a fourth class of glia has emerged called the oligodendrocyte progenitor cell (OPC). OPCs have a stellate morphology and are present

in both the gray and white matter. They belong to the same population of progenitors that give rise to oligodendrocytes during CNS development. However, a large fraction of OPCs do not differentiate and remain in a cycling state throughout adulthood. OPCs represent the largest dividing population among neural cells and are uniformly distributed, making up, on average, 5% of total CNS cells (Dawson et al., 2003). The first described function of adult OPCs was differentiation into oligodendrocytes (Gensert and Goldman, 1997). When myelin repair is needed after CNS injury, local OPC proliferation occurs followed by OPC differentiation into oligodendrocytes (Lytle et al., 2009). OPC differentiation is accompanied by expression of mature oligodendrocyte markers such as proteolipid protein and myelin basic protein. Oligodendrocytes then generate a large amount of plasma membrane and begin to wrap around neuronal axons to form the myelin sheath in a process called myelination (Snaidero et al., 2014, Baron and Hoekstra, 2010). The mammalian brain undergoes myelination beyond postnatal stages and well into adulthood, highlighting the importance of adult OPCs in generating oligodendrocytes (Young et al., 2013). However, the differentiation rate of OPCs into myelinating oligodendrocytes decreases with age, with only a small percentage of adult OPCs giving rise to oligodendrocytes, suggesting that OPCs may have important functions beyond myelination (Zhu et al., 2011, Psachoulia et al., 2009, Rivers et al., 2008).

Adult OPCs are evenly dispersed throughout the CNS and *in vivo* imaging studies have shown that they are poised to detect perturbations within the CNS, by sending numerous filopodia to survey their surroundings (Hughes et al., 2013). For example, OPCs rapidly respond during CNS injury and disease by proliferating extensively and quickly surrounding the lesion site (Simon et al., 2011, Kang et al., 2013a). Although some

OPCs in the lesion differentiate into oligodendrocytes, there is a burgeoning interest in other possible roles of OPCs in response to CNS injury. Furthermore, OPCs can influence neuronal activity by altering the composition of the extracellular matrix (Sakry et al., 2014). Recently, loss of OPCs in the prefrontal cortex has been shown to alter glutamatergic signaling and promote depressive-like behavior in mice (Birey et al., 2015). These studies highlight a novel role of OPCs in modulating neuronal network activity adding to our understanding of glia-neuron interactions. The multifunctional role of OPCs during CNS homeostasis and pathologies will be presented in the following chapters, keeping in mind the gaps that still exist in our knowledge about these fascinating cells.

C. OPCs in the adult CNS

OPC development has been extensively studied and is beyond the scope of this review (Takebayashi and Ikenaka, 2015, Gallo and Deneen, 2014). In adults, OPCs are present across the CNS but their quantity varies between the white and gray matter (Dawson et al., 2003). In the white matter, such as the dorsal column of the spinal cord, OPCs can account for up to 8% of all cells, while in the dorsal horn gray matter OPCs account for only 3% of the cellular content (Dawson et al., 2003). Despite these regional differences in cell number, adult OPCs remain uniformly distributed across the brain and the spinal cord. Live-imaging studies performed in the cortex reveal that OPCs have elegantly ramified processes that constantly survey the environment and maintain an even distribution using self-repulsion mechanisms (Hughes et al., 2013). In the superficial layers of the cortex, each OPC covers its own territory, with clear borders and no apparent overlap (Hughes et al., 2013).

An important characteristic of OPCs is that they represent the major dividing cell population in the CNS. Using BrdU labeling methods, multiple studies have shown that OPCs account for more than 70% of CNS dividing cells, potentially outpacing the need for replacement of mature oligodendrocytes (Gensert and Goldman, 2001, Dawson et al., 2003). Yet, the principal role of adult OPCs was believed to be the generation of new myelinating oligodendrocytes. Given their uniform distribution and constant surveillance of the environment, OPCs are well positioned to sense changes in CNS homeostasis. Indeed, OPCs respond to primary demyelination and several types of CNS injury, with extensive proliferation, migration and morphological changes, but the utility of these actions in the context of CNS repair is not fully understood (Dimou and Gallo, 2015).

D. CNS myelination in adulthood

When they were first phenotypically characterized, adult OPCs were shown to express the same markers as embryonic OPCs. However, questions were raised about whether these cells shared the same lineage and whether they also generated oligodendrocytes. With advances in transgenic reporter mice, it became possible to conduct fate-mapping studies using specific Cre reporter lines, and the functions of adult OPCs began to emerge. Zhu *et al.* used NG2-Cre stop-flox-EGFP reporter mice to examine the fate of postnatal OPCs. In this system, NG2-expressing OPCs express Cre recombinase, allowing for the excision of the stop-flox sequence, and are labeled with EGFP. As expected, 78% of oligodendrocytes in the corpus callosum and striatum are EGFP⁺, indicating that OPCs gave rise to those oligodendrocytes (Zhu et al., 2008). This study, however, was conducted at the peak of myelination (P14) in the mouse CNS, and

OPCs examined here likely belong to the population of progenitors that exist at birth. Therefore, a P14 OPC is probably not the same as an OPC from, for example, a three- or an eight-month old mouse. Rivers *et al.* used an inducible PDGFR α -driven Cre YFP reporter line to label OPCs at P45 and examine their progeny 240 days later (Rivers *et al.*, 2008). The authors found that 29% of oligodendrocytes in the corpus callosum were generated by OPCs between P45 and P255 (Rivers *et al.*, 2008). Finally, three additional independent fate-mapping studies also concluded that adult OPCs produce oligodendrocytes throughout life (Dimou *et al.*, 2008, Kang *et al.*, 2010, Zhu *et al.*, 2011).

Oligodendrocyte generation in gray matter occurs less frequently than in white matter (Dimou *et al.*, 2008). Studies using *in vivo* two-photon imaging of superficial cortical layers in adult mice reported that less than 1% of OPCs mature into oligodendrocytes, while 96% remain stable over a 40-day timespan (Hughes *et al.*, 2013). Though one might expect higher OPC turnover in highly myelinated regions, the overall oligodendrocyte production does not differ between adult structures with varying degrees of myelination (Young *et al.*, 2013). Young *et al.* compared the robustly myelinated optic nerve to the partially myelinated corpus callosum in adult mice and found no long-term change in the number of new oligodendrocytes integrating in those tracts (Young *et al.*, 2013). Whether newly differentiated OPCs replace dying oligodendrocytes to stabilize a circuit or integrate to improve network function is still not known. Evidence to support the latter comes from observations that newly generated oligodendrocytes have significantly shorter internodes compared to neonatal oligodendrocytes suggesting integration into already myelinated axons (Young *et al.*, 2013). At odds with this explanation is the fact that myelinated axons are not encapsulated with myelin uniformly. For example,

myelinated axons from pyramidal neurons in the neocortex have lengthy unmyelinated tracts in which newly generated oligodendrocytes can integrate without restrictions on internode length (Tomassy et al., 2014).

The factors responsible for inducing continuous oligodendrocyte generation in adulthood are also incompletely understood. In mice, physical exercise can cause cortical OPCs to exit the cell cycle and generate oligodendrocytes (Simon et al., 2011). In humans, structural changes associated with white matter can be detected by magnetic resonance imaging after performing complex tasks such as practicing piano (Bengtsson et al., 2005). In rodents, it has been demonstrated that motor skill learning induces myelination (Sampaio-Baptista et al., 2013). More importantly, blocking the differentiation of OPCs into myelinating oligodendrocytes impairs motor skill learning (McKenzie et al., 2014). These findings are consistent with the role of myelin in improving the stability and function of neuronal circuits that are involved in learning. As discussed in more detail below, neuronal activity is implicated in OPC differentiation and proliferation, but myelination is not exclusively activity-dependent (Gibson et al., 2014, Hines et al., 2015). Elucidation of the specific molecular and behavioral triggers mechanisms that control myelination is a fascinating area of future research.

Another intriguing question is whether myelination dynamics seen in rodent models are comparable to higher order species. In the human corpus callosum, the oligodendrocyte number is established early in childhood and remains stable throughout life, such that an annual oligodendrocyte generation rate is estimated at 0.3% (Yeung et al., 2014). This number is strikingly low even when compared to a conservatively calculated rate in mice of 36% (Yeung et al., 2014). Of note, however, is that although

oligodendrocytes are established early in life, the myelin sheath is continuously renewed, suggesting that it is a highly dynamic structure (Yeung et al., 2014). An attractive hypothesis is that human oligodendrocytes have evolved to remodel the myelin sheath without requiring generation of a new oligodendrocyte from an OPC (Yeung et al., 2014). Thereby, oligodendrocyte turnover could result in segments of axons temporarily demyelinated, not conducive for efficient neuronal activity. The discrepancies in adult myelination and OPC function between species remain to be reconciled. It is an essential problem warranting further studies, as much of our understanding of human demyelinating diseases comes from non-human vertebrate models.

E. Neuron-OPC bidirectional crosstalk

Recently, neuronal activity has been studied as a regulator of myelination in the CNS (Gibson et al., 2014, Hines et al., 2015). OPCs were first reported to receive excitatory glutamatergic synaptic input via OPC-expressed AMPA receptors (Bergles et al., 2000). Subsequently, Lin and Bergles showed that OPCs also express GABA_A receptors and are responsive to GABAergic input (Lin and Bergles, 2004). These seminal works established the notion of a bona fide neuron-OPC synapse, but little is known about its significance. Gibson *et al.* used optogenetic technology to stimulate the mouse premotor cortex and showed that neuronal activity promotes OPC proliferation, differentiation and myelination (Gibson et al., 2014). OPC proliferation in the premotor cortex was detectable with three hours of optogenetic stimulation. Newly-formed oligodendrocytes were also detectably four weeks after optogenetic stimulation. The authors also noted a mild but significant increase in myelin thickness in the premotor

cortex, which correlated with increased limb swing speed (Gibson et al., 2014). Follow up studies demonstrated that activity-dependent synaptic vesicle release is necessary to induce myelination during zebrafish development, confirming the hypothesis that endogenous neuronal activity can affect myelination in the CNS (Mensch et al., 2015, Hines et al., 2015).

There are many questions left unanswered regarding the effects of neuronal activity on OPCs. It is important to note that suppressing neuronal activity by blocking voltage-gated sodium channels did not completely prevent myelination during zebrafish development (Hines et al., 2015). Specific deletion of NMDA receptor subunit NR1 in OPCs also does not affect myelination in the developing rodent CNS (De Biase et al., 2011). Yet, NR1 deletion in OPCs results in their upregulation of calcium-permeable AMPA receptors, another avenue by which glutamate signaling might modulate OPC function. Activation of AMPA receptors has been shown to inhibit OPC differentiation *in vitro* and stimulate OPC migration *in vivo*, but OPC-specific deletion of AMPA receptor signaling is needed to fully elucidate their contribution to OPC biology (Harlow et al., 2015, Gallo et al., 1996). In addition, the magnitude of OPC proliferation and the newly derived oligodendrocyte number after optogenetic stimulation did not translate into a robust increase in myelin thickness. In fact, a surprisingly low increase in g-ratio was observed between stimulated and unstimulated mice, suggesting a potential unconventional fate for these newly generated cells (Gibson et al., 2014).

OPCs are well positioned in the CNS to directly modulate neuronal function. At the synapse, OPCs have been shown to make contact with pre and post-synaptic terminals (Ong and Levine, 1999, Bergles et al., 2000). Furthermore, OPCs are known to contact

axons at the nodes of Ranvier, suggesting that OPCs could maintain node function (Butt et al., 1999). Because OPCs receive GABAergic and glutamatergic synaptic input, they could be capable of sensing and modulating network activity. Birey *et al.* have now demonstrated that OPC deletion in the prefrontal cortex (PFC) compromises glutamatergic signaling in pyramidal neurons (Birey et al., 2015). This perturbation in neurotransmission is accompanied by a decrease in astrocytic glutamate uptake following OPC ablation. Aberrations in glutamatergic signaling translated into a behavioral phenotype, as loss of OPCs triggered depressive-like behavior, which was rescued after endogenous OPC repopulation. Likewise, mice susceptible to a social defeat stress paradigm had reduced numbers of OPCs in the PFC, a feature shared by patients with major depressive disorder (Birey et al., 2015). This study is the first to demonstrate a robust physiological and behavioral change after OPC ablation, elucidating a novel role of OPCs in regulating CNS homeostasis. However, as this OPC ablation model does not delete OPCs uniformly across the CNS, novel roles for OPCs outside the PFC remain unknown.

Sakry *et al.* have also demonstrated that ectodomain cleavage of NG2, a proteoglycan highly expressed by OPCs, can also modulate neuronal networks (Sakry et al., 2014). Cleavage of NG2 in OPCs was activity dependent, and its blockade with protease inhibitors resulted in the impairment of NMDAR-dependent long-term potentiation (Sakry et al., 2014). This loss of long-term potentiation was recapitulated using the global NG2 knockout mouse, which also had diminished AMPAR- and NMDAR-mediated neuronal currents but did not present with learning and memory deficits (Sakry et al., 2014). Finally, bath application of the NG2 ectodomain onto brain slices results in

more c-Fos positive neurons compared to controls after glutamate stimulation (Sakry et al., 2014). The lack of an OPC-specific NG2 knockout model questions whether these findings are mediated exclusively by OPCs. A follow up study found that OPCs express neuromodulatory factor neuronal Pentraxin 2 (Nptx2), which affects AMPAR stability and trafficking at the cell surface (Sakry and Trotter, 2015). Taken together, the data suggests that OPC-derived factors can affect neuronal network activity, but the importance of this bidirectional OPC-neuron communication requires further investigation.

Oligodendrocytes also participate in a novel mode of bidirectional crosstalk using the transfer of exosomes from oligodendrocytes to neurons (Fruhbeis et al., 2013). Neuronal activity mediates exosome secretion from oligodendrocytes, which are then endocytosed by the neurons and promote survival under oxidative stress or nutrient deprivation conditions (Fruhbeis et al., 2013). Neurons can also endocytose exosomes from oligodendrocytes during the resting state, but the contents of the exosome cargo and how they impact neurons under these conditions is not known. Exosome secretion is further triggered by the Ca^{2+} influx that results from the glutamate binding NMDA and AMPA receptors on oligodendrocytes (Fruhbeis et al., 2013). Given that OPCs express NMDAR and AMPAR and are part of the oligodendroglial lineage, it is possible that similar modes of communication exist in OPCs (Sakry et al., 2015).

F. OPC heterogeneity

In development, OPCs have distinct spatial and temporal origins, raising the question of whether there is functional heterogeneity among the OPC populations (Takebayashi and Ikenaka, 2015). Ablation of any one OPC population during

development results in compensation by neighboring OPCs of different origin, suggesting that spatial origin does not commit OPCs to a single function (Kessar et al., 2006). However, it is clear that region-specific environments can alter OPC behavior. In fact, fate-mapping studies have shown OPCs in white matter differentiate into oligodendrocytes more frequently than gray matter OPCs (Dimou et al., 2008). In addition, OPCs in white matter have a shorter cell division cycle (10 days in the corpus callosum at P60) compared to gray matter OPCs (36 days in the motor cortex at P60) (Young et al., 2013). Hill *et al.* also demonstrated that white matter perinatal OPCs have a greater proliferative response to PDGF α than gray matter OPCs and that this difference was not due to differential expression of the PDGF α receptor (PDGFR α) (Hill et al., 2013). This suggests that regional differences in environment might affect OPC properties and account for dissimilarities between OPC populations.

Furthermore, transplantation of white matter OPCs into gray or white matter results in comparable amounts of oligodendrocyte differentiation (Vigano et al., 2013). On the other hand, gray matter OPCs exhibited greater oligodendrocyte differentiation when transplanted into white matter than when placed in gray matter. Therefore, it appears that the white matter milieu supports oligodendrocyte maturation, and that this effect is preserved in OPCs even after they have been taken out of the white matter environment (Vigano et al., 2013). These differences highlight the long-term effects that the extracellular environment could have on OPC function. In fact, a recent study has shown that microenvironment stiffness, which increases with aging, affects OPC proliferation and differentiation (Segel et al., 2019). Yet, these observations do not address whether distinct OPC populations exist within the same CNS region or similar environments.

Questions regarding true OPC functional heterogeneity remain highly debated in the field. Marques *et al.* have analyzed the transcriptomes of single cells expressing oligodendrocyte lineage markers from ten different regions in the juvenile and adult mouse CNS (Marques et al., 2016). Gene expression analysis revealed twelve distinct oligodendrocyte lineage populations, largely composed of myelin-forming oligodendrocytes. Surprisingly, their analysis only revealed one population of OPCs using canonical markers like *Pdgfra* and *Cspg4* (also known as NG2). Additionally, there was no regional or age-specific heterogeneity within the OPC population, which was observed in mature oligodendrocytes (Marques et al., 2016). In contrast, Spitzer *et al.* have reported that OPCs become regionally diverse and functionally heterogeneous with age by acquiring distinct ion channels repertoires (Spitzer et al., 2019). It is important to note the limitations of the Marques *et al.* study, for example, the low number of OPCs sequenced (310 cells from 10 CNS regions) and the lack of depth in single-cell RNA sequencing. Furthermore, it is possible that non-homeostatic conditions, like CNS injury, might reveal more noticeable transcriptional and functional heterogeneity within OPCs.

Interestingly, single-cell RNA sequencing of OPCs from EAE spinal cords revealed three distinct OPC populations that were transcriptionally different than the one OPC population found in control mice (Falcao et al., 2018). Most notably, OPCs from EAE spinal cords displayed an upregulation of antigen presentation machinery, suggesting OPCs are active contributors in disease pathogenesis and targets of cytotoxic T lymphocytes (Falcao et al., 2018). It is clear there are disease-specific OPC populations, yet it remains to be seen what the role of each of these OPC populations is during CNS demyelination. While the debate on OPC functional heterogeneity is not settled, these

studies suggest the existence of disease-specific OPC populations in the CNS that might be relevant for developing novel therapeutics for diseases like multiple sclerosis.

G. OPCs respond to CNS Injury

One of the most unique qualities of OPCs is their ability to respond to several types of CNS injury. OPCs respond to secondary demyelinating insults, even when oligodendrocytes are not primarily targeted, for example in mechanical lesions, spinal cord injury, ischemia, and neurodegeneration (Levine, 1994, McTigue et al., 2001, Zhang et al., 2013, Kang et al., 2010). Increased levels of OPCs have also been documented in the prefrontal cortex after acute methamphetamine exposure, perhaps as a part of the alterations to addiction circuitry that needs to be examined further (Somkuwar et al., 2014). OPCs, along with microglia, respond within a day after traumatic brain injury by migrating to and occupying the lesion site, where they become hypertrophic and highly proliferative (Dimou and Gallo, 2015). Surprisingly, *in vivo* imaging of CNS stab wound injuries showed that at 5 days post-injury astrocytes have a low proliferation rate, and do not exhibit migration to the lesion site (Bardehle et al., 2013). Reactive OPCs are also found in models of CNS neurodegeneration, such as the SOD1 (G93A) mutant mouse that recapitulates features of human amyotrophic lateral sclerosis (ALS) (Kang et al., 2010). Progressive motor neuron death in the spinal cord of these mice is accompanied by a robust increase in OPC proliferation and differentiation (Kang et al., 2010). This suggests that OPCs and microglia are playing an immediate role in the CNS injury response that remains to be fully explored.

H. OPCs contribute to glial scar formation

After any kind of CNS injury, glial cells become activated and orchestrate the formation of the glial scar. The glial scar is characterized by a high content of ECM molecules forming an environment known to block axonal regeneration and remyelination (Silver and Miller, 2004, Cregg et al., 2014). Chondroitin sulfate proteoglycans (CSPGs) are a key component of the inhibitory glial scar (Lau et al., 2012, Davies et al., 1997). While reactive astrocytes are the principal cells present within the glial scar, it is now clear that OPC are not bystanders during the scar formation. Following spinal cord injury, OPCs proliferate and upregulate NG2 expression, thereby inhibiting axonal regeneration (Tan et al., 2005). Rhodes *et al.* reported that treatment with antimetabolic drugs, aimed at diminishing glial scar formation by eliminating OPC proliferation in knife wound injuries, results in a slight improvement in axonal regeneration (Rhodes et al., 2003). This result suggests that OPC proliferation and upregulation of NG2 can be detrimental to axon regrowth. Conversely, OPC expression of NG2 has also been shown to support axon growth *in vitro*, even when NG2 was overexpressed in OPCs (Yang et al., 2006). The contribution of the OPC to the glial scar is not limited to only one type of CSPG (Jones et al., 2003). OPC have been shown to also produce keratan sulfate proteoglycan after injury, and can also produce neurocan and versican, CSPGs known to impair CNS repair (Jones and Tuszynski, 2002, Asher et al., 2002, Asher et al., 2000). In conclusion, OPC clearly participate in the formation of the glial scar and produce CSPGs that impair CNS repair and their differentiation into mature myelinating oligodendrocytes.

I. OPCs as active participants in neuroinflammation

Microglia and astrocytes are considered to be the classic innate immune cells of the CNS because of their response to pathogens or tissue damage and their ability to recruit peripheral immune cells (Ransohoff and Brown, 2012). However, the literature contains evidence that OPCs are not simple spectators of the CNS immune response. In a mouse model of cerebral prolonged hypoperfusion, it was shown that OPCs were the first cells to produce MMP9, an enzyme necessary for degradation of the extracellular matrix, prior to the appearance of white matter damage (Seo et al., 2013). Furthermore, authors demonstrated that OPC derived MMP9 could mediate the opening of the BBB and the infiltration of neutrophils that ultimately damage the myelin sheath in this model (Seo et al., 2013). Moyon *et al.* have recently demonstrated that OPCs isolated from the brain of mice undergoing cuprizone-induced demyelination express high levels of CCL-2 and IL-1 β (Moyon et al., 2015). CCL-2 has a critical role in recruiting monocytes (Deshmane et al., 2009) while IL-1 β is a powerful inflammatory cytokine involved in many aspects of the immune response (Sims and Smith, 2010). While authors did not explore the role of these mediators on immune cell recruitment/activation, they concluded their study by demonstrating that CCL-2 could promote OPC migration *in vivo* and was also expressed by OPCs present in active multiple sclerosis (MS) lesions (Moyon et al., 2015). Recent work by Gadani *et al.* also highlights the role that myelinating glia play in repair after spinal cord injury. Oligodendrocytes release IL-33, a nuclear alarmin implicated in orchestrating the recruitment of peripheral immune cells necessary for CNS repair (Gadani et al., 2015b). Although predominantly expressed by oligodendrocytes, OPCs also express IL-33 and participate in promoting CNS repair (Gadani et al., 2015b).

OPCs can also upregulate gene expression of inflammatory cytokines like *Il6* and *Csf2* in response to IL-17 signaling, and disruption of this signaling pathway ameliorated EAE clinical symptoms (Kang et al., 2013b). In line with this novel immunomodulatory role of OPCs, subsequent studies have shown that OPCs in the demyelinating CNS participate in antigen presentation via MHC1 and MHC2, and can activate pathogenic T cells (Falcao et al., 2018, Kirby et al., 2019). Elegant work by Kirby et al. presented evidence showing that OPCs who engage in antigen cross-presentation of myelin peptide are targets of CD8-mediated cytotoxicity, and as a result impair CNS remyelination (Kirby et al., 2019). My own thesis work also suggests that OPCs contribute to neuroinflammation via antigen cross-presentation in the demyelinating CNS (Fernandez-Castaneda et al., 2019), and this work will be presented later. Future studies are needed to tease out whether all OPCs are capable of participating in antigen cross-presentation *in vivo*, or whether only a specialized subset can carry out this role. In addition, a better characterization of the CNS antigens that OPCs can internalize, process, and present to T cells during demyelination is still needed. The discovery that OPCs participate in antigen presentation has definitely shifted our view of OPCs as bystanders in neuroinflammation. A better understanding of the mechanisms that control the immunomodulatory function of OPCs is desperately needed. Targeting this novel function of OPCs has the potential to modulate the inflammatory environment and promote CNS remyelination.

J. Conclusion

Over the past decade, we have greatly expanded our knowledge of OPC biology and function within the CNS. We now appreciate that adult OPCs are responsible for generating myelinating oligodendrocytes throughout life. Yet, myelination is not their only role within the CNS, as discussed in this chapter (**Figure 1**). Recent studies have provided compelling evidence that OPCs are capable of modulating neuronal and astrocytic functions that can ultimately affect behavior (Sakry et al., 2014), providing a new perspective on adult OPC function. After all, adult OPCs are uniformly distributed across the CNS, giving them the ability to survey widespread network activity. However, questions remain regarding adult OPC function. Despite their unique developmental origins within the CNS, no functional differences have been found regarding their myelination potential. It is possible that differences in function might arise in their ability to regulate neuronal activity in distinct regions of the CNS. As the field continues to examine the OPC-neuron synapse, other roles of adult OPCs might become clearer.

OPCs also respond to several types of CNS injury. As microglia and astrocytes have traditionally held the spotlight in CNS injury, the contribution of OPCs to tissue repair would be interesting to explore. Recent work has shown that OPCs upregulate expression of immune signaling molecules CCL-2 and IL-1 β to promote their migration into demyelinating lesions (Moyon et al., 2015). These immune molecules were shown to be important for OPC migration, but they could also be involved in orchestrating an inflammatory response. CCL-2 produced by astrocytes and IL-1 β produced by microglia has been shown to amplify the immune response following CNS injury, which can be beneficial to tissue repair (Gadani et al., 2015a). Surprisingly, OPCs were also shown to

participate in antigen presentation within the demyelinating CNS, indicating that they can actively contribute to neuroinflammation (Kirby et al., 2019, Fernandez-Castaneda et al., 2019). Future studies will be needed to determine whether targeting OPCs presents a viable option to modulate the neuroinflammatory environment during CNS pathology.

The need to target OPCs to promote remyelination in demyelinating diseases such as MS, has long been a therapeutic goal. Although much research has been focused on identifying the factors implicated in inhibition of OPC differentiation and remyelination, it is highly possible that the multi-functionality of OPCs during CNS disease might steer OPCs away from repair to involvement in the immune response and/or the glial scar formation. A deeper understanding of OPC function in the CNS is warranted before we can truly begin to explore their therapeutic potential.

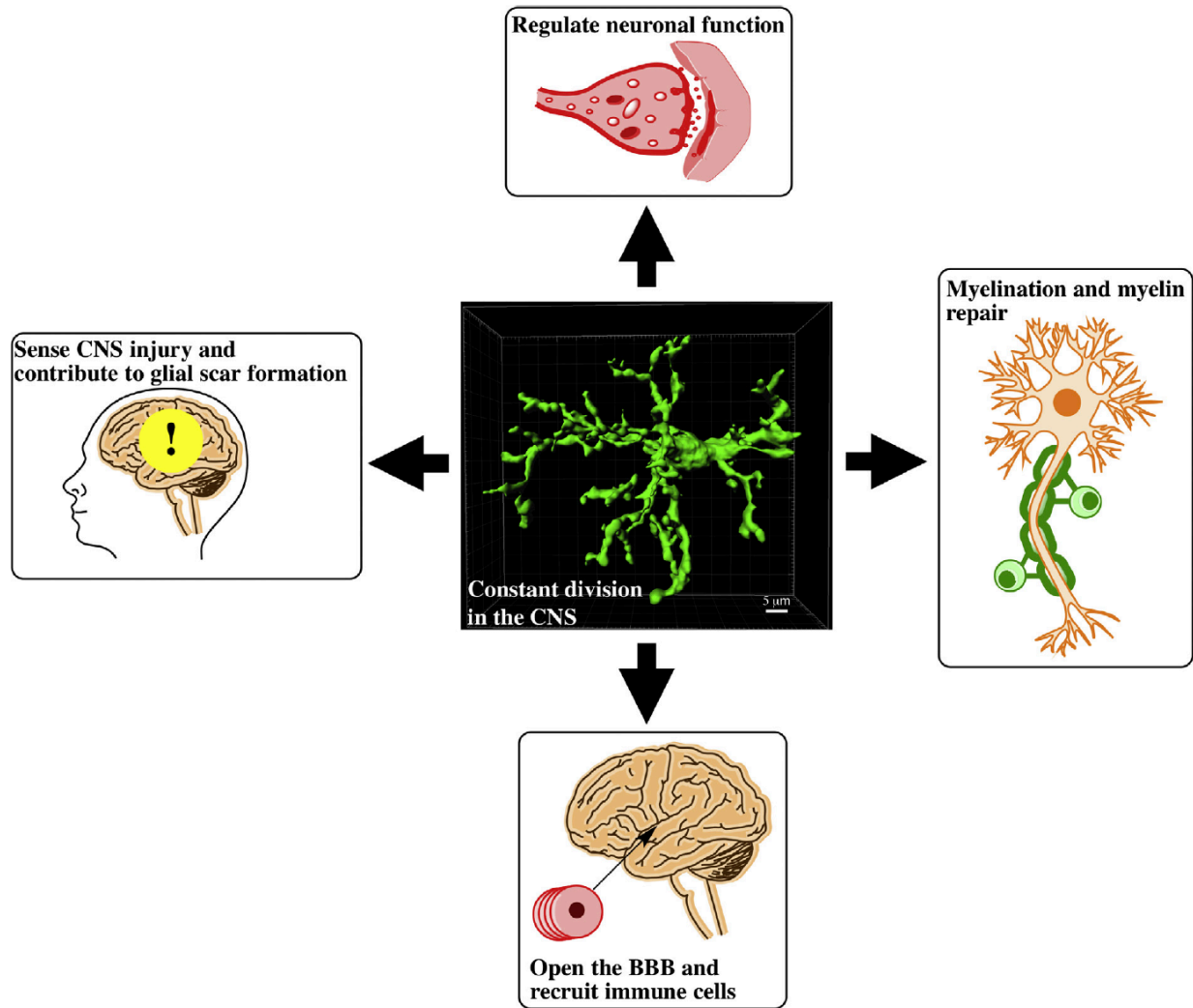


Figure 1 **The multiple functions of OPCs in the CNS.** Central panel represents a 3D rendering of an OPC in the mouse cortex. Figure from review article published in *Brain, Behavior, and Immunity* [Fernandez-Castaneda and Gaultier, 2016]

Chapter 3: The multifunctional low-density lipoprotein receptor-related protein 1 (LRP1)

A. LRP1 overview

While the role of low-density lipoprotein receptor-related protein 1 (LRP1) in central nervous system (CNS) neurons has been investigated, its function in CNS glia remains elusive. Our laboratory has been instrumental in furthering our understanding of LRP1 function in microglia and oligodendrocyte-lineage cells in the context of multiple sclerosis (MS). Here, I will review the relevant literature highlighting LRP1 function in the CNS, and more importantly, its relevance to MS pathogenesis. Considering LRP1 is expressed in several CNS cell types and has numerous high-affinity ligands, it is important to recognize its pleiotropic effects are still poorly understood.

LRP1 was originally discovered as a liver receptor responsible for the clearance of α 2-macroglobulin (α 2M), a proteinase inhibitor found in the blood (Moestrup and Gliemann, 1989). LRP1 is a member of the low-density lipoprotein receptor gene family (Herz, 2001), and is composed of an 85kD cytoplasmic and transmembrane β -chain that is non-covalently linked to a 515kD extracellular α -chain (Zlokovic et al., 2010). Its large extracellular α -chain contains four ligand binding domains, allowing LRP1 to bind and endocytose over 40 structurally distinct ligands that include Rhinovirus, bacterial toxin *Pseudomonas* exotoxin A, proteinases, and lipoproteins (Zlokovic et al., 2010, Herz and Strickland, 2001). Given its wide range of ligands, LRP1 has been assigned a variety of scavenger receptor functions, including the clearance of apoptotic cells (Gardai et al., 2005). Additionally, LRP1 has also been shown to participate in extracellular matrix

remodeling by fibroblasts, in part by regulating matrix metalloproteinase levels (Hahn-Dantona et al., 2001, Gaultier et al., 2010). Genetic deletion of LRP1 in mice results in embryonic lethality, perhaps underlining the importance of this multifunctional receptor in development (Herz et al., 1992, Herz et al.).

The beginning of my thesis career was largely shaped by two unique studies that emphasized the multifaceted nature of LRP1. The first work highlighted the role of LRP1 as a regulator of inflammation via the NF κ b signaling pathway (Gaultier et al., 2008). The second study demonstrated that LRP1 in astrocytes, microglia, and oligodendrocytes was a phagocytic receptor for myelin debris (Gaultier et al., 2009). Given that MS is an inflammatory demyelinating disease of the CNS (Compston and Coles, 2008), it did not take long before I focused my graduate work on the role of LRP1 in glia. Yet, LRP1 is ubiquitously expressed across many tissues, and has cell type-specific functions (Lillis et al., 2008). In the following sections I will summarize some of the important roles LRP1 plays in several CNS cell types.

B. Neuronal LRP1 in the central nervous system

Like other LDL receptor family members, LRP1 binds apolipoprotein E (ApoE), which is known to contribute to late-onset Alzheimer's disease (Beisiegel et al., 1989, Schmechel et al., 1993). LRP1 also binds other ligands associated with Alzheimer's disease, like α 2-macroglobulin (α 2M), β -amyloid precursor protein (APP), amyloid- β ($A\beta$) peptides, and its affinity for these ligands has resulted in several studies investigating the role of LRP1 in CNS pathogenesis (Kounnas et al., 1995, Shinohara et al., 2017). For example, LRP1 in neurons and astrocytes has been shown to mediate the clearance of

A β in the brain (Kanekiyo et al., 2013, Liu et al., 2017). Similarly, pericytes associated with the blood-brain barrier have also been shown to clear A β aggregates in an LRP1-dependent manner (Ma et al., 2018). While it is possible that impaired clearance of A β peptide by LRP1 contributes to disease progression, the exact mechanism by which LRP1 could drive Alzheimer's pathogenesis remains elusive. Indeed, there have been contradictory studies showing whether polymorphisms in the *LRP1* exon 3 is associated with Alzheimer's disease (Kang et al., 1997, Woodward et al., 1998, Beffert et al., 1999, Wang et al., 2017).

In addition to its link with Alzheimer's disease, LRP1 also plays a role in maintaining CNS homeostasis. Deletion of neuronal LRP1 results in hyperactivity and motor abnormalities (May et al., 2004). This phenotype has been attributed to the potential role of LRP1 in modulating synaptic transmission, as LRP1 can be co-immunoprecipitated with postsynaptic density protein PSD95 and subunits of the N-methyl-D-aspartate (NMDA) receptor (May et al., 2004, Nakajima et al., 2013, Maier et al., 2013). Neuronal LRP1 is also important for maintaining proper brain lipid metabolism, as LRP1 deletion in forebrain neurons results in defective cholesterol levels, synapse loss, neurodegeneration, and neuroinflammation (Liu et al., 2010). The authors of the study propose neuronal LRP1 is regulating ApoE/cholesterol transport, which maintains neurite integrity and ultimately CNS function (Liu et al., 2010). LRP1 in neurons has also been shown to regulate insulin signaling and glucose metabolism, as conditional LRP1 knockouts present with higher levels of glucose in the interstitial fluid in the brain (Liu et al., 2015). It remains to be seen whether this impaired insulin signaling is detrimental to CNS function, as no behavioral phenotypes were reported in the study.

C. LRP1 functions as a phagocytic receptor for myelin

Despite the increasing knowledge of LRP1 in neuronal function, the role of LRP1 in CNS glia during CNS pathology has not been extensively explored. Gaultier *et al.* were the first to report that oligodendrocytes express LRP1 (Gaultier et al., 2009). It is important to note that while the authors describe this glial population as “oligodendrocytes”, the isolation protocol used in this study is commonly used to purify oligodendrocyte progenitor cells (OPCs) (O'Meara et al., 2011). We now know that few mature oligodendrocytes express LRP1, and that OPCs are amongst the highest expressers in the CNS (Fernandez-Castaneda et al., 2019, Zhang et al., 2014). It is likely that the authors primarily purified OPCs, with noticeable oligodendrocyte contamination, and mistakenly referred to this glial population as oligodendrocytes. Consistent with these data, was the observation that LRP1 was not detected in purified CNS myelin, which consists of oligodendrocyte cell membrane (Gaultier et al., 2009). For this reason, I will refer to the ill-defined glial population in the study as oligodendroglia, an umbrella term often used to denote OPCs and oligodendrocytes.

It was also demonstrated that astrocytes, microglia, and oligodendroglia phagocytosed myelin vesicles in an LRP1-dependent manner (Gaultier et al., 2009). Additionally, LRP1 expression was upregulated in the cerebellum and spinal cord of mice with experimental autoimmune encephalomyelitis (EAE) when compared to controls (Gaultier et al., 2009). Importantly, LRP1 immunoreactivity was also detected in macrophages (potentially microglia) and astrocytes in the EAE spinal cord, suggesting these cells might participate in debris clearance (Gaultier et al., 2009). This observation

eventually led our laboratory to characterize the LRP1-specific ligands in myelin debris, and our work suggested LRP1 could play a role in necrotic cell clearance (**Appendix A**) (Fernandez-Castaneda et al., 2013).

The data mentioned above had several implications for the trajectory of my graduate work. I was deeply interested in OPC biology and the mechanisms governing white matter repair in the context of MS. It was known that myelin debris clearance was necessary for efficient remyelination in the CNS (Kotter et al., 2001, Kotter et al., 2006). Yet, myelin debris clearance during demyelination was predominantly thought to be performed by microglia via Fc and complement receptors (Smith, 2001, Yamasaki et al., 2014). Although myelin debris was shown to inhibit OPC differentiation into mature oligodendrocytes (Syed et al., 2008, Baer et al., 2009), the OPC receptors mediating this effect remained unknown. Given the robust expression of LRP1 in oligodendroglia and microglia, LRP1 seemed like an ideal candidate to contribute to the myelin-mediated block of remyelination. In one scenario, the phagocytic function of LRP1 in microglia could be hindered in the demyelinating CNS, resulting in inefficient myelin debris clearance and inhibition of white matter repair. Alternatively, OPCs could be actively phagocytosing myelin debris in an LRP1-dependent manner, causing a block in OPC differentiation and remyelination (**Figure 1**). The role of LRP1 in these two glial cell types is something our laboratory would explore further. I decided to pursue the role of LRP1 in OPCs for my doctoral work, and that role was undoubtedly more complex than originally thought.

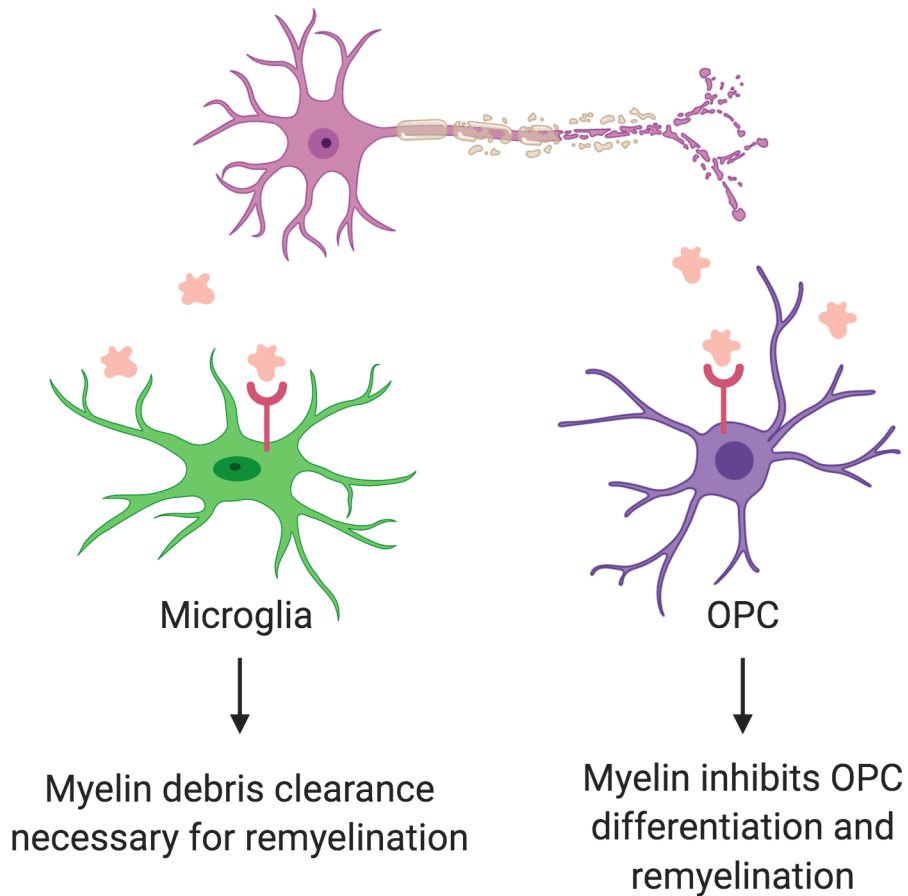


Figure 1 Potential cell-type specific consequences of LRP1 participating in myelin debris phagocytosis.

D. LRP1, microglia, and neuroinflammation

Although some groups had attempted to examine the role of LRP1 in microglia, this was done solely in an *in vitro* setting or with the use of genetic models not specific for microglia (Pocivavsek et al., 2009, Zhang et al., 2009). Our laboratory was the first to generate a microglia-specific LRP1 knockout, in which we studied the role of microglial LRP1 in EAE, the murine mouse model of MS described earlier (Chuang et al., 2016). LRP1-deficient microglia presented with amoeboid morphology, a hallmark of myeloid cell

activation, in the naïve brain (Chuang et al., 2016). This suggests that LRP1 might play a role in microglial homeostatic function. More importantly, deletion of LRP1 in microglia resulted in worsening of EAE disease, which was characterized by greater demyelination in the spinal cord, and an increase in CNS-infiltrating immune cells (Chuang et al., 2016). Mechanistic studies showed microglia and myeloid cells lacking LRP1 responded to LPS, a bacterial cell-wall component, with increased proinflammatory cytokine gene expression, likely mediated by disruption in NF κ b signaling (Chuang et al., 2016). This is consistent with previous studies demonstrating LRP1-deficient peritoneal macrophages have increased NF κ b activation (Gaultier et al., 2008). Although the exact mechanism by which microglial LRP1 is protective during EAE remains unknown, it is clear that LRP1 can modulate neuroinflammation in a cell-type specific manner, as LRP1 deletion in peripheral myeloid cells did not recapitulate the phenotype (Chuang et al., 2016).

The role of microglial LRP1 and neuroinflammation has also been studied in the context of neuropathic pain. Peripheral nerve injury can cause sensory neurons to express and transport CSF1 into the spinal dorsal horn where it can activate microglia (Guan et al., 2016). This microglial activation is thought to contribute to neuropathic pain by increasing the mechanical sensitivity of nociceptive neurons (Guan et al., 2016). Interestingly, mice lacking microglial LRP1 had decreased inflammatory cytokine gene expression after partial sciatic nerve ligation, when compared to controls (Brifault et al., 2019). Additionally, these LRP1 deficient mice did not develop mechanical hypersensitivity, a neuropathic pain-related behavior, after partial sciatic nerve ligation (Brifault et al., 2019). The decrease in neuroinflammation in this model is perplexing, as

one would expect neuroinflammation to worsen in the absence of microglial LRP1 given our work in the EAE model.

Brifault and colleagues suggest that unlike membrane-bound LRP1 that serves an anti-inflammatory role (May et al., 2013, Mantuano et al., 2016), LRP1 that is proteolytically cleaved from the cell membrane is inflammatory (Gorovoy et al., 2010, Brifault et al., 2017). In agreement with this explanation, it was shown that CSF1 increases in the spinal dorsal horn after sciatic nerve injury, and CSF1 can induce LRP1 shedding from spinal cord microglia (Brifault et al., 2019). Additionally, microglial LRP1 and proteinases that are responsible for LRP1 shedding from the cell membrane are also upregulated in the spinal cord after partial sciatic nerve ligation (Brifault et al., 2019), suggesting that shed LRP1 but not membrane bound LRP1, drives neuroinflammation in this model. While our laboratory has not examined whether LRP1 is proteolytically cleaved in spinal cord microglia during EAE, our data suggest that the anti-inflammatory membrane-bound LRP1 is responsible for our phenotype. Understanding if and how shedding of LRP1 is regulated in different disease contexts would be beneficial when developing therapeutics to modulate neuroinflammation.

It should be noted that despite the role of LRP1 in apoptotic cell and myelin debris clearance *in vitro* (Gardai et al., 2005, Gaultier et al., 2009), the *in vivo* contribution of LRP1 as a scavenger receptor in the CNS has been difficult to examine. These studies discussed above do not eliminate a contribution of LRP1 as an endocytic receptor for cellular debris, and how that cellular debris affects microglia function. Previous studies suggest that engulfment of apoptotic cells can activate anti-inflammatory pathways (Henson and Bratton, 2013), and the role of LRP1 in this process remains unclear.

E. Rationale for studying the role of LRP1 in OPCs during CNS demyelination

In a previous chapter I outlined several inhibitors of OPC differentiation and remyelination in MS. These inhibitors included myelin debris, inflammatory cytokines, and certain components of the extracellular matrix (ECM). Interestingly, the scavenger receptor LRP1 intersects with each of these remyelination inhibitors. Not only is LRP1 highly expressed in OPCs, but it is also a phagocytic receptor for myelin, it can regulate neuroinflammation, and is involved in ECM remodeling (Gaultier et al., 2009, Gaultier et al., 2010, Chuang et al., 2016). This was the foundation on which I would build my graduate work. Even in those early years, it seemed likely that LRP1 was uniquely positioned to affect OPC differentiation and remyelination. The next chapter details several years of my work on the role of LRP1 in OPCs during CNS demyelination.

Chapter 4: The active contribution of OPCs to neuroinflammation is mediated by LRP1

This chapter consists of the publication authored by Anthony Fernández-Castañeda, Megan S. Chappell, Dorian A Rosen, Scott M. Seki, Rebecca M. Beiter, David M. Johanson, Delaney Liskey, Emily Farber, Suna Onengut-Gumuscu, Christopher C. Overall, Jeffrey L. Dupree, Alban Gaultier. 2019. The active contribution of OPCs to neuroinflammation is mediated by LRP1. Acta Neuropathologica

A. ABSTRACT

Oligodendrocyte progenitor cells (OPCs) account for about 5% of total brain and spinal cord cells, giving rise to myelinating oligodendrocytes that provide electrical insulation to neurons of the CNS. OPCs have also recently been shown to regulate inflammatory responses and glial scar formation, suggesting functions that extend beyond myelination. Low-density lipoprotein receptor-related protein 1 (LRP1) is a multi-faceted phagocytic receptor that is highly expressed in several CNS cell types, including OPCs. Here, we have generated an oligodendroglia-specific knockout of LRP1, which presents with normal myelin development, but is associated with better outcomes in two animal models of demyelination (EAE and cuprizone). At a mechanistic level, LRP1 did not directly affect OPC differentiation into mature oligodendrocytes. Instead, animals lacking LRP1 in OPCs in the demyelinating CNS were characterized by a robust dampening of inflammation. In particular, LRP1-deficient OPCs presented with impaired antigen cross-presentation machinery, suggesting a failure to propagate the inflammatory response and

thus promoting faster myelin repair and neuroprotection. Our study places OPCs as major regulators of neuroinflammation in an LRP1-dependent fashion.

B. INTRODUCTION

Chronic demyelination is the major reason for disease progression and increased disability in multiple sclerosis (MS) patients, as exposed neurons are prone to neurodegeneration (Irvine and Blakemore, 2008). Understanding the mechanisms of remyelination is critical in preventing neuronal loss, and is paramount to improving the quality of life of MS patients (Franklin, 2002). The adult CNS contains a large population of oligodendrocyte progenitor cells (OPCs) that have the potential to differentiate into mature oligodendrocytes and remyelinate denuded axons (Franklin, 2002). Despite OPCs being efficiently recruited into MS lesions (Chang et al., 2002), the process of axon remyelination is impaired (Kuhlmann et al., 2008). A multitude of factors in MS plaques inhibit OPC differentiation into mature oligodendrocytes, including myelin debris, the glial scar, and cytotoxic inflammation (Butovsky et al., 2006, Kotter et al., 2006, Cantuti-Castelvetri et al., 2018, Back et al., 2005, Lau et al., 2012).

Beyond their role in myelination, OPCs have now been shown to be active players in CNS pathology. OPCs, similar to microglia, are constantly surveilling their environment and can migrate to sites of CNS injury (Hughes et al., 2013). In mouse models of MS, OPCs can upregulate cytokine production in response to IL-17 signaling, and greatly contribute to CNS pathogenesis (Kang et al., 2013). Surprisingly, OPCs also upregulate antigen presentation machinery in the demyelinating CNS, and can regulate CD4 T cell proliferation and survival *in vitro* (Falcao et al., 2018b). In addition, OPCs can cross-

present antigen via MHC1 and activate CD8 T cells, further shaping the inflammatory milieu (Kirby et al., 2018a). Taken together, these studies highlight the dynamic role OPCs play in the diseased CNS.

Low-density lipoprotein receptor-related protein 1 (LRP1) is a member of the LDL receptor gene family, which functions in receptor-mediated endocytosis and cell signaling (Lillis et al., 2008). With regards to white matter repair, LRP1 is known to be expressed by the oligodendrocyte lineage (Auderset et al., 2016) and to function as a phagocytic receptor for myelin debris (Fernandez-Castaneda and Gaultier, 2016, Gaultier et al., 2009). The phagocytic properties of LRP1 have also been shown to greatly influence extracellular matrix remodeling and expression of matrix metalloproteinases (Gaultier et al., 2010a, Song et al., 2009). Additionally, LRP1 has a central role in inflammation due to its ability to regulate cytokine production (Gaultier et al., 2008, Mantuano et al., 2016, Yang et al., 2016, Brifault et al., 2017). LRP1 has also been shown to play a role in dendritic cell efferocytosis and MHC1-dependent antigen cross-presentation (Subramanian et al., 2014). Taken together, this evidence places LRP1 as a potential key player in the context of remyelination, but the contribution of LRP1 in OPCs during neuroinflammation remains unclear.

Herein, we report LRP1 expression in OPCs in adult mice and human oligodendroglia. Using two animal strains lacking LRP1 in the oligodendrocyte lineage, we show that the inflammatory environment was significantly dampened in LRP1-deficient mice, resulting in neuroprotection and enhanced myelin regeneration in the Experimental Autoimmune Encephalomyelitis (EAE) and cuprizone models, respectively. Mechanistically, we show that LRP1-deficient OPCs have no intrinsic defect involved in

their differentiation into mature oligodendrocytes but have impaired MHC1-dependent antigen cross-presentation, which could explain the enhanced neuroprotection and remyelination.

C. RESULTS

Cells of the oligodendrocyte lineage dynamically express LRP1.

LRP1 expression in the CNS is differentially regulated during development, with glial cells and, in particular, OPCs expressing high levels of LRP1 into adulthood. Oligodendrocytes and myelin are not reported to express LRP1 in the adult CNS (Auderset et al., 2016, Zhang et al., 2014, Gaultier et al., 2009). Indeed, the majority of PDGFR α ⁺ OPCs in the corpus callosum expressed LRP1 (**Fig. 1a, b**, arrows, 97.5%), while only a small percentage of CC1⁺ oligodendrocytes (**Fig. 1a, b**, hollow arrowheads, 7.6%) were LRP1 positive. Additional staining for LRP1 performed on *Mobp*-EGFP mice (Gong et al., 2003) revealed that GFP⁺ oligodendrocytes are LRP1 negative (**Fig. S1b**), suggesting that LRP1 expression might be progressively lost during OPC differentiation into oligodendrocytes, a finding consistent with published results (Zhang et al., 2014). To analyze whether human OPCs also express LRP1, we examined postmortem human white matter Olig2⁺ cells, and discovered that a subset of these cells also expressed LRP1 and had typical OPC morphology (**Fig. 1c**). Furthermore, we detected LRP1 expression in OPCs during pathological conditions. We found PDGFR α ⁺ Olig2⁺ LRP1⁺ OPCs in tissue isolated from mice undergoing cuprizone-mediated demyelination and EAE (**Fig. 1d, e**). Taken together, our results confirm and highlight LRP1 expression in human and murine adult OPCs during homeostatic and pathological conditions.

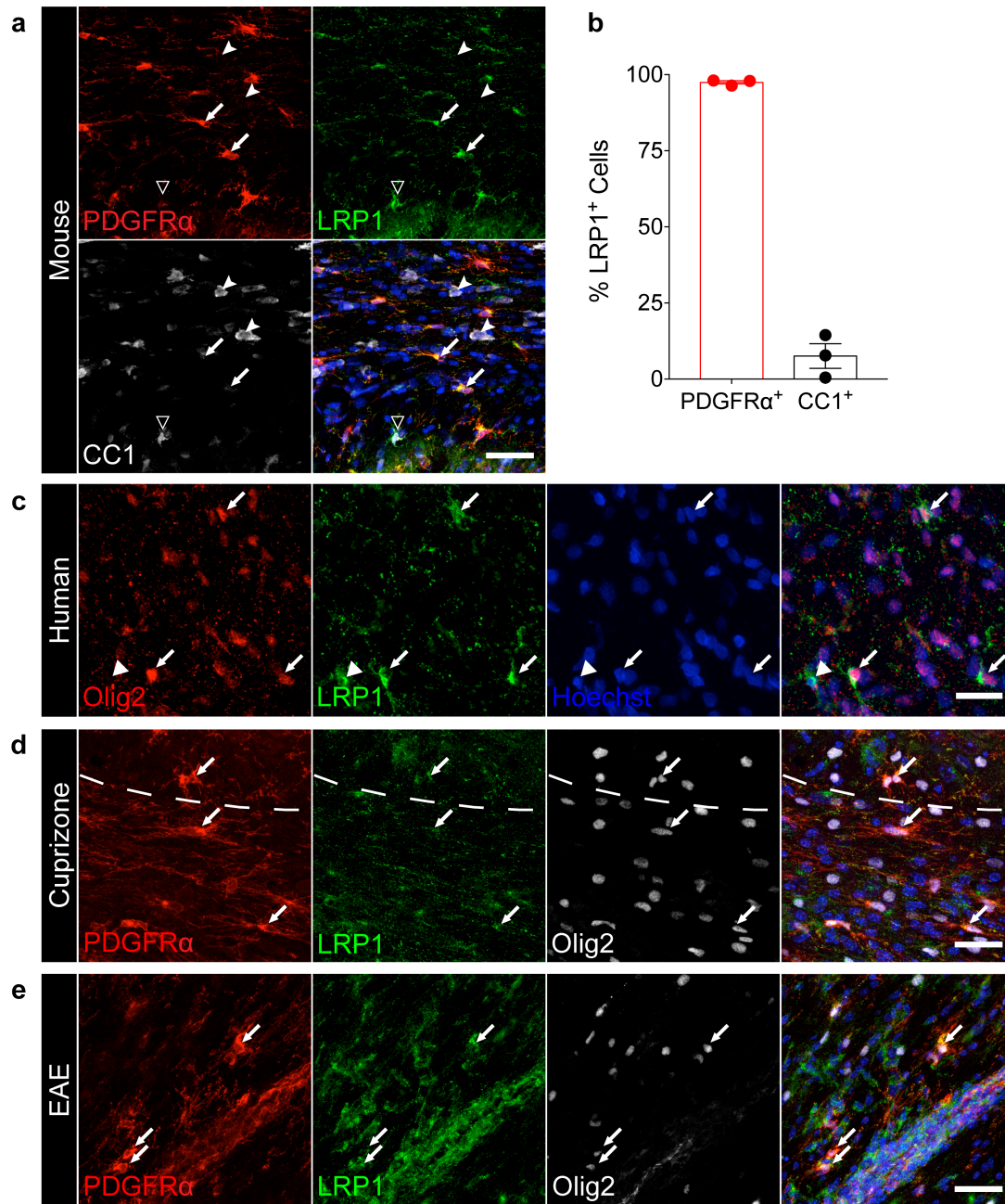


Figure 1 LRP1 is dynamically expressed in oligodendroglia in the homeostatic and pathological CNS. (a) Staining in the adult mouse corpus callosum for PDGFR α , LRP1, and CC1 (arrows = PDGFR α ⁺ LRP1⁺ cells; dented arrowheads = CC1⁺ LRP1⁺ cells; hollow arrowhead = CC1⁺ LRP1⁺ cell). Scale bar 40 μ m. (b) Quantification of PDGFR α ⁺ and CC1⁺ cells expressing LRP1 in the adult mouse corpus callosum (n=3 mice; error bars represent +/- SEM). (c) Human white matter stained for Olig2 and LRP1 (arrows = Olig2⁺ LRP1⁺ cells; arrowheads = Olig2⁻ LRP1⁺ cells). Scale bar 20 μ m. (d) Staining for PDGFR α , LRP1, and Olig2 in the mouse corpus callosum after cuprizone-induced demyelination (arrows = PDGFR α ⁺ LRP1⁺ Olig2⁺ cells). Dashed line demarcates the border between the cortex and corpus callosum. Scale bar 30 μ m. (e) EAE spinal cord stained for PDGFR α , LRP1, and Olig2 (arrows = PDGFR α ⁺ LRP1⁺ Olig2⁺ cells). Scale bar 40 μ m.

Myelin homeostasis is normal in animals lacking LRP1 in oligodendrocyte lineage.

To study the function of LRP1 in the oligodendrocyte lineage *in vivo*, we crossed *Lrp1^{fl/fl}* animals with mice expressing Cre recombinase under the *Olig1* promoter (Lu et al., 2002). *Lrp1^{fl/fl}Olig1^{Cre}* and *Olig1^{Cre}* (Cre-expressing wild type) mice were born according to Mendelian ratios, and appeared healthy and fertile. As expected, LRP1 expression was undetectable by immunofluorescence in PDGFR α ⁺ OPCs in the *corpus callosum* of adult *Lrp1^{fl/fl}Olig1^{Cre}* mice, but remained detectable in NeuN⁺ cortical neurons (**Fig. 2a, Fig. S2c**). LRP1 transcript and protein were not detected in purified primary OPCs isolated from *Lrp1^{fl/fl}Olig1^{Cre}* mice (**Fig. S2a, b**). As a control, we also performed IBA1 staining in adult brains to visualize microglia, the resident immune cells in the CNS, and found that deletion of LRP1 in OPCs did not result in perturbation of microglial number or morphology (**Fig. S2c**). These findings confirmed specific deletion of LRP1 in OPCs in our model. To address whether deletion of LRP1 in OPCs was associated with a myelination defect, we began by quantifying myelin protein expression in adult mice (5 months). Protein extracts were prepared from the cerebrum and cerebellum of *Lrp1^{fl/fl}Olig1^{Cre}* and control *Olig1^{Cre}* mice and expression of MBP and CNP was analyzed via immunoblot. In the cerebellum, CNP and MBP expression was similar across genotypes, whereas the cerebrum of *Lrp1^{fl/fl}Olig1^{Cre}* mice had a modest, but statistically significant decrease in MBP and CNP expression (**Fig. 2b-d**). To further analyze the contribution of LRP1 in myelination, optic nerves from 8-week-old *Lrp1^{fl/fl}Olig1^{Cre}* and *Olig1^{Cre}* mice were prepared for transmission electron microscopy (TEM) analysis of myelin ultrastructure and determination of the *g*-ratio (**Fig. 2e**). Linear fitting of the *g*-ratio data showed no differences between the two groups of mice (**Fig. 2f**). Taken together,

our results show that overall myelin structure in adult mice appears normal following specific deletion of LRP1 in OPCs, with a modest decrease in MBP and CNP expression that is unique to the cerebrum.

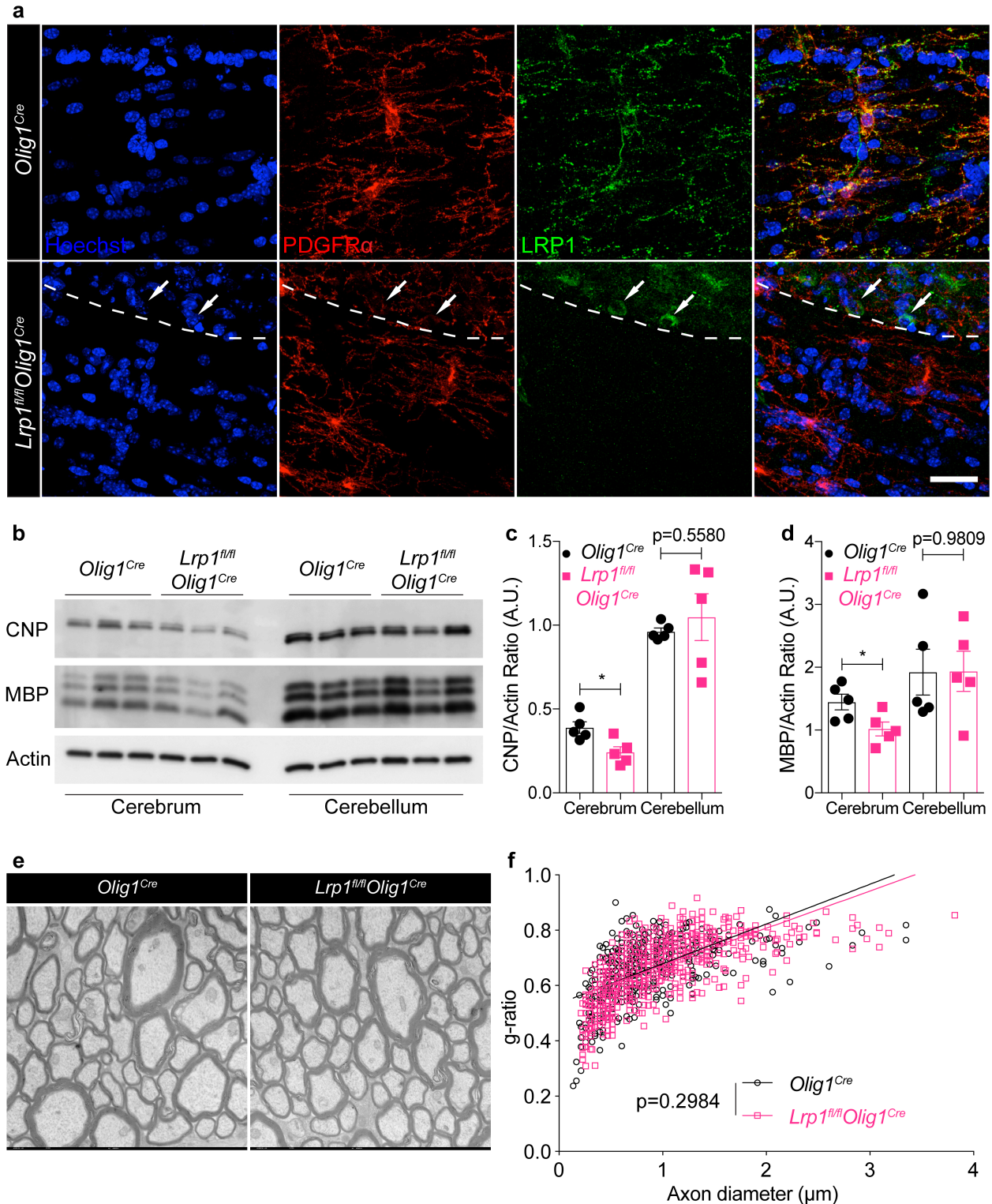


Figure 2 Deletion of LRP1 in OPCs is not associated with severe myelin defects. (a) Staining for PDGFR α and LRP1 in the corpus callosum in *Olig1^{Cre}* and *Lrp1^{fl/fl}Olig1^{Cre}* mice (arrows = LRP1⁺ PDGFR α cells). Dashed line demarcates the border between the cortex and corpus callosum. Scale bar 25 μ m. (b) Representative immunoblot and (c,d) densitometry analysis for CNP, MBP, and actin from cerebrum and cerebellum (unpaired t-test, MBP * $p=0.0329$, CNP * $p=0.0150$; $n=5$ mice per genotype, 2 independent

experiments combined; error bars represent +/- SEM). (e) Representative TEM images and (f) calculated g-ratio of optic nerves (6,000x magnification; n=4 mice per genotype, 10 fields per mouse; linear regression analysis with slopes comparison).

Enhanced OPC differentiation in LRP1-deficient mice after cuprizone-induced demyelination.

Since LRP1 has been shown to regulate pathological conditions applicable to demyelination, such as the inflammatory response and the removal of myelin debris (Gaultier et al., 2008, Gaultier et al., 2009, Fernandez-Castaneda et al., 2013), we subjected our mice to a pathological model of demyelination: the cuprizone model. Cuprizone is a copper chelator that induces reversible demyelination in the *corpus callosum* by inducing selective oligodendrocyte apoptosis (Kipp et al., 2009, Goldberg et al., 2013). Once the animals are returned to their regular diet, OPCs differentiate and remyelination in the *corpus callosum* occurs. Mice were fed a 0.3% cuprizone diet for 5 weeks and then returned to a normal diet to allow for remyelination in the CNS (**Fig. 3a**). We quantified OPC (Olig2⁺ PDGFR α ⁺) and oligodendrocyte (Olig2⁺ CC1⁺) numbers in the *corpus callosum* during homeostatic conditions, peak demyelination, or two remyelination stages, as indicated in **Fig. 3a (left panel)**. Under homeostasis, we found no differences in the number of OPCs or mature oligodendrocytes in the *corpus callosum* of *Lrp1^{fl/fl}Olig1^{Cre}* and *Olig1^{Cre}* mice (**Fig. 3c, e, Unt; Fig. S3b, c**). This is in agreement with our data suggesting no major defects in myelination in LRP1-knockout animals (**Fig. 2**). *Lrp1^{fl/fl}Olig1^{Cre}* mice also experienced similar oligodendrocyte loss and comparable OPC expansion at the peak of cuprizone-induced demyelination (**Fig. 3c, e, Dem; Fig. S3d, e**). Notably, the loss of mature oligodendrocytes correlated with an equal decrease in MBP expression in the *corpus callosum* (**Fig. S4a**). The number of Ki67⁺ OPCs or total

Ki67⁺ cells between genotypes at the peak of demyelination was comparable, which indicated that the deletion of LRP1 does not affect OPC proliferation (**Fig. 3f-h**). Surprisingly, we noted a significant increase in the oligodendrocyte numbers in *Lrp1^{fl/fl}Olig1^{Cre}* mice, compared to *Olig1^{Cre}* controls at both remyelination time points examined (**Fig. 3b, c, 0.5 and 1 Wk Rem**). This increase in oligodendrocytes correlated with a significant decrease in the number of OPCs (**Fig. 3d, e, 0.5 Wk Rem**), suggesting enhanced OPC differentiation in the absence of LRP1. Overall, our data suggest that the deletion of LRP1 in OPCs enhances OPC differentiation into oligodendrocytes following cuprizone-induced demyelination. To explore if the increase in oligodendrocyte numbers in *Lrp1^{fl/fl}Olig1^{Cre}* mice translates into increased myelin synthesis, we analyzed MBP expression on coronal brain sections by immunofluorescence. We saw a significant increase in MBP coverage in *Lrp1^{fl/fl}Olig1^{Cre}* mice (**Fig. 4a, b**). We also analyzed myelin ultrastructure in the *corpus callosum* of *Lrp1^{fl/fl}Olig1^{Cre}* mice by TEM and observed a trend towards a higher percentage of myelinated axons (**Fig. 4c, d**). No difference in myelin g-ratios was observed between the genotypes (**Fig. S4b**). Collectively, these results indicate that the deletion of LRP1 in OPCs accelerates myelin repair after cuprizone-induced demyelination.

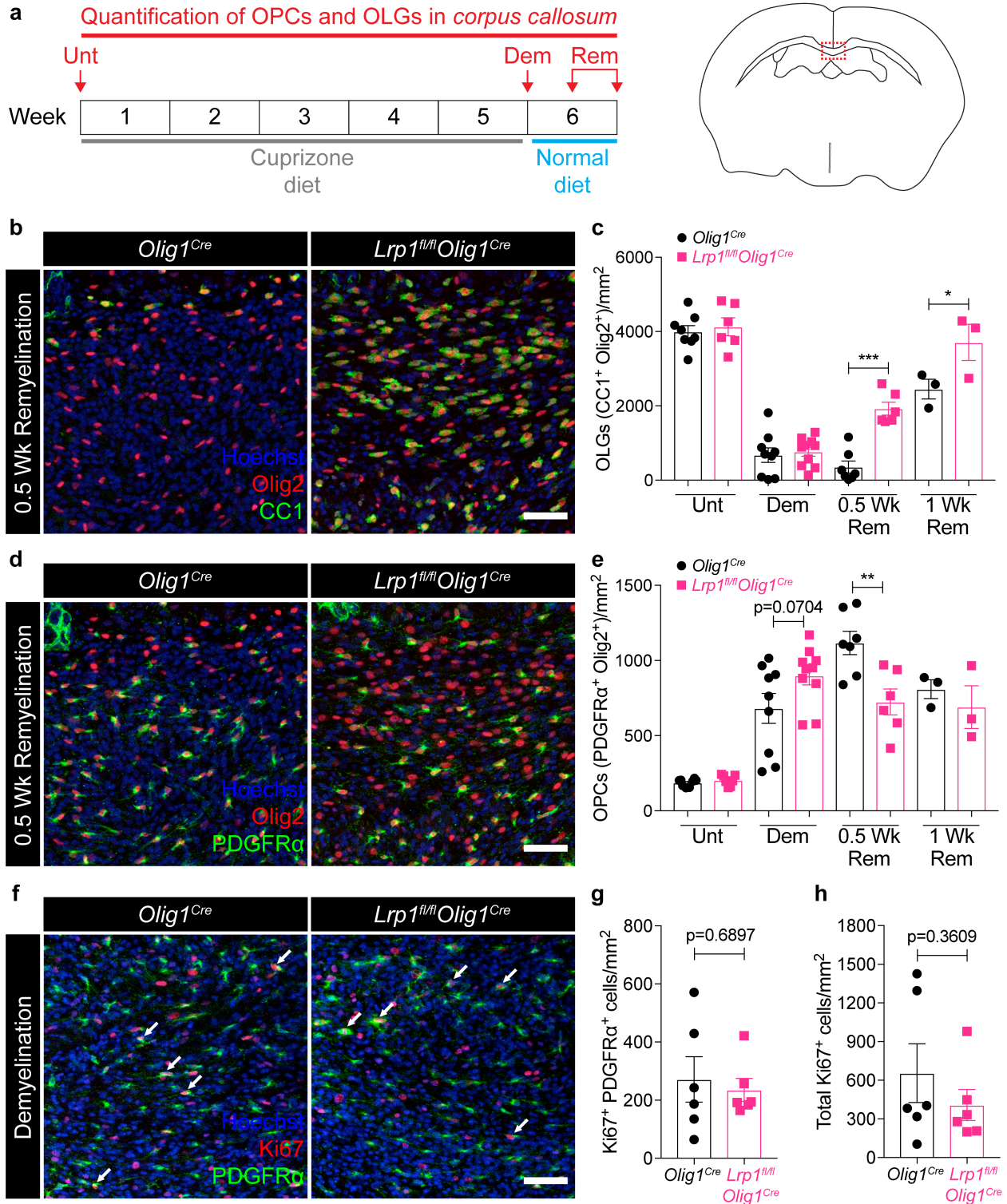


Figure 3 Mice lacking LRP1 in OPCs display enhanced oligodendrogenesis after cuprizone-induced demyelination. (a) Schematic illustrating the cuprizone diet timeline and the timepoints at which the corpus callosum was imaged in *Olig1^{cre}* and *Lrp1^{fl/fl}Olig1^{cre}* mice. (b) Representative images and (c) quantification of oligodendrocytes (CC1⁺ Olig2⁺ cells) in the remyelinating corpus callosum (Two-way ANOVA with Sidak's multiple comparisons test, * $p=0.0153$, *** $p<0.0001$; 3 independent experiments combined). (d)

Representative images and (e) quantification of OPCs (PDGFR α ⁺ Olig2⁺ cells) in the remyelinating corpus callosum (Two-way ANOVA with Sidak's multiple comparisons test, **p=0.0027; 3 independent experiments combined). (f) Ki67 and PDGFR α staining in the corpus callosum at the peak of demyelination (arrows = Ki67⁺ PDGFR α ⁺ cells). (g) Quantification of Ki67⁺ PDGFR α ⁺ cells and (h) total Ki67⁺ cells in the corpus callosum at the peak of demyelination (unpaired t-test; 2 independent experiments combined). Each data point represents an individual mouse. All error bars represent +/- SEM. All scale bars 50 μ m.

Oligodendrocyte maturation *in vitro* does not require LRP1 expression in OPCs.

To determine whether enhanced remyelination in LRP1-deficient mice was cell-intrinsic, we isolated primary OPCs from *Lrp1^{fl/fl}Olig1^{Cre}* and *Olig1^{Cre}* neonate (post-natal day 8) animals and induced their differentiation into myelinating oligodendrocytes with triiodothyronine (T3) for 48 hours (Emery and Dugas, 2013). We then analyzed the expression of myelin genes *Mrf*, *Mbp*, and *Cnp* by qPCR. To our surprise, we found no significant differences between *Lrp1^{fl/fl}Olig1^{Cre}* and *Olig1^{Cre}* OPCs (**Fig. 4e-g**). In addition, when cultured OPCs derived from *Plp*-EGFP reporter mice were cultured in the absence of T3 and treated with increasing concentrations of receptor-associated protein (RAP), an LRP1 antagonist that blocks ligand binding to LRP1 (Herz et al., 1991), we found no differences in the percent of *Plp*-EGFP positive cells, compared to vehicle control (**Fig. 4h,i**). These data suggest that enhanced OPC differentiation in *Lrp1^{fl/fl}Olig1^{Cre}* mice after cuprizone treatment is not likely to be mediated by a cell-intrinsic mechanism in OPCs.

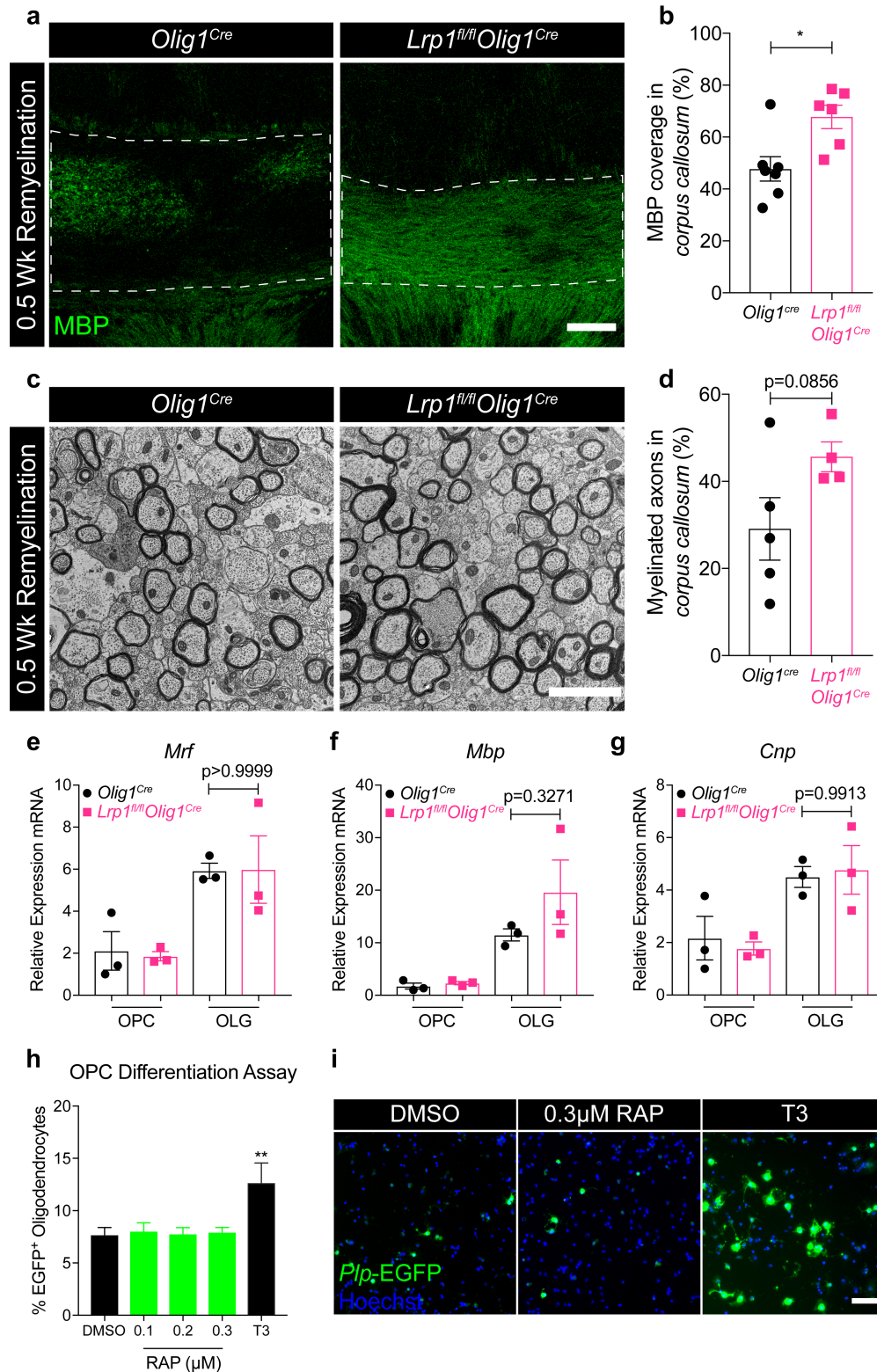


Figure 4 Enhanced remyelination in mice lacking oligodendroglial LRP1 is not cell-autonomous. (a) Representative images and (b) quantification of MBP expression in the remyelinating corpus callosum of *Olig1^{Cre}* and *Lrp1^{fl/fl}Olig1^{Cre}* mice after 0.5 Wk Rem (unpaired *t*-test; 2 independent experiments combined; scale bar 100μm). (c) Representative TEM images and (d) quantification of axons in the remyelinating

corpus callosum after 0.5 Wk Rem (unpaired t-test; n=4-5 mice per genotype; scale bar 2 μ m). (e-g) qPCR for *Mrf*, *Mbp*, and *Cnp* from primary OPCs cultured in proliferation (OPC) or differentiation (OLG) media (unpaired t-test; n=3 mice per genotype). (h) Quantification and (i) representative images of *Plp*-EGFP OPCs treated with DMSO, T3, or increasing concentrations of the specific LRP1 inhibitor, RAP (One-way ANOVA with Dunnett's multiple comparisons test, DMSO vs T3 **p=0.0072; conditions plated in sextuplicate; error bars represent +/- SEM; scale bar 150 μ m).

Oligodendroglial LRP1 regulates the inflammatory environment and promotes myelin repair.

Given the unexpected lack of a cell-autonomous differentiation phenotype in *Lrp1^{fl/fl}Olig1^{Cre}* OPCs *in vitro*, and the fact that naïve *Lrp1^{fl/fl}Olig1^{Cre}* mice have similar numbers of OPCs and oligodendrocytes in the *corpus callosum*, we postulated that OPCs lacking LRP1 could influence the local environment to promote remyelination via an indirect mechanism under pathological demyelination. To test this, we performed unbiased RNA-sequencing analysis on micro-dissected *corpus callosum* from homeostatic or remyelinating mice post-cuprizone treatment (**Fig. 5a**). Principal component analysis (PCA) revealed that *Lrp1^{fl/fl}Olig1^{Cre}* and *Olig1^{Cre}* *corpus callosum* samples under homeostatic conditions were comparable (**Fig. 5b**). However, striking gene expression differences between the remyelinating *corpus callosum* of *Lrp1^{fl/fl}Olig1^{Cre}* and *Olig1^{Cre}* mice were detected (**Fig. 5c, d**). Gene ontology (GO) terms associated with myelination and oligodendrocyte differentiation were elevated in *Lrp1^{fl/fl}Olig1^{Cre}* mice (**Fig. 5e**), supporting our histological analysis (**Fig. 4**). Indeed, prototypical genes involved in myelination (*Cnp*, *Mbp*, *Plp1*) were significantly elevated in the *corpus callosum* of *Lrp1^{fl/fl}Olig1^{Cre}* mice (**Fig. 5f**). Surprisingly, *Lrp1^{fl/fl}Olig1^{Cre}* mice also had a dampened inflammatory signature, compared to *Olig1^{Cre}* mice (**Fig. 5g**). The change in the inflammatory response was detectable at week 5 (**Fig. S5c**), a stage preceding remyelination (Skripuletz et al., 2011) (**Fig. S5b**), without an overall change in IBA1

immunoreactivity (**Fig. S5d, e**). Collectively, our data suggest that LRP1 expression in OPCs might modulate the immune landscape in the cuprizone model.

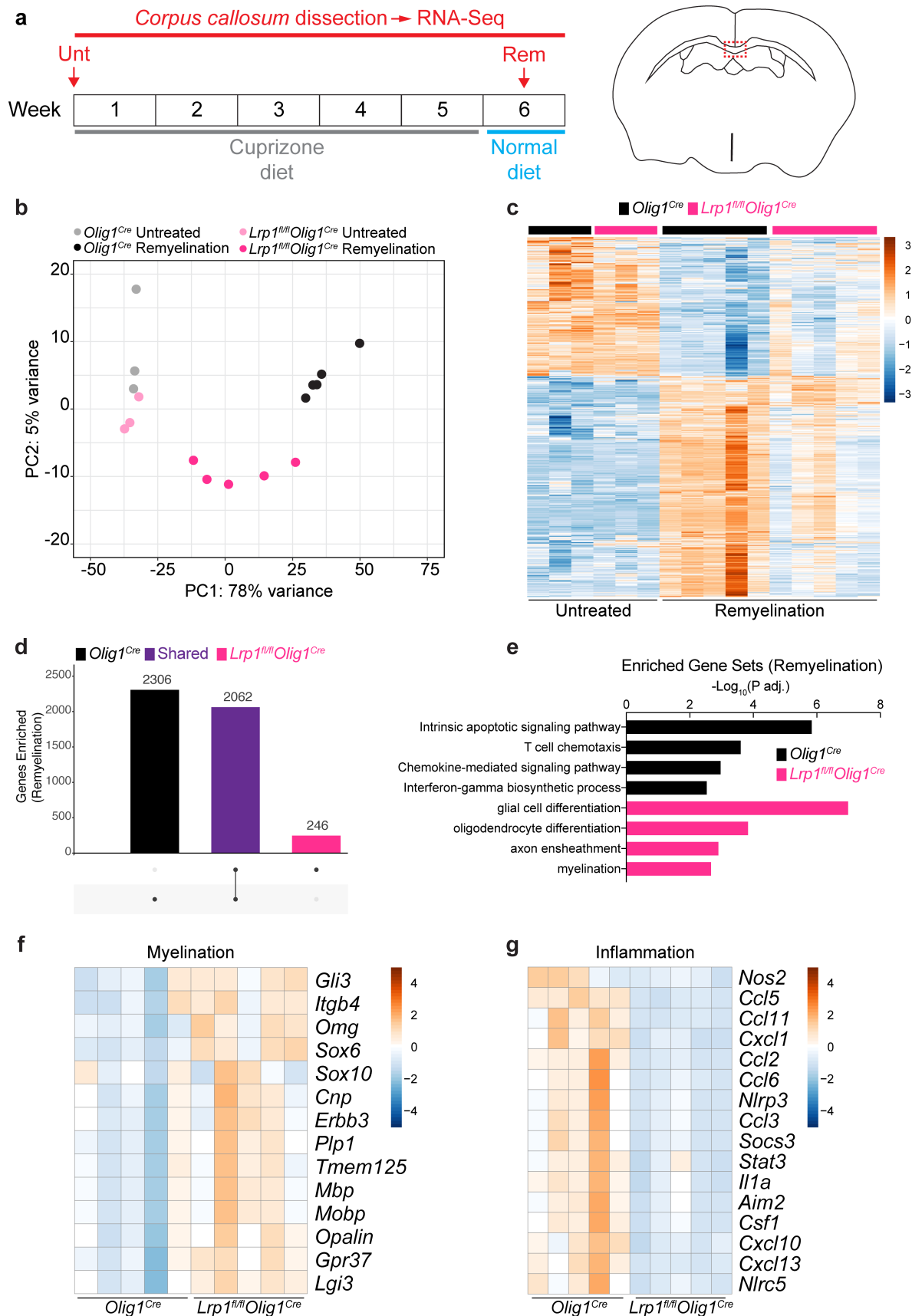


Figure 5 Oligodendroglial LRP1 modulates the inflammatory landscape and enhances myelin repair. (a) Schematic illustrating the cuprizone diet timeline and timepoints at which the corpus callosum was dissected and analyzed by RNA-seq. (b) Principal component analysis (PCA) plot and (c) heat map of the transcriptomes of *Olig1^{cre}* and *Lrp1^{fl/fl}Olig1^{cre}* mice. (d) UpSet plot showing the number of significantly upregulated genes (compared to untreated mice) that are unique (single dots) or shared (connected dots) in mice undergoing remyelination. (e) Gene ontology (GO) terms illustrating unique biological processes upregulated in the remyelinating corpus callosum of *Olig1^{cre}* and *Lrp1^{fl/fl}Olig1^{cre}* mice. (f) Heat maps for myelination- and (g) inflammation-related genes in the remyelinating corpus callosum. Heat maps have a normalized count scale with z-score normalization.

LRP1 deletion in OPCs is protective in experimental autoimmune encephalomyelitis.

The unexpected inflammatory phenotype in the cuprizone model of demyelination prompted us to further explore OPC LRP1 function in neuroinflammation. For this, we chose experimental autoimmune encephalomyelitis (EAE), a well-accepted model of the neuroinflammatory human disease multiple sclerosis (MS). We tested *Lrp1^{fl/fl}Olig1^{Cre}* and control *Olig1^{Cre}* mice in EAE, and found reduced clinical scores and delayed incidence of disease onset in *Lrp1^{fl/fl}Olig1^{Cre}* mice, compared to control mice (**Fig. 6a, b**). This phenotype was recapitulated with an alternate inducible model of LRP1 deletion in OPCs (*Lrp1^{fl/fl}Pdgfra^{CreERT2}*). In this model, mice were injected with tamoxifen (to induce LRP1 deletion) at 8 weeks of age, followed by EAE immunization 4 weeks later. Tamoxifen is known to inhibit inflammation explaining the milder EAE clinical score and incidence obtained with this inducible Cre strain (Behjati and Frank, 2009); nevertheless, LRP1 deletion also resulted in a significant decrease in clinical score (**Fig. S6a**). To explore the pathological conditions associated with lower EAE clinical scores in *Lrp1^{fl/fl}Olig1^{Cre}* mice, we performed flow cytometry analysis at the peak of the disease (day 17). Our results reveal that the numbers of TCR β ⁺ T cells (TCR β ⁺ CD8⁻), CD8 T cells (TCR β ⁺ CD8⁺), and myeloid cells (CD11b⁺ CD45⁺) were decreased in animals lacking LRP1 expression in

OPCs, compared to control mice (**Fig. 6c-f**). T regulatory cell (TCR β^+ CD4 $^+$ FoxP3 $^+$) numbers were equivalent in the spinal cord and the draining inguinal lymph nodes across genotypes during EAE (**Fig. S6b**). Importantly, the number of OPCs (CD45 $^-$ PDGFR α^+) was similar across genotypes (**Fig. 6g-i**).

To rule out immune dysfunction in *Lrp1^{fl/fl}Olig1^{Cre}* mice as the driver of our immunomodulatory phenotype, we tested the antigen recall response of lymph node T cells 7 days after immunization. Treatment with the MOG₃₅₋₅₅ peptide resulted in a mild increase in IFN γ without significant differences in the production of IL-17A, as determined by multiplex immunoassay (**Fig. 6j, k**). Importantly, the analysis of the spleen 7 days post-immunization did not reveal differences in T cell numbers (**Fig. S6c**), ruling out an LRP1-dependent defect in immunization as the origin of our phenotype. EAE resistance was not due to the baseline differences in immune cell composition, as demonstrated by immunophenotyping analysis of the immune organs of *Lrp1^{fl/fl}Olig1^{Cre}* and *Olig1^{Cre}* animals under homeostatic conditions (cervical lymph nodes and spleen; **Fig. S6d-f**). One exception being a small decrease in the frequency of CD8 T cells in naïve spleens of *Lrp1^{fl/fl}Olig1^{Cre}*. Taken together, our results show that mice lacking LRP1 expression in OPCs have reduced inflammation in EAE, paralleling our results obtained with the cuprizone model.

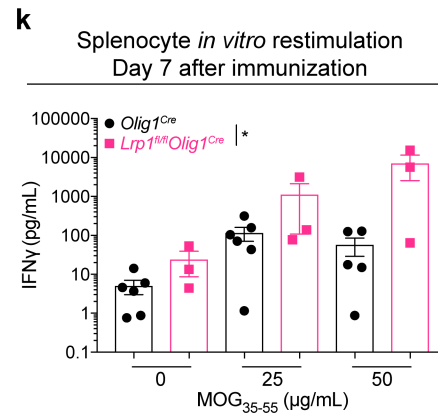
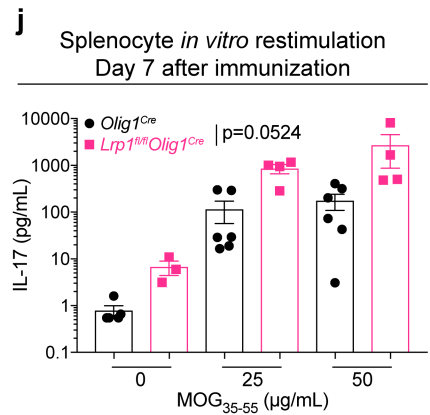
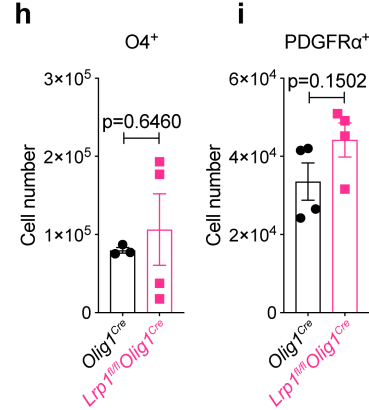
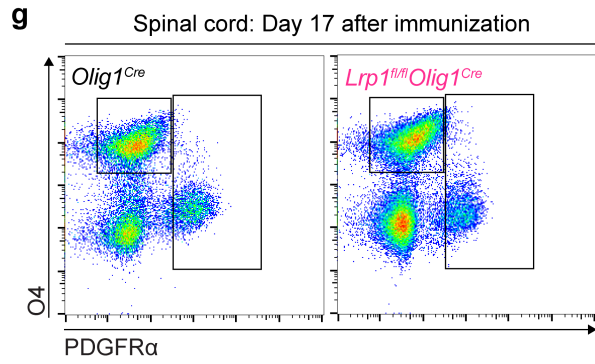
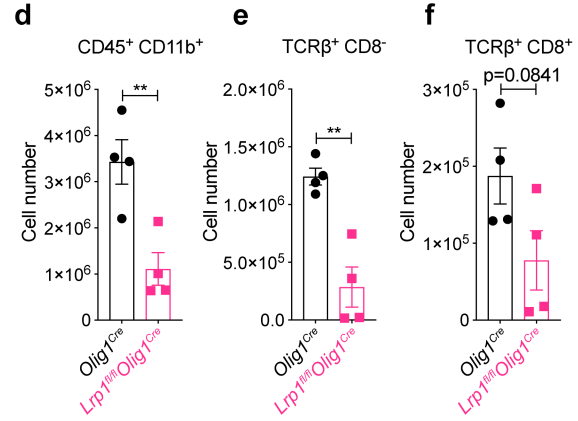
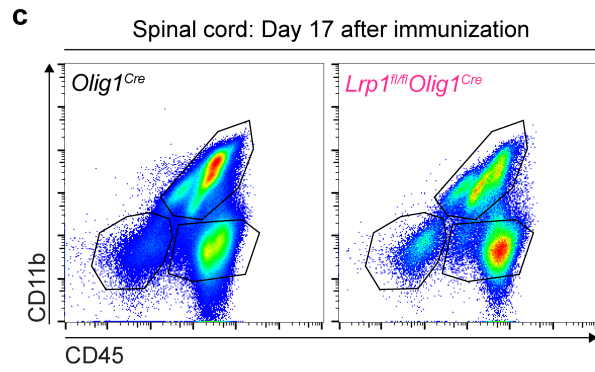
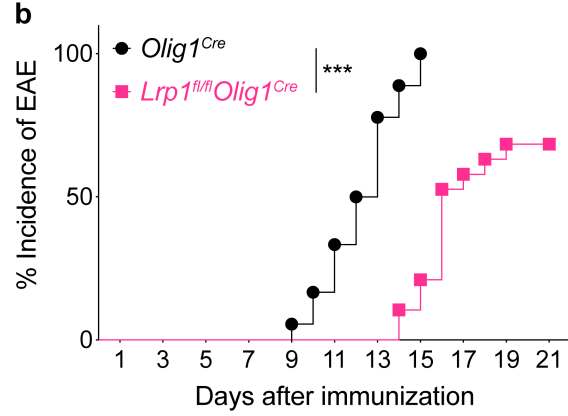
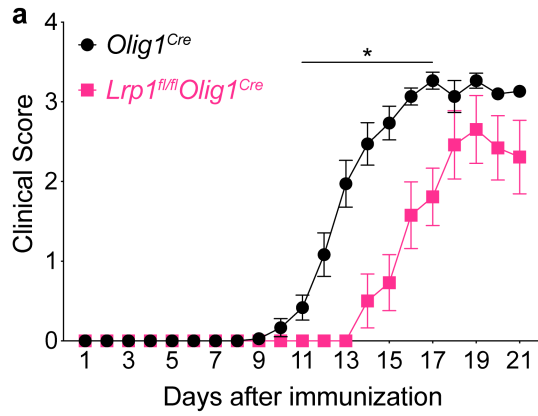


Figure 6 Deletion of LRP1 in OPCs is protective in experimental autoimmune encephalomyelitis. (a) EAE clinical scores and (b) incidence of disease in *Olig1^{Cre}* and *Lrp1^{fl/fl}Olig1^{Cre}* female mice (EAE scores: Mann-Whitney U test, * $p < 0.05$, $n = 13-18$ mice with disease per genotype; incidence: Log-rank test, *** $p < 0.0001$, $n = 18-19$ total mice per genotype; 2 independent experiments combined). (c) Representative flow plots and (d-f) quantification of immune cells in EAE spinal cords on day 17 after immunization (unpaired t-test; $n = 4$ mice per genotype; ** $p < 0.01$). (g) Representative flow cytometry plots and (h,i) quantification of oligodendroglial cells in EAE spinal cords on day 17 after immunization (unpaired t-test; $n = 3-4$ mice per genotype). (j) Levels of IL-17A and (k) IFN γ from splenocytes after antigen restimulation with MOG₃₅₋₅₅ (Two-way ANOVA, * $p = 0.0184$; 2 independent experiments combined).

LRP1 regulates antigen cross-presentation by OPCs.

Recently, OPCs have been shown to cross-present antigen via MHC1 in demyelinating conditions (Kirby et al., 2018a). Antigen cross-presentation was of particular interest because of the documented role of LRP1 in internalizing antigenic stimuli that is processed and presented to CD8 T cells via MHC1 (Subramanian et al., 2014, Hart et al., 2004, Binder and Srivastava, 2004, Basu et al., 2001). We began by measuring the expression of MHC1 at the peak of EAE in *Lrp1^{fl/fl}Olig1^{Cre}* and *Olig1^{Cre}* mice and found that LRP1-deficient OPCs have significantly lower levels of MHC1 (**Fig. 7a, b**). We next examined myeloid cells (CD45⁺ CD11b⁺) and detected two populations based on MHC1 expression (MHC1^{Mid} and MHC1^{High}, **Fig. 7c-e**). Backgating showed that MHC1^{High} cells are CD45^{High} CD11b⁺ and that MHC1^{Mid} cells are CD45^{Mid} CD11b⁺ (**Fig. 7f**); an expression pattern that has been used to loosely classify microglia and invading myeloid cells (Denker et al., 2007). Our results suggest that MHC1 expression does not change in CD45^{Mid} CD11b⁺ MHC1^{Mid} (microglia, **Fig. 7d**) but is decreased in CD45^{High} CD11b⁺ MHC1^{High} (peripheral myeloid cells, **Fig. 7e**). Next, we isolated OPCs and myeloid cells from EAE spinal cords to further explore antigen cross-presentation defects in LRP1-deficient OPCs and the consequences on the inflammatory environment (**Fig. S7a, b**). The labeling strategy for cell sorting was designed to eliminate contaminating

endothelial cells (CD31⁺) and pericytes (CD13⁺) that are known to also express PDGFR α (**Fig. 7g**). RNA-sequencing analysis revealed decreased expression of antigen cross-presentation machinery, including MHC1, in OPCs (PDGFR α ⁺) lacking LRP1 (**Fig. 7h**). Excitingly, decreased MHC1-related gene expression was conserved in our cuprizone model RNA-sequencing data set (**Fig. 7i**). Because myeloid cells are critical orchestrators of demyelination (Ajami et al., 2011, Goldmann et al., 2013), we also analyzed gene expression in isolated myeloid cells (CD45⁺ CD11b⁺) from the spinal cords of *Lrp1^{fl/fl}Olig1^{Cre}* and *Olig1^{Cre}* mice subjected to EAE. We found that the inflammatory response to IFN γ , a cytokine produced by antigen-stimulated CD8 and CD4 T cells, was robustly elevated in myeloid cells from *Olig1^{Cre}* mice, when compared to the cells from *Lrp1^{fl/fl}Olig1^{Cre}* mice (**Fig. 7j**). This observation also phenocopied our cuprizone results, as IFN γ response genes were also decreased in remyelinating *corpus callosum* of *Lrp1^{fl/fl}Olig1^{Cre}* mice (*Nos2*, *Ccl5*, *Nlrc5*; **Fig. 5g**). We next quantified CD8 T cells present in the brain of cuprizone-fed mice, and EAE spinal cords and did not detect any significant changes between genotypes (**Fig. S8a, b, d, e**). However, the number of CD8 T cells associating with OPCs (**Fig. 7k**) was trending lower in the cuprizone and EAE models in *Lrp1^{fl/fl}Olig1^{Cre}* mice (**Fig. S8 c, f**). To assess the role of LRP1 in antigen cross-presentation, we treated primary OPCs with IFN γ to induce MHC1 expression (Kirby et al., 2018b). OPCs were then incubated with ovalbumin (OVA) protein in the presence or absence of RAP, an LRP1 inhibitor (Herz et al., 1991). After a media wash, OPCs were cocultured with OT-I CD8 T cells (OVA-specific) for 48h. Finally, CD8 T cell proliferation was quantified by flow cytometry. Our results show that blocking LRP1 with RAP is able to significantly decrease CD8 T cell proliferation *in vitro* (**Fig. 7l**). Taken together, our

results suggest that LRP1 deletion in OPCs may disrupt antigen cross-presentation to lymphocytes and thus could influence the function of T cells and myeloid cells in the demyelinating CNS.

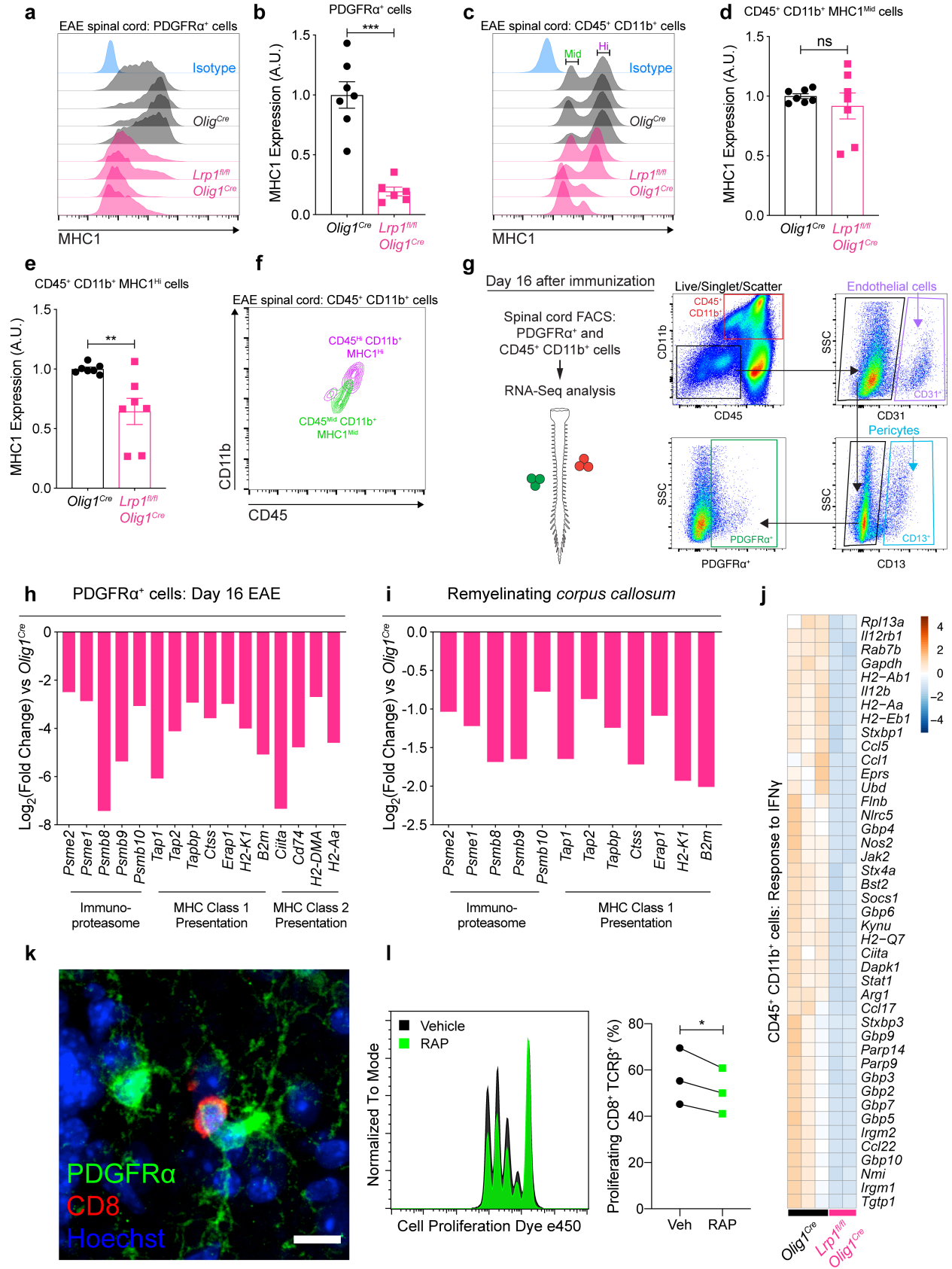


Figure 7 LRP1 modulates MHC1-dependent antigen presentation in OPCs. (a) Representative histograms and (b) MHC1 expression in PDGFR α ⁺ and (c-e) CD45⁺ CD11b⁺ cells from EAE spinal cords (day 17) detected by flow cytometry in *Olig1*^{cre} and *Lrp1*^{fl/fl}*Olig1*^{cre} mice (unpaired t-test, ****p*<0.0001, ***p*=0.0076; n=6-7 mice per genotype; 2 independent experiments combined). (f) Backgating of MHC1 Mid (Middle) and Hi (High) expressing CD45⁺ CD11b⁺ cells in (c). (g) FACS gating strategy for sorting PDGFR α ⁺ and CD45⁺ CD11b⁺ cells from EAE spinal cords (gates based on FMOs; CD31: endothelial cells; CD13: pericytes; SSC: side scatter area). (h) Antigen presentation genes downregulated in PDGFR α ⁺ cells from *Lrp1*^{fl/fl}*Olig1*^{cre} EAE spinal cords. (i) Antigen presentation genes downregulated in the remyelinating corpus callosum of *Lrp1*^{fl/fl}*Olig1*^{cre} mice. (j) Genes related to IFN γ response in CD45⁺ CD11b⁺ cells from EAE spinal cords (GO:0034341). Heat map has a normalized count scale with z-score normalization. (k) OPC-CD8 cell association in the EAE spinal cord. Scale bar 10 μ m. (l) Histogram and quantification of OT-I CD8 T cell proliferation after coculture with OVA-laden OPCs in the presence or absence of RAP, an LRP1 inhibitor (n=3 independent cocultures; paired t-test, **p*=0.0484).

D. DISCUSSION

Understanding the mechanisms that control neuroinflammation and promote neuroprotection in MS is paramount for the development of critically needed therapeutics. Here, we have presented evidence further highlighting the role of OPCs in actively shaping the neuroinflammatory landscape. Using two distinct models of demyelination, we have shown that the immunomodulatory function of OPCs relies on the multifunctional receptor LRP1. The specific removal of LRP1 in OPCs (*Lrp1*^{fl/fl}*Olig1*^{Cre} or *Lrp1*^{fl/fl}*Pdgfra*^{CreERT2} mice) reduces the inflammatory response during CNS demyelination and promotes repair and neuroprotection.

Intriguingly, in our hands, *Lrp1*^{fl/fl}*Olig1*^{Cre} mice appear to have unperturbed developmental myelination, in contrast with a recent study that utilized *Olig2*-Cre mediated deletion of LRP1 (Lin et al., 2017). We did not observe myelin ultrastructure abnormalities in adult *Lrp1*^{fl/fl}*Olig1*^{Cre} animals, though we noted modestly decreased MBP and CNP expression in the cerebrum of these mice. There are several possible explanations for the observed differences in the role of LRP1 in developmental myelination between our study and Lin *et al* (Lin et al., 2017). One, it is possible that a transient myelination deficit exists in *Lrp1*^{fl/fl}*Olig1*^{Cre} mice at earlier developmental time

points, which is not apparent in the adult animals we examined. The slight decrease in MBP and CNP expression detected in the cerebellum, but not present in the cerebrum, could be linked to the significant difference in myelin quantity between these two CNS regions. Perhaps, a mild developmental myelin defect is only detectable in heavily myelinated areas in our strain, but the role of LRP1 in pathological inflammatory conditions (antigen cross-presentation) outweighs this mild phenotype. Furthermore, we did not observe differences in the *in vitro* differentiation of OPCs (isolated from newborn mice) after either genetic or pharmaceutical inactivation of LRP1. Second, our mouse model employs the use of the *Olig1*-Cre knock-in allele (Lu et al., 2002). Because *Olig1* deficiency has been reported to cause remyelination and developmental myelination deficits (Arnett et al., 2004, Dai et al., 2015), we utilized *Olig1^{Cre}* animals as controls for *Lrp1^{fl/fl}Olig1^{Cre}* mice (to minimize any differences due to the inactivation of one *Olig1* allele). Such consideration could perhaps mask the subtle LRP1-dependent phenotype observed during myelin formation by Lin *et al.* (Lin et al., 2017). Third, there are fundamental differences in the models selected for our study - cuprizone and EAE are associated with extensive demyelination and induction of immune responses, compared to the focal lysolecithin demyelination model used by Lin *et al.* (Ransohoff, 2012).

In this study, we demonstrate that the removal of LRP1 in OPCs is associated with a better outcome in animal models of demyelination (cuprizone and EAE). This improvement was not due to a direct effect on the differentiation of OPCs into oligodendrocytes, but was mediated by the modulation of the inflammatory environment. Specifically, we observe a downregulation of genes involved in MHC1 antigen cross-presentation in LRP1-deficient OPCs. In addition, the CNS of these mice also presents

with a dampened inflammatory profile. Our results are consistent with a previous study that shows wild type OPCs upregulate antigen cross-presentation machinery in the demyelinating CNS (Falcao et al., 2018b). LRP1 blockade or genetic deletion has been shown to prevent antigen presenting cells from engulfing exogenous peptides or apoptotic cells, thereby negatively affecting MHC1-mediated cross-presentation (Binder et al., 2000, Binder and Srivastava, 2004, Subramanian et al., 2014). We propose OPCs internalize antigen in an LRP1-dependent fashion, which is then processed and cross-presented to CD8 T cells during CNS demyelination (**Fig. 8**). CD8 T cells can then engage in a multitude of effector functions to exacerbate CNS pathology, for example, production of perforin and granzyme B, or secretion of IFN γ and TNF α (Zhang and Bevan, 2011). It has been well documented that IFN γ and TNF α can stunt OPC differentiation (Lin et al., 2006, Chew et al., 2005). Furthermore, CD8-derived IFN γ plays a crucial role in EAE pathogenesis, specifically in models where oligodendrocytes are engineered to cross-present antigen to CD8 lymphocytes (Huseby et al., 2001, Ford and Evavold, 2005, Na et al., 2008, Na et al., 2009). Indeed, we observed a downregulation of cross-presentation machinery in LRP1-deficient OPCs, which is accompanied by decreased expression of IFN γ -related genes in the CNS (**Fig. 5g; Fig. 7h**). Another possible explanation for our results is the potential role of LRP1 on cell migration (Lillis et al., 2008). Perhaps, LRP1-deficient OPCs migrate faster to the site of remyelination from adjacent regions of the parenchyma or stem cell niches to accelerate myelin repair (Butti et al., 2019).

Our results are in agreement with recent work showing that OPCs can participate in antigen-cross presentation and activate CD8 T cell effector functions, leading to impaired myelin repair in the cuprizone model (Kirby et al., 2018a). Future studies will be

critical to understand if LRP1 is needed to mediate CD8 T cell cytotoxicity toward OPCs in the context of MS and to identify the antigens involved in this pathological process. Other studies are also needed to determine if the change of the inflammatory environment is downstream of CD8 T cells or an independent arm of LRP1 function in OPCs. Clearly, LRP1 in OPCs might also influence other immune cells such as CD4 and myeloid cells in the context of demyelination; further work is needed to tease apart the effect of LRP1 in OPCs on different inflammatory cell types.

Based on our results, targeting LRP1 in the context of MS appears to be an attractive therapeutic intervention, but caution should be taken due to the pleiotropic and multifunctional nature of LRP1 (Gonias and Campana, 2014). Other cells in the CNS, such as microglia and neurons, express LRP1 and LRP1 function can vary greatly across cell types (Lillis et al., 2008). LRP1 deletion in microglia results in higher pro-inflammatory cytokines and increased EAE severity (Chuang et al., 2016). This phenotype is mediated in part by increased NF- κ B activity (Chuang et al., 2016). Yet, abrogating NF- κ B signaling in oligodendroglia does not mirror the findings presented here (Raasch et al., 2011), strengthening the point that other LRP1-dependent mechanism(s) are at play in our system. Furthermore, LRP1 deletion in neurons has been reported to be associated with motor dysfunction, likely due to impaired neurotransmission (May et al., 2004). While the precise targeting of LRP1 in OPCs might be technically challenging, future studies are needed to determine upstream and downstream pathways associated with LRP1 to discover OPC-based treatments to promote remyelination and neuroprotection.

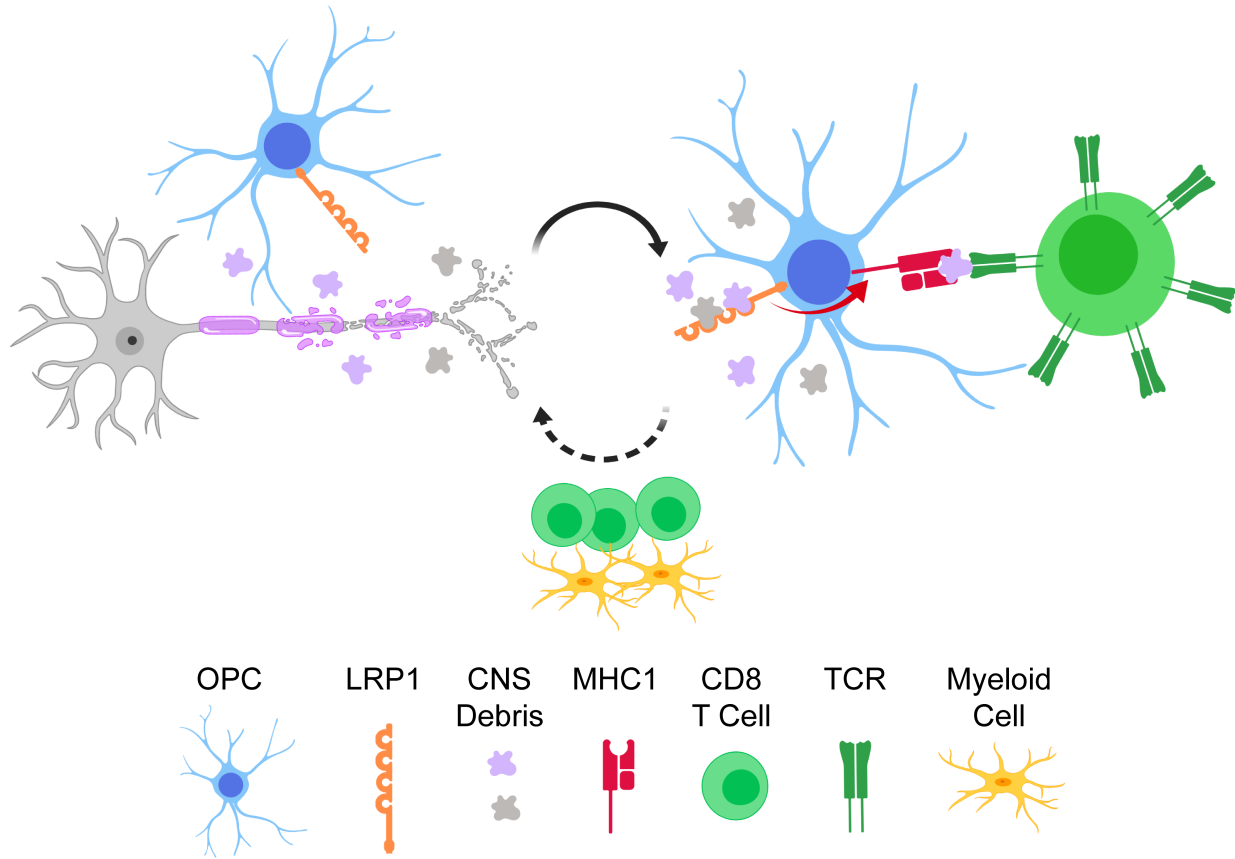


Figure 8 Proposed model by which LRP1 in OPCs regulates the inflammatory landscape. OPCs expressing LRP1 are present in areas of CNS demyelination. LRP1 can mediate the internalization of exogenous antigen that is then processed and cross-presented via MHC1 to CD8 lymphocytes. This cross-presentation can activate CD8 effector functions, which can further exacerbate CNS pathogenesis.

E. METHODS

Human subjects

Fresh-frozen brain tissues from multiple sclerosis patients with pathological evaluations were obtained from the Rocky Mountain MS center Brain Bank.

Animals

Mice in the C57BL/6J background with loxP sites flanking the *LRP1* gene (Jackson #012604) were crossed with *Olig1^{Cre/Cre}* (Jackson #011105) or *Pdgfra^{CreERT2}* (Jackson

#018280) mice to generate *Lrp1^{fl/fl}Olig1^{Cre}* mice and *Lrp1^{fl/fl}Pdgfra^{CreERT2}*. *Olig1^{Cre}* mice were used as a negative control across all the studies when using *Lrp1^{fl/fl}Olig1^{Cre}* mice. *Lrp1^{fl/fl}Pdgfra^{CreERT2-}* mice were used as negative controls when studying *Lrp1^{fl/fl}Pdgfra^{CreERT2+}* mice. Mice were maintained in the C57BL/6J background by performing backcrossing every 2-3 generations. OT-I mice were purchased from Jackson (#003831). *Mobp*-EGFP mice were purchased from MMRRC (#030483-UCD). The age of experimental animals is indicated in **Table S1**. All animal experiments were approved and complied with regulations of the Institutional Animal Care and Use Committee at University of Virginia (#3918).

Reagents

Primary antibodies used for immunofluorescence were against LRP1 (ab92544, 1:5000, Abcam), PDGFR α (AF1062, 1:200, R&D Systems), CC1 (OP80, 1:200, Millipore), Olig2 (AB9610, 1:500, Millipore), Olig2 (MABN50, 1:500, Millipore), MBP (ab7349, 1:500, Abcam), CD8 (14-0081-82, 1:200, eBioscience), and Ki67 (ab15580, 1:300, Abcam). Primary antibodies used for immunoblotting were against LRP1 (L2170, 1:1000, Sigma), MBP (SMI-94, 1:1000, Covance), CNP (CNP, 1:2000, Aves Labs), and actin (A2228, 1:5000, Sigma). GST-RAP was expressed in bacteria and purified as previously described (Herz et al., 1991).

Animal models of demyelination

For the cuprizone model, adult male mice (ages in **Table S1**) were fed regular chow mixed with 0.3% cuprizone (Sigma #14690) ad libitum for 5 weeks to induce demyelination as

previously described (Sachs et al., 2014). For EAE, *Lrp1^{fl/fl}Olig1^{Cre}* and *Olig1^{Cre}* mice were immunized and scored as previously described (Seki et al., 2017).

Tamoxifen (T5648, Sigma) was prepared at 20mg/mL in 0.2µm filtered corn oil (C8267, Sigma) by shaking overnight at 37°C. *Lrp1^{fl/fl}Pdgfra^{CreERT2}* adult mice received two IP injections of 200mg/kg tamoxifen, 2 days apart. No more than 4mg tamoxifen per injection was administered to adult mice. Mice were allowed to recover for 4 weeks after the final tamoxifen injection before EAE immunizations. *Lrp1^{fl/fl}Pdgfra^{CreERT2-}* and *LRP1^{fl/fl}Pdgfra^{CreERT2+}* mice were immunized twice, three weeks apart, due to the immunomodulatory effects of tamoxifen (Gonzalez et al., 2016, Behjati and Frank, 2009). EAE scores for *Lrp1^{fl/fl}Pdgfra^{CreERT2}* mice were collected after the second immunization.

Immunofluorescence and transmission electron microscopy

Mice were euthanized and perfused with PBS containing 5U/mL heparin followed by 10% buffered formalin. Tissue was post-fixed at least 24h and allowed to sink in 20% sucrose at 4°C. Free-floating cryosections were cut (30-40µm) and collected in PBS containing 0.02% sodium azide and stored at 4°C until further analysis. Sections were blocked in PBS, 0.3% Triton-X 100, 1% BSA, 2% serum for at least 2h at room temperature. When using mouse antibodies on mouse tissue, M.O.M Blocking Reagent (Vector Labs) was also used for 1h at room temperature. Sections were then placed in primary antibody cocktail overnight at 4°C. Tissue was washed three times in PBS, incubated in corresponding secondary antibodies at 2µg/mL (Jackson Immuno Research), and counterstained with Hoechst. Sections were mounted using Aqua-Mount (Lerner Labs)

mounting medium, imaged using a Leica TCS SP8 confocal microscope, and analyzed in Imaris (Bitplane) or Fiji (Schindelin et al., 2012). Mouse tissue was prepared for transmission electron microscopy as previously described (Marcus et al., 2006). Fresh-frozen human tissue samples were acquired from the Rocky Mountain MS Center Tissue Bank at the University of Colorado.

Immunoblot

Cerebrum and cerebellum protein were extracted in RIPA buffer with cOmplete Protease Inhibitor Cocktail (Roche). Lysates were centrifuged (13,000 x g, 4°C) for 15min and protein concentration was quantified using BCA assay. Protein samples were loaded on a Protean TGX gel (Bio-Rad) and transferred into a PVDF membrane. Membranes were blocked in 5% milk in TBS-Tween 0.1% for 1h at room temperature and primary antibody was incubated overnight at 4°C. Washes were performed in TBS-Tween 0.1% and membranes were incubated with secondary antibodies conjugated to HRP (Amersham) for 1h at room temperature and developed using Western Lightning Plus ECL (Perkin Elmer). Densitometry was performed using Fiji (Schindelin et al., 2012).

RNA sequencing and analysis

Mice were euthanized and perfused with PBS containing 5U/mL heparin. The brain was harvested and coronal slices were cut using an adult mouse matrix (69080-C, Electron Microscopy Sciences). Coronal slices (cut to include bregma -0.88 to -1.855) were prepared from untreated animals (3mm thick) and cuprizone-treated animals (2 mm) to normalize total RNA quantity. The corpus callosum was then micro-dissected, flash-

frozen in liquid nitrogen, and RNA was extracted using the Isolate II RNA Mini Kit (Bioline). OPCs and myeloid cells from EAE spinal cords were sorted using a BD FACSAria Fusion, and RNA was extracted using the Isolate II Micro Kit (Bioline). RNA-seq (Illumina) was performed by the Genomic Sciences Lab or the Genome Analysis and Technology Core at the University of Virginia. The sequencing data have been deposited in the National Center for Biotechnology Information (NCBI) Gene Expression Omnibus (GEO) and is accessible through GEO Series accession number GSE136863.

Quantified reads mapped to Ensembl gene transcript IDs and imported into the R-programming environment with the tximport R package. Gene dispersion values were estimated using DESeq2 (v1.22.1), after which pairwise comparisons were made between cuprizone-fed and untreated mice at each timepoint (3wk, 5wk, 5.5wk) after cuprizone administration. The resulting differentially expressed genes were selected using a q-value threshold of 0.05. From these lists, any genes that were found to be differentially expressed between *Lrp1^{fl/fl}Olig1^{Cre}* and *Olig1^{Cre}* mice at 0 weeks after cuprizone administration were removed (**Table S2**) from the gene lists obtained from pairwise comparisons between genotypes in the subsequent three time points. These gene lists were further subdivided into “up-regulated” and “down-regulated” gene lists using log₂ fold change (L2FC) thresholds of $\pm\log_2(1.5)$.

Resulting gene lists from the differential expression analysis were imported into the R package ClusterProfiler (v3.10.1) to perform an over-representation analysis on gene lists against the Gene Ontology Consortium’s Biological process (BP) database (v3.7.0). In

this implementation, Fischer's exact test was applied to each gene list against a background of all genes in the data set while excluding the genes that were differentially expressed among genotypes before cuprizone administration (0wk). Any Gene Ontology terms with a q-value greater than 0.05 were thrown out as insignificant.

Curated gene lists were made from the lists of differentially expressed genes to represent genes specific for neuroinflammation, myelination and oligodendrocyte identity. The corresponding DESeq2 normalized counts were visualized using the R package pheatmap (v1.0.10) and standardized with z-score normalization across all samples. Up Set plots were created using the R package UpSetR (v1.3.3).

Flow cytometry

Flow cytometric analyses were performed as previously described (Seki et al., 2017). eBioscience antibodies were used unless otherwise specified: TCR β (H57-597), CD4 (RM4-5), CD8 (53-6.7), CD19 (eBio1D3), CD45 (30-F11), CD11b (M1/70), CD44 (IM7), CD62L (MEL14), CD11c (N418), Ly6G (1A8), PDGFR α (APA5), O4 (O4; Miltenyi), CD13 (R3-242; BD), CD31 (390; BioLegend), MHC1 (28-8-6; BioLegend), and CD16/CD32 (93). Viability was assessed using a Zombie Aqua Fixable Viability kit (cat. no. 423101, BioLegend) or Ghost Dye Violet 510 (cat. no. 13-0870, Tonbo Biosciences).

Antigen Recall

Single cell suspensions were prepared from inguinal lymph nodes 7 days after immunization as previously described (Seki et al., 2017). Cells were treated with various

concentrations of MOG₃₅₋₅₅ peptide for 48-72h and the concentration of secreted IFN- γ and IL-17A was determined using a Luminex multiplex immunoassay.

Primary OPC cultures

Primary OPC cultures were prepared from P4-8 mouse pups as previously described with minor modifications (Emery and Dugas, 2013). In short, cortices were dissected and the meninges was removed before being digested in 4-5mL Accutase (A11110501, Thermo Fisher) for 45min at 37°C in 5% CO₂ and triturating every 15min. Cell suspensions were then filtered through a 40 μ m strainer, spun down, resuspended in panning buffer, and sequentially incubated in two BSL-1 plates, and finally a rat anti-PDGFR α (APA5) coated plate to select for OPCs. Cells were cultured and expanded for 6 days in poly-L-lysine coated tissue culture plates in OPC proliferation media (DMEM, Pen/Strep, B27, N2, CNTF, NT-3, PDGF-AA, forskolin), and then replated in OPC differentiation media (DMEM, B27, N2, CNTF, T3, forskolin) for 2-3 days to generate oligodendrocytes for gene expression analysis.

The following assay was performed by Renovo Neural (Cleveland, OH). In brief, OPCs from *P1p*-EGFP mice were plated at a density of ~7,000 cells per well in a 96-well plate. Cells were treated with RAP, 0.1% DMSO, and T3 (six wells per condition) in OPC differentiation media for 5 days, with one media change at 48h. Cells were then fixed with 4% PFA, stained with Hoechst, and 20 images per well were captured using a Cellomics VTI scanner. Total and pyknotic nuclei, as well as EGFP⁺ cells were quantified.

Antigen Cross-Presentation Assay

Assay was performed as described with minor modifications (Kirby et al., 2018b). Cultured OPCs were plated in a 96-well plate at 20,000 cells per well. The next day, OPCs were treated with 10ng/mL IFN γ for 12h. OPCs were then pre-treated with 300nM GST-RAP or GST (vehicle) for 1h in IFN γ -containing OPC media. Next, OPCs were incubated with 500 μ g/mL of OVA (77120, Thermo Fisher) in IFN γ -containing OPC media in the presence of GST-RAP or GST for 8h. During the 8h OVA incubation, OT-I CD8 T cells were isolated (19853, Stem Cell Technologies) from spleen and lymph nodes and labeled with Cell Proliferation Dye e450 (65-0842-85, eBioscience). OPCs were then washed with PBS and 160,000 OT-I CD8 T cells were added in a 50/50 mix of RPMI complete and OPC media. OT-I CD8 T cell proliferation was examined using flow cytometry after 48h of coculture.

RT-qPCR

RNA was extracted using the Isolate II Mini Kit (Bioline). cDNA was prepared using iScript cDNA Synthesis Kit (Bio-Rad) or SensiFAST cDNA Synthesis Kit (Bioline). RT-qPCR was performed using NO-ROX SensiFAST Probe or SYBR Mix (Bioline). Taqman probes (Thermo Fisher) were used for *Mbp*, *Cnp*, *Lrp1*, and *Gapdh*. Primers were used for *Mrf* (Forward: CGGCGTCTCGACAGCCTCAA, Reverse: GACACGGCAAGAGAGCCGTCA). Samples were run and analyzed on a PikoReal PCR system (Thermo Fisher).

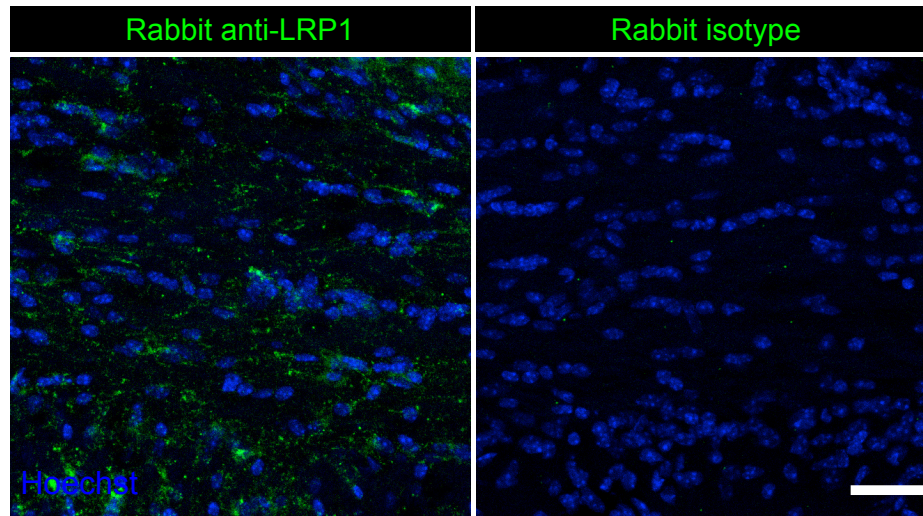
Statistical Analyses

All statistical analyses were performed in Prism 8 (GraphPad software). The results of the statistical tests are presented within the results section. For all analyses, significance was set at $p < 0.05$. Repeats for each experiment, are indicated in the figure legend corresponding to the respective panel.

Acknowledgements

We thank Dr. Sanja Arandjelovic, Courtney Rivet-Noor and Andrea R. Merchak (University of Virginia) for critical reading of the manuscript. We thank Dr. Ioana A. Marin (Stanford) for insightful scientific discussions. Dr. Timothy Bullock (University of Virginia) generously provided OT-I mice for this study. The authors are supported by grants from the NINDS R01 NS083542 and R21 NS111204, the National Multiple Sclerosis Society PP1978, the Double Hoo Research Grant, and the Owens family foundation. A.F.C. is supported by T32 GM008328. D.R. is supported by T32 GM007055. S.M.S. is supported by T32 GM007267 and F31 NS103327.

a



b

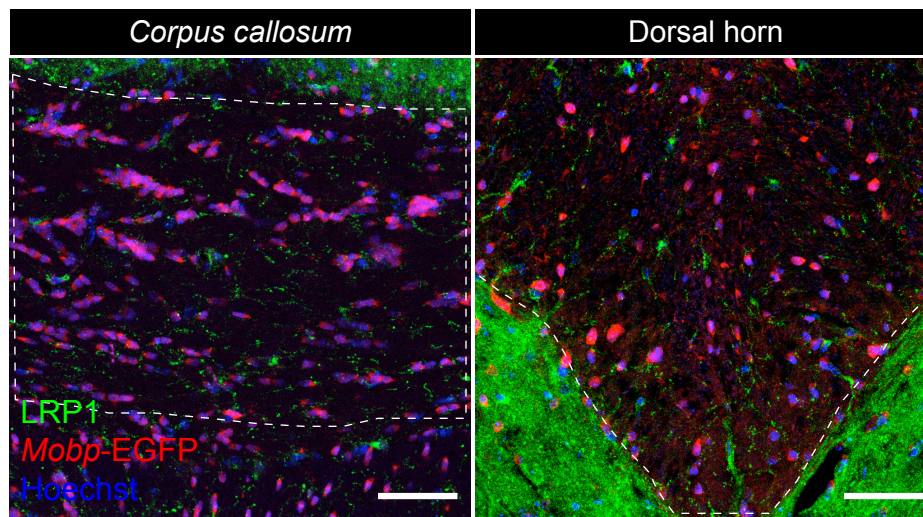


Fig. S1 LRP1 expression in mature oligodendrocytes (a) *Corpus callosum* staining with rabbit anti-LRP1 antibody and rabbit isotype control. Scale bar 30 μ m. (b) Brain (*corpus callosum*) and spinal cord (dorsal horn) slices from *Mobp*-EGFP reporter mice stained for LRP1. Dashed lines demarcate white matter borders. Scale bars 50 μ m.

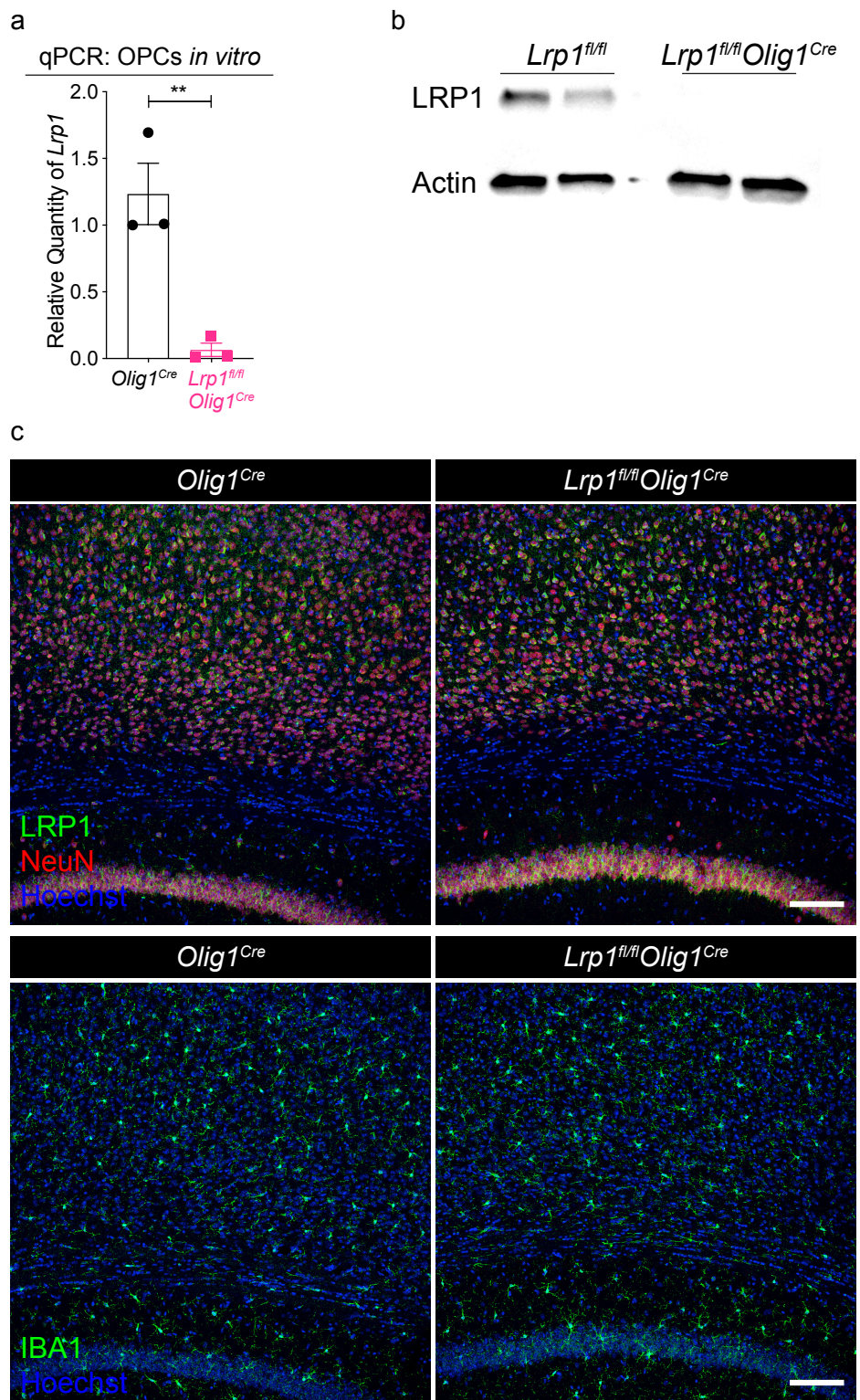


Fig. S2 Silencing of LRP1 in OPCs does not affect neuronal and myeloid compartments (a) qPCR for *Lrp1* from cultured OPCs (unpaired t-test, ** $p=0.0077$; $n=3$ mice per genotype; error bars represent \pm SEM). (b) Western blot for LRP1 and actin from cultured OPCs (2 mice per genotype). (c) Cortical slices stained for LRP1 and NeuN from *Olig1^{Cre}* and *Lrp1^{fl/fl}Olig1^{Cre}* mice (upper panels). IBA1 staining in cortical slices from *Olig1^{Cre}* and *Lrp1^{fl/fl}Olig1^{Cre}* mice (lower panels). Scale bar 100 μ m.

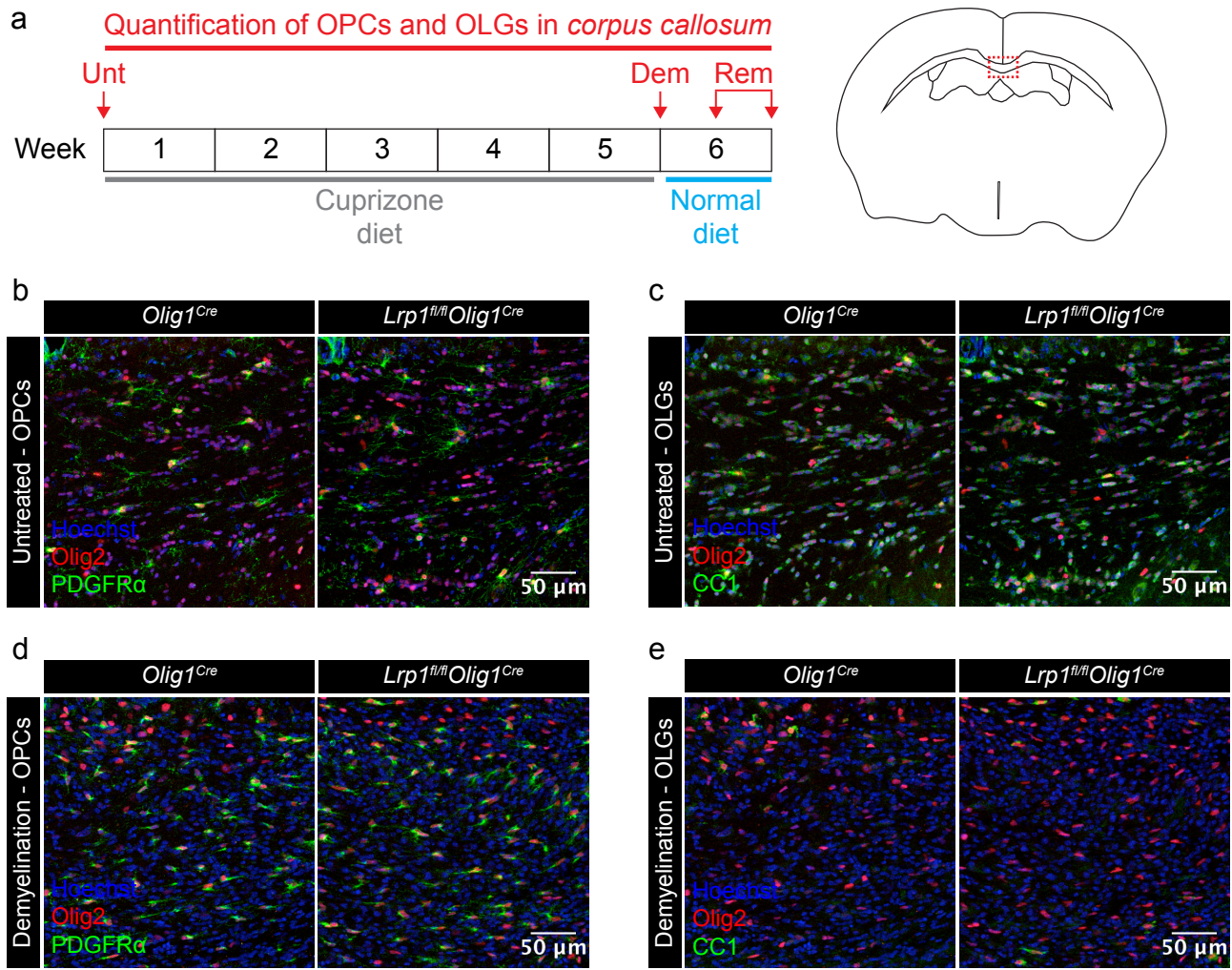


Fig. S3 OPCs and oligodendrocytes in the naïve and demyelinating corpus callosum (a) Schematic illustrating the cuprizone diet timeline and the timepoints at which the corpus callosum was imaged in *Olig1^{Cre}* and *Lrp1^{fl/fl}Olig1^{Cre}* mice. (b) Representative images of OPCs and (c) mature oligodendrocytes in the untreated corpus callosum. (d) Representative images of OPCs and (e) mature oligodendrocytes in the demyelinating corpus callosum.

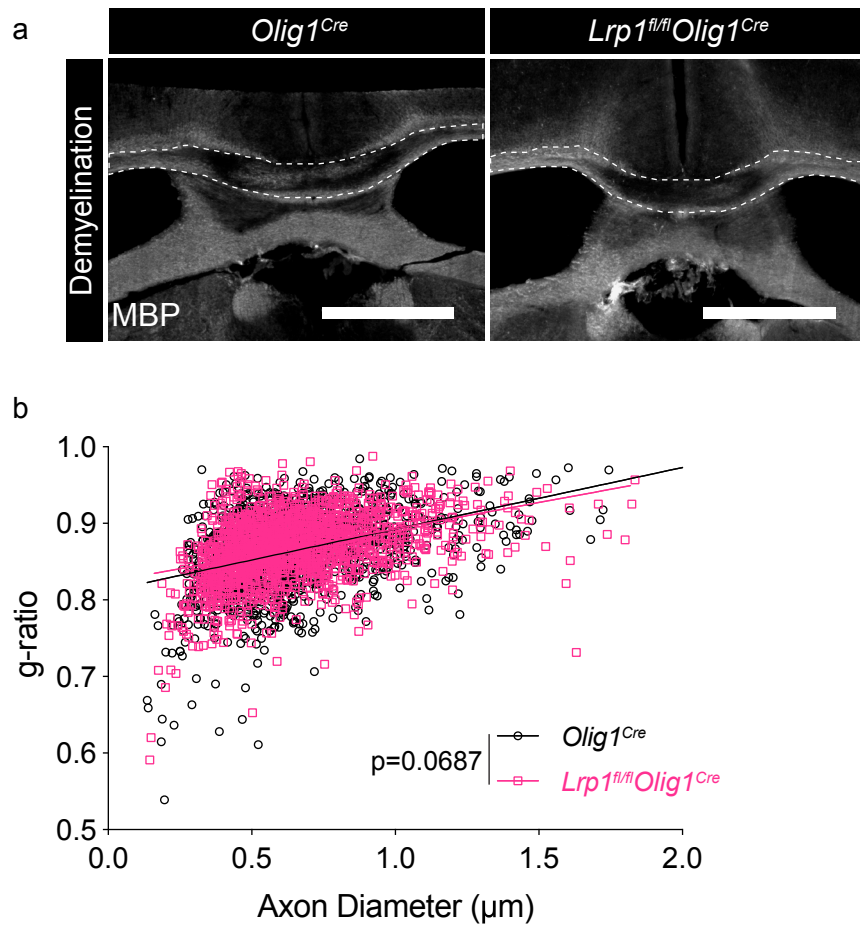


Fig. S4 MBP staining during demyelination and G-ratio analysis in the remyelinating *corpus callosum* (a) MBP immunofluorescence staining at 4 weeks of cuprizone treatment in the *corpus callosum* of *Olig1^{Cre}* and *Lrp1^{fl/fl}Olig1^{Cre}* mice. Scale bars 1000 μm . (b) Calculated g-ratios from axons in the remyelinating (0.5 Wk Rem) *corpus callosum* of *Olig1^{Cre}* and *Lrp1^{fl/fl}Olig1^{Cre}* mice (linear regression analysis with slopes comparison).

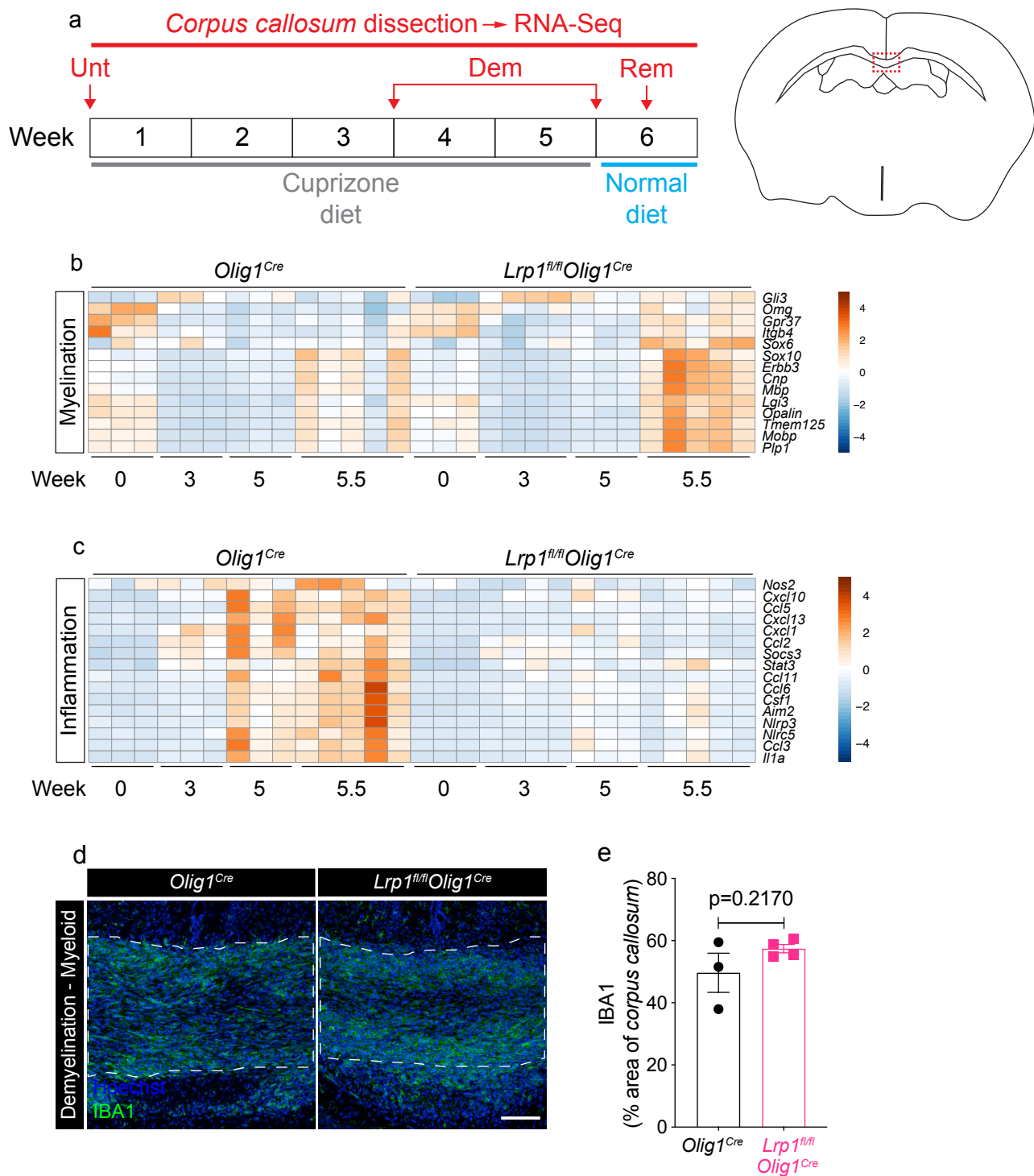


Fig. S5 RNA-seq analysis of the *corpus callosum* over the course of cuprizone treatment (a) Schematic illustrating the cuprizone diet timeline and timepoints at which the *corpus callosum* was dissected and analyzed by RNA-seq. **(b)** Heat map of myelination- and **(c)** inflammation-related genes in *Olig1^{Cre}* and *Lrp1^{fl/fl}Olig1^{Cre}* mice. Heat maps have a normalized count scale with z-score normalization. **(d)** Staining and **(e)** quantification of IBA1 in the *corpus callosum* of *Olig1^{Cre}* and *Lrp1^{fl/fl}Olig1^{Cre}* mice after 5 weeks of cuprizone treatment (unpaired t-test; n=3-4 mice per genotype; error bars represent +/- SEM). Scale bar 50µm.

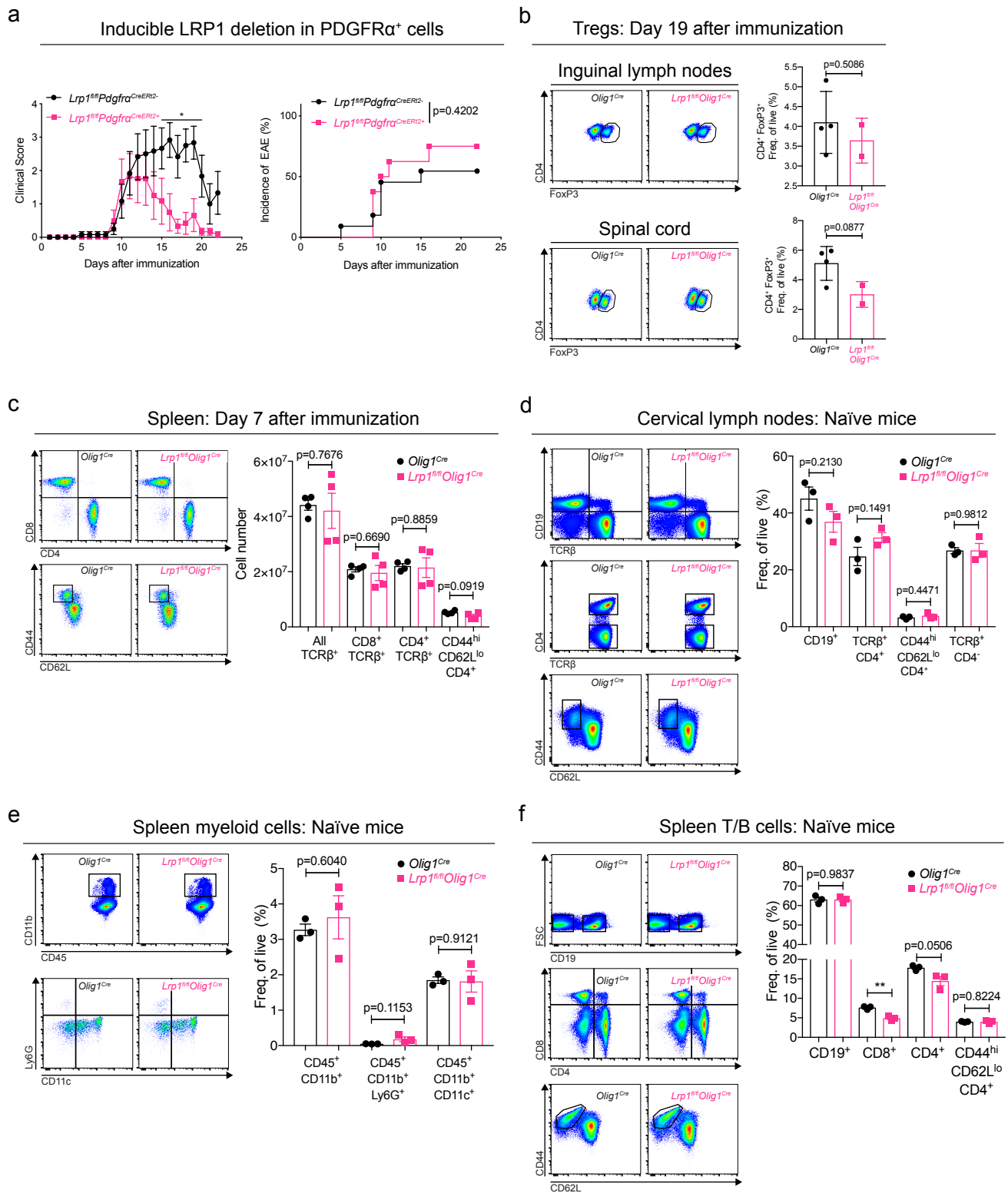


Fig. S6 Inflammatory phenotype in LRP1-deficient mice is not mediated by peripheral immune defects (a) EAE clinical scores and incidence from *Lrp1^{fl/fl}Pdgrfa^{CreERT2}* mice (EAE scores: Mann-Whitney U test, * $p < 0.05$; $n = 6$ mice with disease per genotype; incidence: Log-rank test; $n = 8-11$ total mice per genotype). (b) Flow cytometric analysis of Tregs (TCR β^+ CD4⁺ FoxP3⁺) in the draining lymph nodes (inguinal) and spinal cord during EAE in *Olig1^{Cre}* and *Lrp1^{fl/fl}Olig1^{Cre}* mice (unpaired t-test; $n = 2-4$ mice per genotype). (c) Representative flow plots and quantification of T cell subsets in the spleen 7 days after EAE immunization. (d) T and B cell populations in the cervical lymph nodes of naïve mice. (e) Myeloid cells and (f) T and B cell populations in the spleen of naïve mice (FSC: forward scatter height). Error bars represent \pm SEM.

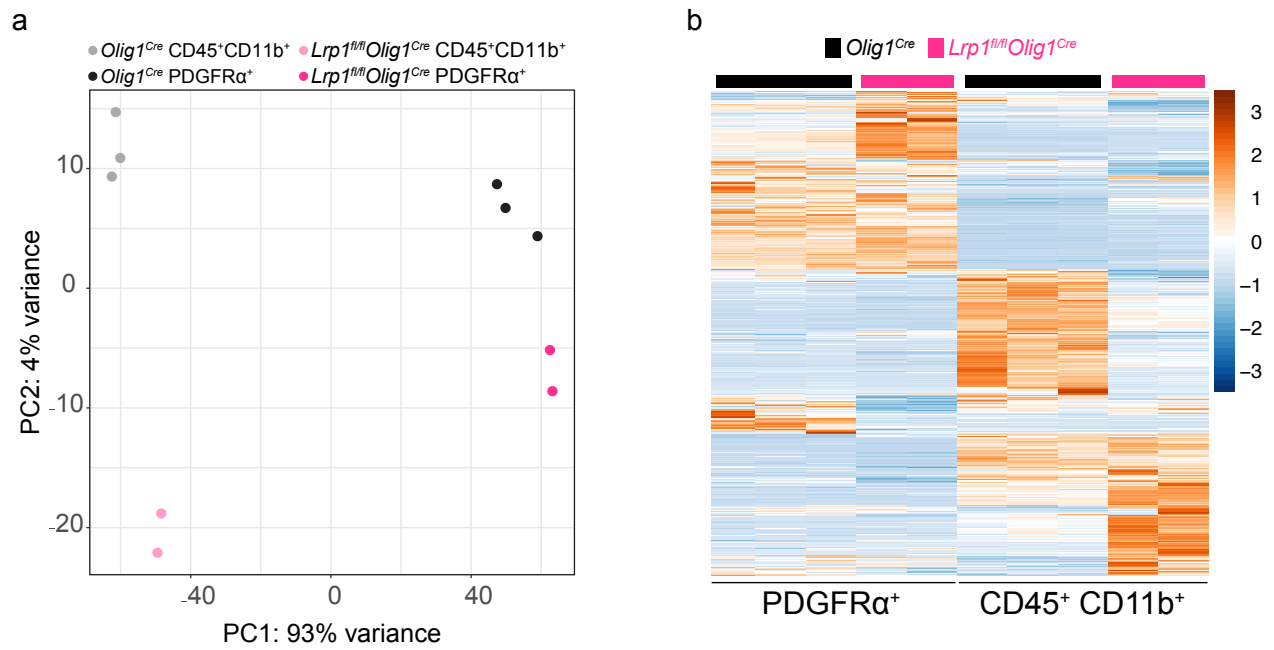


Fig. S7 Transcriptional profiling of the EAE spinal cord (a) Principal component analysis (PCA) plot and (b) heat map of the transcriptomes of sorted cells from EAE spinal cords of *Olig1^{Cre}* and *Lrp1^{fl/fl}Olig1^{Cre}* mice. Heat maps have a normalized count scale with z-score normalization.

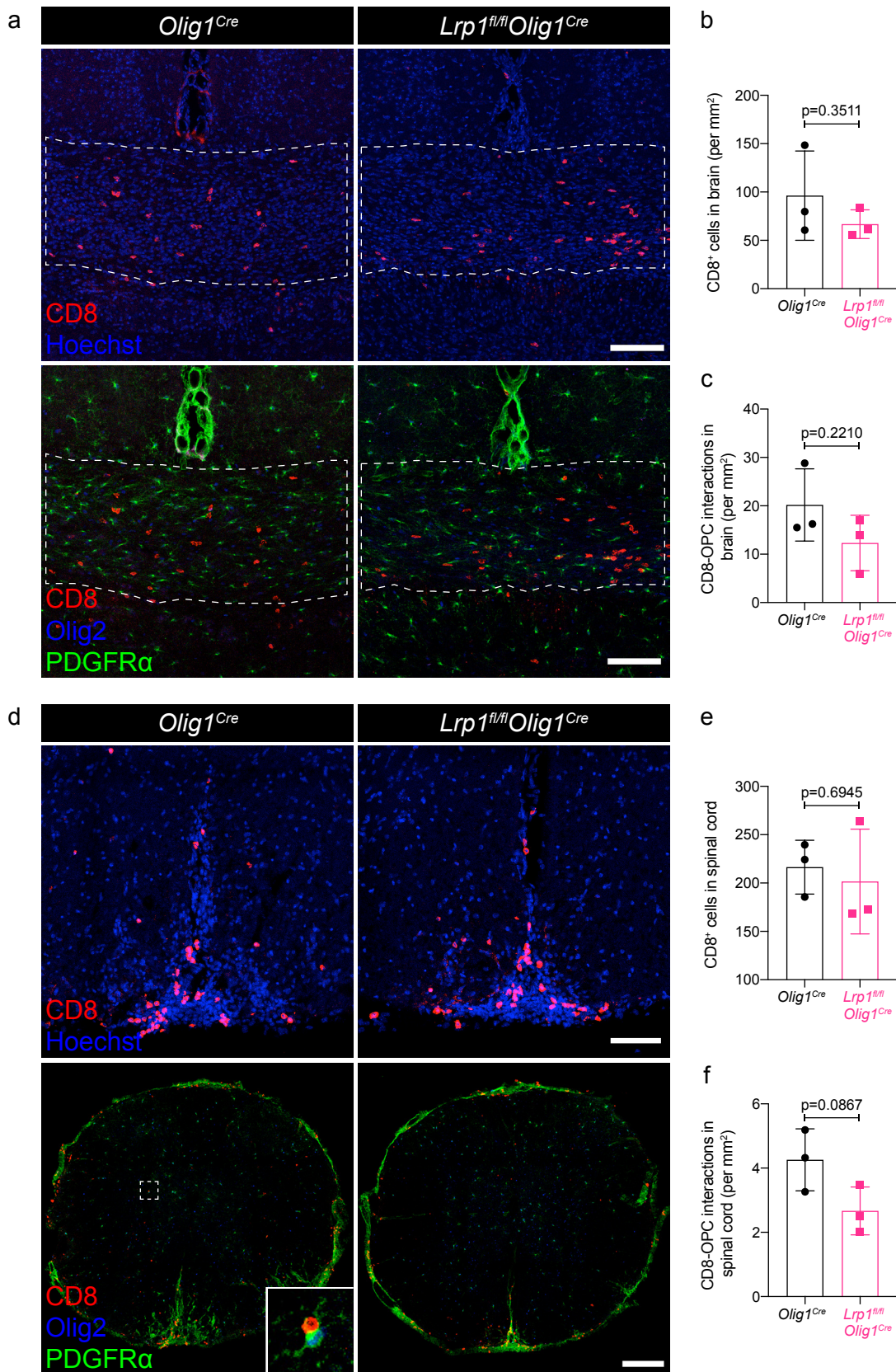


Fig. S8 CD8 cells in the cuprizone brain and EAE spinal cord. (a) Staining for CD8 (top panels), Olig2 and PDGFR α (lower panels) in the remyelinating brain (1 Wk Rem) of *Olig1^{Cre}* and *Lrp1^{fl/fl}Olig1^{Cre}* mice (dashed line outlines the *corpus callosum*). Scale bars 100 μ m. (b) Quantification of CD8 cells and (c) CD8-OPC interactions in remyelinating brains (unpaired t-test; n=3 mice per genotype). (d) Staining for CD8 (top panels), Olig2 and PDGFR α (lower panels) in EAE spinal cords (genotypes have similar disease scores; scale bars 75 μ m and 200 μ m, respectively.). (e) Quantification of CD8 cells and (f) CD8-OPC interactions in chronic EAE spinal cords (unpaired t-test; n=3 mice per genotype). Error bars represent +/- SEM.

Table S1 Ages of mice at experimental endpoints

Figure Panel	Age (weeks)
Fig. 1a,b	8
Fig. 1d	16
Fig. 1e	16
Fig. 2a	35-42
Fig. 2b-d	22
Fig. 2e,f	8
Fig. 3b-e cohort 1	35-42
Fig. 3b-e cohort 2	34
Fig. 3b-e cohort 3	22-25
Fig. 3f-h cohort 1	34
Fig. 3f-h cohort 2	22-25
Fig. 4a,b cohort 1	34
Fig. 4a,b cohort 2	22-25
Fig. 4c,d	17
Fig. 5b-g	16-25
Fig. 6a,b cohort 1	17-22
Fig. 6a,b cohort 2	12-16
Fig. 6c-i	17-24
Fig. 6j,k	26
Fig. 7a-f cohort 1	17-24
Fig. 7a-f cohort 2	27
Fig. 7g-j	14-17

Table S2 Differentially expressed genes in the corpus callosum of *Olig1^{Cre}* and *Lrp1^{fl/fl} Olig1^{Cre}* mice at week 0

ENSEMBL	baseMean	log2FoldChange	lfcSE	stat	pvalue	padj	SYMBOL	Up/Down in <i>Lrp1^{fl/fl} Olig1^{Cre}</i>
ENSMUSG00000068396	421.2400213	9.530674878	1.736238796	5.489265013	4.04E-08	8.46E-05	Rpl34-ps1	Up
ENSMUSG00000028736	37.47535702	9.02157036	2.270849669	3.972773047	7.10E-05	0.027931427	Pax7	Up
ENSMUSG00000001504	48.48650706	7.970635908	1.863623722	4.276955596	1.89E-05	0.01291707	Irx2	Up
ENSMUSG00000053747	12.55659766	7.471338108	1.751783964	4.264988298	2.00E-05	0.013003975	Sox14	Up
ENSMUSG00000097623	11.18597684	6.551515034	1.516299073	4.320727455	1.56E-05	0.011283259	B230323A14Rik	Up
ENSMUSG00000034384	10.36146052	6.517949801	1.425595754	4.572088393	4.83E-06	0.004470185	Barhl2	Up
ENSMUSG00000015619	35.09825765	6.456802394	1.194455419	5.405645359	6.46E-08	0.000121815	Gata3	Up
ENSMUSG00000034917	20.06535515	6.210961029	1.588280445	3.910493925	9.21E-05	0.033413795	Tjp3	Up
ENSMUSG00000026805	19.56004358	6.043340257	1.597548017	3.782884892	0.000155021	0.046417751	Barhl1	Up
ENSMUSG00000039217	39.14688581	6.012681851	1.386571577	4.336366007	1.45E-05	0.01093038	Il18	Up
ENSMUSG00000059246	18.50645027	5.967154128	1.501081423	3.975236811	7.03E-05	0.027931427	Foxb1	Up
ENSMUSG00000048349	100.4290744	5.619795882	1.467248871	3.8301586	0.000128061	0.040863014	Pou4f1	Up
ENSMUSG00000027833	68.25695807	5.582516376	1.283151106	4.350630529	1.36E-05	0.01093038	Shox2	Up
ENSMUSG00000028280	5.940707506	5.171579938	1.351310943	3.827083593	0.00012967	0.040863014	Gabrr1	Up
ENSMUSG00000000263	17.49708288	4.149583683	1.031500597	4.022861154	5.75E-05	0.026452626	Gira1	Up
ENSMUSG00000018486	8.831628702	4.131912452	1.100040539	3.756145621	0.00017255	0.04993454	Wnt9b	Up
ENSMUSG00000031734	23.81825338	3.924533766	1.014238242	3.869439746	0.000109086	0.037414424	Irx3	Up
ENSMUSG00000073555	40.180958	3.639119902	0.932770798	3.901408482	9.56E-05	0.034038706	Gm4951	Up
ENSMUSG00000010476	94.56881644	3.173719797	0.827496831	3.835325622	0.000125398	0.040863014	Ebf3	Up
ENSMUSG00000011658	86.48116341	3.074140031	0.773822705	3.97266714	7.11E-05	0.027931427	Fuz	Up
ENSMUSG00000015652	69.46564362	3.020226594	0.696081089	4.338900515	1.43E-05	0.01093038	Steap1	Up
ENSMUSG00000028717	155.9155353	2.845562154	0.590197912	4.821369401	1.43E-06	0.001582091	Tal1	Up
ENSMUSG00000020264	12.72961554	2.730695834	0.721681133	3.783798286	0.000154453	0.046417751	Slc36a2	Up
ENSMUSG00000031111	220.6344737	2.251598642	0.493146305	4.565782244	4.98E-06	0.004470185	Igfbp1	Up
ENSMUSG00000030111	3015.893843	2.171765339	0.421805924	5.148731247	2.62E-07	0.000412264	A2m	Up
ENSMUSG00000058174	44.60359428	1.406446466	0.302718681	4.646051109	3.38E-06	0.003359273	Gm5148	Up
ENSMUSG00000026042	147.9687002	1.371897225	0.322869909	4.249071186	2.15E-05	0.013497739	Col5a2	Up
ENSMUSG00000047181	694.7309031	1.136422284	0.230525264	4.929708199	8.24E-07	0.000970936	Samd14	Up
ENSMUSG00000041741	148.6116826	1.126290706	0.222945187	5.051872701	4.37E-07	0.000589499	Pde3a	Up
ENSMUSG00000001665	114.8214899	0.906853974	0.222096184	4.083158733	4.44E-05	0.02290317	Gstt3	Up
ENSMUSG00000021338	595.167337	0.770960846	0.185698329	4.151684349	3.30E-05	0.018311244	Carmil1	Up
ENSMUSG00000070003	1051.250896	0.743426912	0.197887787	3.756810479	0.000172093	0.04993454	Ssbp4	Up
ENSMUSG00000021010	415.3598054	0.626778105	0.156023944	4.017191767	5.89E-05	0.026452626	Npas3	Up
ENSMUSG00000022842	521.3676328	0.611221364	0.159903453	3.82244005	0.000132138	0.040863014	Ece2	Up
ENSMUSG00000025911	353.7523585	0.590167477	0.153232652	3.85144725	0.000117422	0.03955438	Adhfe1	Up
ENSMUSG00000028648	902.5765363	0.567960494	0.144037475	3.943143911	8.04E-05	0.030340995	Ndufs5	Up
ENSMUSG00000020022	970.6741304	0.547566286	0.102303218	5.352385755	8.68E-08	0.000148858	Ndufa12	Up
ENSMUSG00000032393	3009.22146	-0.284923446	0.066659502	-4.274311078	1.92E-05	0.01291707	Dpp8	Down
ENSMUSG00000040472	645.1176357	-0.321813847	0.080849648	-3.980398851	6.88E-05	0.027931427	Rabggta	Down
ENSMUSG00000020458	10287.49286	-0.33538891	0.089364748	-3.753033698	0.000174707	0.04993454	Rtn4	Down
ENSMUSG00000026678	1109.633241	-0.44228736	0.111271328	-3.974854683	7.04E-05	0.027931427	Rgs5	Down
ENSMUSG00000055447	2634.556336	-0.616731154	0.111794282	-5.516660969	3.46E-08	8.15E-05	Cd47	Down
ENSMUSG00000029822	534.8044443	-0.620285526	0.150414901	-4.123830303	3.73E-05	0.02008334	Osbpl3	Down
ENSMUSG00000030067	926.4256622	-0.655569697	0.171346553	-3.825987079	0.000130249	0.040863014	Foxp1	Down
ENSMUSG00000021113	368.5847104	-0.920066736	0.184733944	-4.980496351	6.34E-07	0.000797588	Snape1	Down
ENSMUSG00000049044	10111.08226	-0.967815674	0.244361416	-3.960591196	7.48E-05	0.028782781	Rapgef4	Down
ENSMUSG00000054000	58.70720416	-0.979590916	0.242800644	-4.034548255	5.47E-05	0.026452626	Tusc1	Down
ENSMUSG00000078894	209.0884403	-1.461538794	0.377514264	-3.871479656	0.000108177	0.037414424	2210418O10Rik	Down
ENSMUSG00000090622	33.70827551	-1.526679645	0.363176917	-4.203680287	2.63E-05	0.015011731	A930033H14Rik	Down
ENSMUSG00000041460	76.99514516	-1.594431686	0.364521437	-4.374040936	1.22E-05	0.010458158	Cacna2d4	Down
ENSMUSG00000026315	107.0030684	-1.77682184	0.447069186	-3.974377786	7.06E-05	0.027931427	Serp1nb8	Down
ENSMUSG00000097325	20.50082525	-1.796406958	0.426051588	-4.216407141	2.48E-05	0.014632889	Gm16897	Down
ENSMUSG00000085956	15.3493593	-1.931422114	0.455358589	-4.241540973	2.22E-05	0.013508471	NA	Down
ENSMUSG00000039985	76.53830595	-2.070667921	0.508970515	-4.068345535	4.73E-05	0.02350461	Sinhcaf	Down
ENSMUSG00000098702	144.6240394	-3.636872761	0.233142296	-15.59936922	7.35E-55	6.93E-51	1500015A07Rik	Down
ENSMUSG00000054618	5.131686195	-3.785431095	0.962105531	-3.934527942	8.34E-05	0.03083353	NA	Down
ENSMUSG00000044211	65.18925315	-4.138946576	0.868951404	-4.763150798	1.91E-06	0.001997418	NA	Down
ENSMUSG00000067017	284.8246694	-4.492358243	0.477648304	-9.405159004	5.20E-21	2.45E-17	NA	Down
ENSMUSG00000082536	450.8296124	-4.618081693	0.349168388	-13.22594441	6.22E-40	3.91E-36	NA	Down
ENSMUSG00000047347	15.4528267	-5.585769586	1.010443997	-5.528034808	3.24E-08	8.15E-05	Tdg-ps	Down
ENSMUSG00000085666	43.7829745	-6.073844302	0.674836738	-9.00046479	2.25E-19	8.48E-16	NA	Down
ENSMUSG00000080893	185.4966096	-6.240963838	0.362462183	-17.2182482	1.94E-66	3.66E-62	NA	Down
ENSMUSG00000049580	32.68772593	-7.006851592	1.37688116	-5.088929818	3.60E-07	0.000522518	Tsku	Down
ENSMUSG00000081824	131.712625	-7.192723894	1.290232257	-5.574751254	2.48E-08	7.79E-05	NA	Down
ENSMUSG00000061062	35.23638137	-7.411780592	1.842261284	-4.023197282	5.74E-05	0.026452626	NA	Down
ENSMUSG00000057335	69.97080255	-15.99524949	3.919842067	-4.08058519	4.49E-05	0.02290317	Cep170	Down

Chapter 5: Unanswered questions and future directions

A. Overview

In the previous chapter I have attempted to demonstrate that OPCs are active players in the neuroinflammatory landscape, and that this novel role is mediated in part by the multifunctional receptor LRP1. Using two models of CNS demyelination, I have shown that mice lacking LRP1 in OPCs have a dampened inflammatory response, resulting in increased remyelination (cuprizone) and a better clinical outcome (EAE). Mechanistic studies suggest that OPCs modulate inflammation by participating in antigen cross-presentation, and that antigen internalization is partially regulated by the scavenger receptor LRP1. Despite the advancement in our understanding of novel OPC function that this work has provided, there are still numerous questions that remain to be addressed. Here, I will discuss the implications of this work on CNS pathogenesis, as well as propose future studies to address unanswered questions. Finally, I would like to propose how to utilize the RNA sequencing data sets generated in my thesis project to discover novel MS therapeutics.

B. Future directions

Relevance in human disease

My thesis work is only the third study to suggest OPCs participate in antigen cross-presentation in the demyelinating CNS (Falcao et al., 2018, Kirby et al., 2019, Fernandez-Castaneda et al., 2019). While I focused on the contribution of LRP1 to neuroinflammation during my graduate work, moving forward I would like to focus on better understanding

antigen cross-presentation by OPCs. Whether this process occurs in human disease remains to be determined. It is important to consider the limitations of existing studies and outline *in vivo* experiments to elucidate this process further. One important caveat to consider, is that the classic EAE model is characterized by pathogenic CD4 T cells (Stromnes and Goverman, 2006), which depend on antigen presentation via MHC2 for their activation and effector functions. In contrast, MS lesions are predominantly occupied by CD8 T cells (Machado-Santos et al., 2018), raising the possibility that antigen cross-presentation via MHC1 might play a larger role in human disease than in mouse models. Investigating whether OPCs cross-present antigen to CD8 T cells in humans seems like an incredible challenge, but one that must be addressed.

To begin with, I propose to perform immunostaining for CD8 and PDGFR α in MS tissue to quantify OPC-CD8 associations. The presence of these OPC-CD8 interactions would be great preliminary evidence to support the existence of cross-presentation in the human CNS. Another ideal experiment would be to analyze fresh postmortem MS tissue by flow cytometry to examine MHC1 expression in OPCs, and perhaps even sort this cell population to conduct cross-presentation assays *in vitro* using human CD8 T cells. Considering the limited availability of fresh MS tissue, further experiments using mouse models will be necessary.

Disrupting MHC1 function specifically in OPCs

The first genetic mouse model to perturb MHC1 function in a cell-type specific manner has been recently developed. This was achieved by flanking the *B2m* gene, a protein subunit of MHC1, with loxP sites in order to mediate its excisions by Cre

recombinase (Bern et al., 2019). Our laboratory has just obtained these mice, and they will be an invaluable tool to decipher the contribution of OPC antigen cross-presentation to neuroinflammation. These MHC1 loss-of-function experiments will be necessary to definitively claim OPCs participate in antigen presentation *in vivo*. I propose to generate a mouse where *B2m* deletion in the OPC population can be induced by the administration of tamoxifen (*Pdgfra*^{CreERT2}*B2m*^{fl/fl} mice). After tamoxifen has been administered, I will subject these mice to the EAE model of CNS demyelination. This will allow me to inhibit antigen cross-presentation via MHC1 in OPCs, and evaluate its true effect on disease pathogenesis.

Disease severity would be monitored in control (*Pdgfra*^{CreERT2}-*B2m*^{fl/fl}) and *Pdgfra*^{CreERT2+}*B2m*^{fl/fl} mice, and spinal cords would be collected at the onset (day 7-10) and peak of disease (day 16-19). Spinal cords will be processed for flow cytometry to analyze cell surface expression of MHC1 in OPCs, and to characterize immune cell infiltrates. I expect *Pdgfra*^{CreERT2+}*B2m*^{fl/fl} mice to have decreased EAE clinical scores and less immune cell infiltration in their spinal cords. In particular, I anticipate the levels of CD8 T cells in the spinal cord to be significantly decreased in *Pdgfra*^{CreERT2+}*B2m*^{fl/fl} mice. Analyzing the degree of demyelination in these spinal cords would also be informative, which can be done by immunostaining for the myelin markers MBP and PLP. Lower levels of demyelination in the spinal cord in *Pdgfra*^{CreERT2+}*B2m*^{fl/fl} mice would be consistent with a dampened inflammatory response in the CNS. The completion of these studies would provide convincing evidence supporting the inflammatory role of OPCs in the demyelinating CNS.

Additionally, *Pdgfra*^{CreERT2}*B2m*^{fl/fl} mice can also be used to assess the role of antigen cross-presentation on remyelination failure in MS. Work by Kirby *et al.* suggests that OPCs that participate in antigen cross-presentation become targets for cytotoxic CD8 T cells (Kirby *et al.*, 2019). Disrupting MHC1 function in OPCs during EAE-induced demyelination could potentially prevent OPC cytotoxicity and allow remyelination to occur. Remyelination in the EAE spinal cord is rarely reported, likely due to the strong inflammatory component of the model. Quantifying differences in OPC cell death in EAE spinal cords between control and *Pdgfra*^{CreERT2}*B2m*^{fl/fl} mice would address the issue of cytotoxicity. Performing TEM on EAE spinal cords from these mice to analyze the number of myelinated axons would be a powerful readout of remyelination in this model. Given that there are no approved therapies to promote myelin repair in MS, modulating OPC cross-presentation could be a viable target to promote remyelination.

Although I have focused on the contribution of OPCs to neuroinflammation in the context of MS, this process could also be active in other CNS diseases. For example, spinal cord injury is also characterized by oligodendrocyte death and white matter damage (Gadani *et al.*, 2015), and CD8 T cell infiltration has also been reported in this model (Wu *et al.*, 2017). It is possible that OPCs are also exacerbating neuroinflammation in spinal cord injury by activating CD8 lymphocytes. Performing spinal cord injury on *Pdgfra*^{CreERT2}*B2m*^{fl/fl} mice would also be an interesting proposition.

Antigen specificity

Characterizing the antigens that OPCs internalize and process for cross-presentation would be invaluable in our understanding of MS pathogenesis. Are these

antigens myelin-specific? If so, OPCs could be directly orchestrating the destruction of oligodendrocytes and their myelin sheath. In the previous chapter I presented evidence that LRP1 is involved in the internalization of antigen that is processed and presented to CD8 T cells (Fernandez-Castaneda et al., 2019). Additionally, our laboratory has previously characterized LRP1 ligands in myelin debris (**Appendix A**) (Fernandez-Castaneda et al., 2013). Notable LRP1 ligands include MBP, MAG, and MOG (Fernandez-Castaneda et al., 2013). It is possible that OPCs internalize myelin proteins via LRP1, and this cargo is eventually processed and presented to CD8 lymphocytes. Considering how many CNS ligands bind LRP1, the search for specific antigens will be challenging. It is also obvious that other phagocytic receptors in OPCs are involved in the internalization of antigenic cargo. Characterizing other phagocytic receptors in OPCs would be a great step forward in trying to understand antigen internalization and processing.

Discovering new MS therapeutics

While the experiments above might add to our understanding of OPC function during neuroinflammation, I believe our laboratory could leverage my existing data to discover novel MS therapeutics. During my thesis project, I was fortunate to perform RNA sequencing on the naïve and remyelinating CNS (**Chapter 4, Figure 5**). Fortunately, mice that lacked LRP1 in OPCs presented with an enhanced myelination phenotype when compared to controls. Thus, we have a unique transcriptional signature that represents myelin repair occurring in the CNS. We can now use bioinformatics to find existing therapeutics that might elicit similar transcriptional changes in the CNS.

The Connectivity Map (CMap, version 02) is a computational resource consisting of hundreds of gene-expression profiles from cells treated with bioactive compounds (Lamb et al., 2006). CMap allows you to upload your own transcriptional signatures, and their pattern-matching algorithm will generate a list of compounds that generated similar transcriptional changes in its dataset. Therefore, I uploaded the transcriptional signature of the remyelinating CNS found in LRP1 deficient animals, and CMap generated a list of bioactive molecules that have the potential to induce myelin repair. Ideally, bioactive molecules that are known to cross the blood-brain barrier will be selected and tested *in vivo* using the cuprizone and EAE models. It is important to note that a similar approach has been applied to discover drugs that promote axonal regeneration, which showed promise in models of optic nerve injury (Chandran et al., 2016). The ultimate goal would be to discover existing drugs that can be repurposed to promote CNS myelin repair and neuroprotection.

Identification of the Low Density Lipoprotein (LDL) Receptor-related Protein-1 Interactome in Central Nervous System Myelin Suggests a Role in the Clearance of Necrotic Cell Debris^{*S}

Received for publication, December 18, 2012; Published, JBC Papers in Press, December 21, 2012; DOI 10.1074/jbc.M112.384693

Anthony Fernandez-Castaneda[‡], Sanja Arandjelovic[§], Travis L. Stiles[¶], Ryan K. Schlobach[‡], Kerri A. Mowen[§], Steven L. Gonias[¶], and Alban Gaultier^{‡1}

From the [‡]Department of Neuroscience and Center for Brain Immunology and Glia, University of Virginia, Charlottesville, Virginia 22908, the [§]Department of Chemical Physiology, The Scripps Research Institute, La Jolla, California 92037, and the [¶]Department of Pathology, University of California at San Diego, La Jolla, California 92093

Background: LRP1 is a scavenger receptor involved in the clearance of apoptotic cells and myelin vesicles.

Results: Novel ligands for LRP1 were discovered in CNS myelin by affinity purification combined with proteomics.

Conclusion: Some ligands are intracellular proteins, suggesting a function for LRP1 in the clearance of necrotic debris.

Significance: LRP1 mediates the removal of cellular waste and could maintain homeostasis.

In the central nervous system (CNS), fast neuronal signals are facilitated by the oligodendrocyte-produced myelin sheath. Oligodendrocyte turnover or injury generates myelin debris that is usually promptly cleared by phagocytic cells. Failure to remove dying oligodendrocytes leads to accumulation of degraded myelin, which, if recognized by the immune system, may contribute to the development of autoimmunity in diseases such as multiple sclerosis. We recently identified low density lipoprotein receptor-related protein-1 (LRP1) as a novel phagocytic receptor for myelin debris. Here, we report characterization of the LRP1 interactome in CNS myelin. Fusion proteins were designed corresponding to the extracellular ligand-binding domains of LRP1. LRP1 partners were isolated by affinity purification and characterized by mass spectrometry. We report that LRP1 binds intracellular proteins via its extracellular domain and functions as a receptor for necrotic cells. Peptidyl arginine deiminase-2 and cyclic nucleotide phosphodiesterase are novel LRP1 ligands identified in our screen, which interact with full-length LRP1. Furthermore, the extracellular domain of LRP1 is a target of peptidyl arginine deiminase-2-mediated deimination *in vitro*. We propose that LRP1 functions as a receptor for endocytosis of intracellular components released during cellular damage and necrosis.

Multiple sclerosis (MS)² is an autoimmune disease in which CNS myelin is destroyed and the survival of myelin-producing

^{*} This work was supported by National Institutes of Health Grants R21 NS071347 (to A. G.), R01 HL-060551 (to S. L. G.), and R01 GM085117 and R01 AI067460 (to K. A. M.). This work was also supported by the Philip S. Magaram, Esq., Research Award from the Arthritis Foundation (to S. A.).

^S This article contains supplemental Table 1 and Fig. 1.

¹ To whom correspondence should be addressed: Dept. of Neuroscience, University of Virginia, 409 Lane Rd., Charlottesville, VA 22908. Tel.: 434-243-1903; Fax: 434-982-4380; E-mail: ag7h@virginia.edu.

² The abbreviations used are: MS, multiple sclerosis; LRP1, low density lipoprotein receptor related-1; CNP, cyclic nucleotide phosphodiesterase; CCR, cluster of complement repeats; PAD2, peptidyl arginine deiminase 2; ABTS, 2,2'-azino-bis(3-ethylbenzthiazoline-6-sulphonic acid); GLG1, golgi glyco-

oligodendrocytes is compromised (1). The etiology of MS is poorly understood, but, in some cases, oligodendrocyte apoptosis is detected without the involvement of immune cell infiltrates (2). Thus, the failure to clear apoptotic cells and cellular debris may initiate inflammation and the autoimmune response characteristic for MS (3).

Low density lipoprotein receptor-related protein-1 (LRP1) is a scavenger receptor with key roles in the phagocytosis of myelin debris (4) and apoptotic cells (5, 6). LRP1 is a member of the LDL receptor gene family, first recognized as a receptor for apolipoprotein E and the serum protease inhibitor α_2 -macroglobulin (7, 8). To date, >40 different ligands for LRP1 have been identified, including proteases, growth factors, heat shock proteins, extracellular matrix proteins, and foreign toxins (9). LRP1 is a two-chain receptor in which the ligand-binding α chain is entirely extracellular and non-covalently associated with the membrane-spanning β chain (9). Upon binding to LRP1 on the cell surface, LRP1 ligands are internalized, dissociate in acidified endosomes, and are delivered to lysosomes, whereas LRP1 is recycled to the cell surface (10). LRP1 also mediates endocytosis of cell surface receptors (11) and, in this manner, participates in the regulation of cell signaling events (12, 13).

In addition to its function as a phagocytic receptor for myelin, LRP1 also participates in myelin-mediated inhibition of axon formation (14). The goal of this study was to characterize the interactome of LRP1 in myelin. We designed fusion proteins corresponding to the second and fourth clusters of complement-like repeats (CCR2 and CCR4), two major extracellular ligand-binding domains in LRP1 (15). CCR2 or CCR4 fusion proteins were incubated with myelin protein extracts in the presence or absence of RAP, an LRP1 ligand binding inhib-

protein 1; MBP, myelin basic protein; PLP1, proteolipid protein 1; CNP, 2',3'-cyclic nucleotide 3' phosphodiesterase; CFSE, carboxyfluorescein diacetate succinimidyl ester; RAP, receptor associated protein.

itor (16), and associated partners were identified by tandem mass spectrometry.

Using this approach, we have identified >70 LRP1 ligands in CNS myelin. Validation studies were performed for two myelin-specific LRP1 ligands: cyclic nucleotide phosphodiesterase (CNP, also called CNPase) and peptidyl arginine deiminase-2 (PAD2). CNP is an enzyme highly expressed in oligodendrocytes, with functions in tubulin polymerization and oligodendrocyte process outgrowth (17). CNP is an abundant component of myelin, accounting for up to 4% of the total protein content (18). Although myelination is normal in CNP knock-out mice, they succumb to axonal loss and neurodegeneration due to impaired communication between cells (19). Furthermore, CNP is a potential auto-antigen in MS, as CNP-reactive T cells can be found in MS patients with active disease (20, 21). Another potential auto-antigen in MS is the myelin basic protein (MBP), which we previously identified as a ligand for LRP1 (4). MBP is a substrate for our second chosen target for validation, enzyme peptidyl arginine deiminase 2, or PAD2 (22). PAD2 catalyzes the conversion of protein arginine residues into citrulline, in a reaction called deimination or citrullination (23). Similar to CNP, PAD2 is a component of the myelin sheath and is the only member of the PAD family expressed in the healthy CNS (23, 24). MS patients contain higher levels of MBP citrullination, which is thought to contribute to MBP degradation and loss of myelin sheath integrity (25–28). Similarly, MBP citrullination and PAD2 activity correlate with disease in animal models of MS (29, 30). Our studies demonstrate that both CNP and PAD2 interact with LRP1 CCRs as well as with the full-length LRP1. Finally, we show that LRP1 can be citrullinated by endogenous PAD2 *in vitro* and that citrullination decreases the endocytic function of LRP1.

Interestingly, many of the newly identified LRP1 ligands were intracellular proteins, indicating a novel role for LRP1 in the clearance of cellular debris, potentially released during necrosis. We further demonstrate for the first time that LRP1 regulates the removal of necrotic cells and cellular debris using model T cells and oligodendrocytes. Necrotic waste is harmful to surrounding cells and is generated during catastrophic events such as trauma and hypoxia or when the apoptotic cell clearance system is saturated (31). Furthermore, necrotic debris has been shown to initiate a proinflammatory response by macrophages (32). During MS, improper clearance of apoptotic cells and necrotic debris would thus generate an inflammatory environment, which would further fuel disease severity. Taken together, the data presented here suggest that, by mediating cellular and myelin-associated debris removal after cell damage, LRP1 may inhibit the immune response generated by excessive cellular debris at sites of inflammation.

EXPERIMENTAL PROCEDURES

Reagents and Cell Culture—Glutathione *S*-transferase (GST), GST-RAP, human shed LRP1, and rat LRP1 were purified as described previously (33). The following antibodies were used: 8G1 anti-LRP1 (sc-57353, Santa Cruz Biotechnology), anti-LRP1 C-terminal (L2170, Sigma), anti-LRP1 N-terminal (L2420, Sigma), anti-CNP (5664, Cell Signaling Technologies), CD11b-Alexa Fluor 488 (53-0112, eBioscience), and anti-

GRP78 (610978, BD Biosciences). Anti-PAD2 serum was obtained by immunizing PAD2^{-/-} mice with GST-PAD2. Anti-citrulline (modified) detection kit was used to detect protein citrullination (17-347, Millipore). BV2, LRP1-positive (PEA10), and LRP1-deficient (MEF2) fibroblasts were obtained from ATCC and cultured in DMEM high glucose, supplemented with 2 mM L-glutamine, 10% FBS, and 1% penicillin/streptomycin. The RAW 264.7 murine macrophage cell line and Jurkat lymphocyte cell line were obtained from ATCC and cultured in RPMI 1640, supplemented with 2 mM L-glutamine, 10% FBS, and 1% penicillin/streptomycin. The N20.1 oligodendrocyte cell line was cultured in DMEM high glucose/F12 at 34 °C, supplemented with 10% FBS, sodium bicarbonate, 100 μg/ml G418, 20 μg/ml gentamycin, and 1% penicillin/streptomycin. For differentiation into oligodendrocytes, cells were switched to DMEM high glucose/F12, supplemented with 1% FBS, 100 μg/ml G418, and 1% penicillin/streptomycin, and cultures were maintained at 39 °C for 3 to 5 days as described (34).

Cloning, Expression, and Purification of CCRII and CCRIV—CCRII and CCRIV from human LRP1 were cloned into pFuserFC2 (Invivogen, San Diego, CA) as described in the literature (15) to generate Fc-fusion proteins. CCRII includes EGF repeat 4 and complement repeats 3 to 10 (LRP1 amino acids 806 to 1184). CCRIV spans complement repeats 21 to 31 (LRP1 amino acids 3332 to 3778). CCRII and CCRIV were expressed in CHO-K1 cells and purified from the culture supernatants on protein A-agarose resin (GE Healthcare).

CCR Pulldowns and Proteomics—Myelin vesicles were purified from mouse brains as described previously (35). Myelin-associated proteins were solubilized in radioimmune precipitation assay buffer, containing 100 mM Tris, pH 7.5, 150 mM NaCl, 1% Triton X-100, 0.5% deoxycholate, and 0.1% SDS, supplemented with 1 mM CaCl₂ and complete protease inhibitor mixture (Roche Applied Science). Protein extracts (2 mg) were incubated with 1 pm of CCRII, CCRIV, or Fc with or without 20 pm of GST-RAP for 16 h at 4 °C. CCRII, CCRIV, and Fc were recovered by adding protein A-agarose beads for 1 h at 20 °C. After extensive washing with radioimmune precipitation assay buffer, proteins were either digested with trypsin or eluted with SDS sample buffer for SDS-PAGE and immunoblot analysis. Trypsin digestion was performed in the presence of Protease-MAX surfactant as described by the manufacturer (Promega, Madison, WI). Proteins associated with CCRII, CCRIV, and Fc were identified by LC-MS/MS as described previously (36).

Cloning, Expression, and Purification of PAD2-His, GFP-RAP, and GST-CNP—Murine PAD2 open reading frame (ORF) was cloned into pET-30a(+) vector (Novagen). Human RAP ORF was cloned downstream of GFP into pET-30a(+). pET-30A(+) allows bacterial expression and contains a histidine tag for affinity purification. Murine CNP ORF was cloned into pGEX-2T (GE Healthcare) to allow bacterial expression and GST tag-mediated purification. PAD2-His and GST-CNP were purified by affinity chromatography using the Profinia purification kit and chromatography system (Bio-Rad).

Immobilization Binding Studies—Purified BSA, rat LRP1, or fibronectin (25 nM) (Sigma) were diluted in PBS and absorbed on ELISA plates for 12 h at 4 °C. Wells were blocked for 1 h with

LRP1 Ligands in CNS Myelin

PBS containing 1% BSA. PAD2-His (25 nM) was added to the wells for 1 h at 20 °C. The wells were washed, and retained PAD2-His was detected using anti-PAD2 serum, in an ELISA format using ABTS as a colorimetric substrate. Alternatively, purified BSA, GST, GST-CNP, or GST-RAP (350 nM) were diluted in PBS and absorbed on ELISA plates for 12 h at 4 °C. Wells were blocked for 1 h with PBS containing 1% BSA. Human shed LRP1 (50 nM) was added to the wells for 1 h at 20 °C. The wells were washed with PBS, and retained LRP1 was detected with antibody 8G1, in an ELISA format using ABTS as a colorimetric substrate.

Citrullination Assay—RAW 264.7 cell extract and brain protein extract were prepared in ice-cold extraction buffer (50 mM HEPES, 150 mM NaCl, 1% Triton X-100, 10% glycerol) containing complete protease inhibitor mixture without EDTA (Roche Applied Science). Equal amounts of protein extracts were incubated with 10 μg of PAD2-His for 3 h at 37 °C in the presence or absence of 10 mM CaCl₂. LRP1 was recovered by adding 10 μg of GST-RAP and glutathione-agarose beads (33). Glutathione-agarose beads were washed with the extraction buffer. Proteins were eluted with SDS sample buffer for SDS-PAGE and immunoblot analysis. For cell surface citrullination, LRP1-expressing and -deficient fibroblasts were treated for 6 h at 37 °C with 150 nM recombinant PAD2 in DMEM containing 0.3% BSA. Cell surface proteins were labeled with biotin and purified as described (36).

GFP-RAP Endocytosis—LRP1-positive (PEA10) and LRP1-deficient (MEF2) fibroblasts were treated for 3 h at 37 °C with 150 nM recombinant PAD2 in DMEM containing 0.3% BSA. After washing, cells were treated with 500 nM of GFP-RAP for 3 h at 37 °C. After washing with PBS, cells were detached with trypsin and washed twice with PBS containing 5% FBS. Cells were analyzed by flow cytometry on a BD FACSCalibur (BD Biosciences). Data were plotted using the FlowJo software (Tree Star).

Phagocytosis of Necrotic Cells—LRP1-positive (PEA10) and LRP1-deficient (MEF2) fibroblasts were labeled with CFSE according to the manufacturer's instructions (Invitrogen). To prepare necrotic cells, Jurkat or N20.1 cells were heat shocked at 55 °C for 20 min and then incubated for 4 h at 37 °C. Necrosis was confirmed by microscopy using trypan blue exclusion, or by flow cytometry using annexin V-FITC and 7-amino-actinomycin D staining, according to manufacturers instructions (eBioscience). Necrotic and live cells were labeled with Cypher5 (10 μM, GE Healthcare) for 20 min at 37 °C in DMEM, and excessive dye was quenched by resuspending the cells in DMEM containing 10% FBS. Necrotic and live cells were then added to the CFSE-labeled fibroblasts in DMEM containing 10% FBS for 2 h at 37 °C (10 to 1). After washing with PBS, cells were detached with trypsin and washed twice with PBS containing 5% FBS. In experiments with BV2 cells, necrotic and live cells were added for 30 min at 37 °C (4:1). BV2 cells were distinguished from N20.1 by staining with CD11b-Alexa Fluor 488 antibody. Cells were analyzed by flow cytometry on a BD FACSCalibur (BD Biosciences). Data were plotted using the FlowJo software (Tree Star).

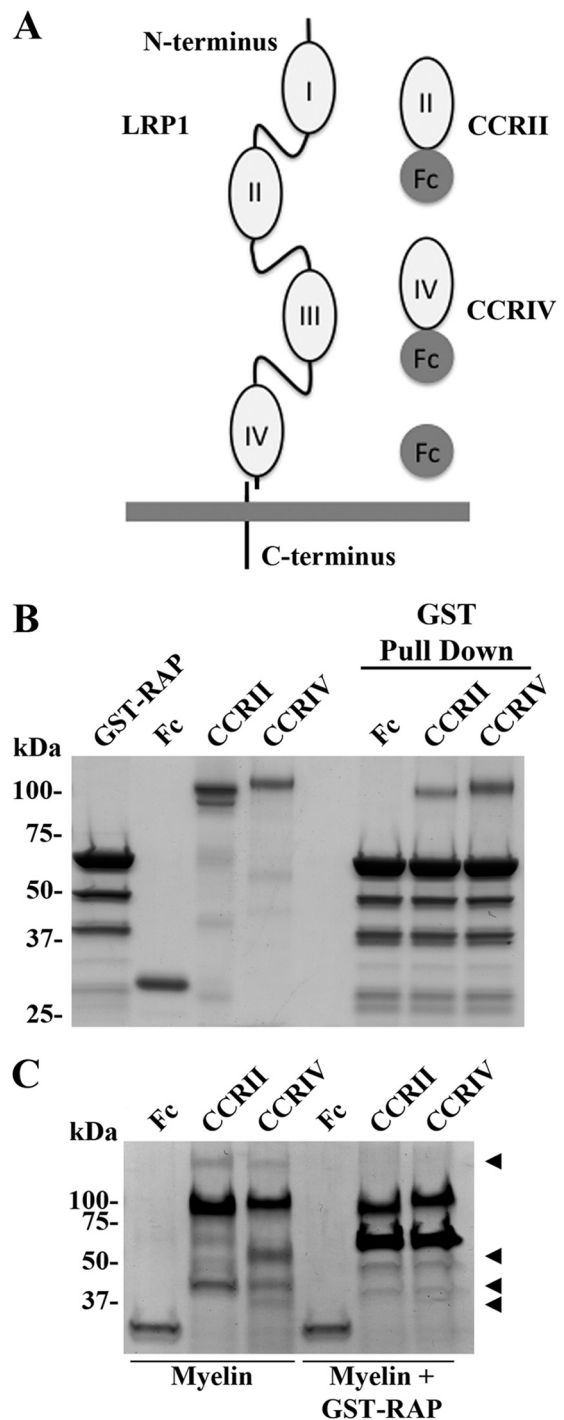


FIGURE 1. CCRII and CCRIV bind LRP1 ligands. *A*, schematic representation of LRP1 and CCRII and CCRIV constructs. *B*, Fc, CCRII, and CCRIV were incubated with GST-RAP as described under "Experimental Procedures," and GST-RAP was recovered by incubation with glutathione-agarose beads. Samples and purified proteins were analyzed by Coomassie staining. *C*, Fc, CCRII, and CCRIV were incubated with myelin protein extract in the presence or absence of GST-RAP. Fc and CCRs were recovered by adding protein A-agarose beads. Samples were analyzed by Coomassie staining.

RESULTS

Preparation of CCRII and CCRIV—To identify LRP1 ligands present in CNS myelin, we prepared two fusion proteins corresponding to CCRII and CCRIV of human LRP1 (Fig. 1*A*). These two CCRs mediate the binding of LRP1 ligands, with the possi-

TABLE 1

Myelin proteins associating with CCRII and CCRIV

The gene products below were identified by tandem mass spectrometry as partners for LRP1 CCRs with (+) or without (–) RAP. Mean spectral counts and S.D. are shown ($n = 3$).

Gene name	Fc	CCRII	CCRIV	Fc	CCRII	CCRIV
RAP	–	–	–	+	+	+
<i>Cnp</i>	0 ± 0	83.7 ± 0.2	73.7 ± 0.3	7.6 ± 0.9	6.7 ± 1.1	11 ± 0.4
<i>Sept7</i>	0 ± 0	33.7 ± 7	34.2 ± 0.37	0 ± 0	0 ± 0	0.7 ± 1.3
<i>Mtap1b</i>	0 ± 0	20.7 ± 0.8	27.7 ± 0.7	0 ± 0	0 ± 0	0 ± 0
<i>Sept2</i>	0 ± 0	19 ± 0.4	17.5 ± 0.2	0 ± 0	0 ± 0	0 ± 0
<i>Sept8</i>	0 ± 0	18.2 ± 0.2	23.5 ± 0.3	0.3 ± 1.7	0 ± 0	0.2 ± 2
<i>Padi2</i>	0 ± 0	17.7 ± 0.3	0 ± 0	0 ± 0	0 ± 0	0 ± 0
<i>Mtap1a</i>	0 ± 0	17.2 ± 0.4	22.7 ± 0.5	0 ± 0	0 ± 0	0 ± 0
<i>Plcb1</i>	0 ± 0	16.7 ± 0.7	3.5 ± 1.8	0 ± 0	0 ± 0	0 ± 0
<i>Sept4</i>	0 ± 0	13 ± 0.5	14.7 ± 0.8	0 ± 0	0 ± 0	0 ± 0
<i>Glul</i>	0 ± 0	12.2 ± 0.2	19 ± 0.2	0 ± 0	6 ± 0.5	5.5 ± 0.2
<i>Pacsin1</i>	0 ± 0	11 ± 0.1	2 ± 0.5	0 ± 0	0 ± 0	0 ± 0
<i>Rock2</i>	0 ± 0	10.5 ± 0.8	11.5 ± 0.6	0 ± 0	0 ± 0	0 ± 0
<i>Anln</i>	0 ± 0	8.7 ± 0.6	4.5 ± 0.8	0 ± 0	0 ± 0	0 ± 0
<i>Mbp</i>	0 ± 0	8.5 ± 0.4	9.5 ± 0.6	1 ± 1.7	10 ± 0	8.7 ± 0.5
<i>Gnao1</i>	0 ± 0	8.2 ± 0.3	8.2 ± 0.3	0 ± 0	2 ± 0.5	1.25 ± 0.8
<i>Slk</i>	0 ± 0	7.7 ± 0.9	11.7 ± 0.6	0 ± 0	0 ± 0	0 ± 0
<i>Myo18a</i>	0 ± 0	7.5 ± 0.3	0 ± 0	0 ± 0	0 ± 0	0 ± 0
<i>Plp1</i>	1.7 ± 0.7	7 ± 0.2	6 ± 0.2	1 ± 0	5.7 ± 0.3	5 ± 0.3
<i>Ank2</i>	0 ± 0	6.75 ± 0.3	6.2 ± 0.1	0 ± 0	0 ± 0	0 ± 0
<i>Csrp1</i>	0 ± 0	6.5 ± 0.7	5.5 ± 0.6	0 ± 0	0 ± 0	0 ± 0

ble exception of α_2 -macroglobulin (9, 15). CCRII and CCRIV were expressed as soluble Fc-fusion proteins in CHO-K1 cells (Fig. 1A) and tested by examining binding of GST-RAP in a pulldown assay. RAP binds to LRP1 and blocks the binding of most known LRP1 ligands (9). Equivalent amounts of CCRII, CCRIV, or Fc (control) were incubated with GST-RAP, followed by incubation with glutathione-agarose beads. After washing, samples were separated by SDS-PAGE alongside the purified proteins, and the gel was stained with Coomassie Blue. CCRII and CCRIV, but not Fc alone, bound to GST-RAP (Fig. 1B).

Next, equivalent amounts of CCRII, CCRIV, or Fc were incubated with CNS myelin protein extracts in the presence or absence of excess GST-RAP. Fc fusion proteins were recovered by pull down with protein A-agarose beads. As shown in Fig. 1C, several protein bands are purified from myelin with CCRII and CCRIV, but not with Fc (arrowheads). Treatment with GST-RAP blocks the binding of these proteins to CCRs (Fig. 1C). These results demonstrate that the recombinant Fc-fusion proteins, CCRII and CCRIV, are functional in ligand binding and may be used to identify LRP1 ligands.

Identification of LRP1 Ligands in CNS Myelin by Tandem Mass Spectrometry—CCRII, CCRIV, or Fc were incubated with CNS myelin protein extracts. Associated proteins were recovered by protein A-agarose pulldown as described above. As a control, CCRII, CCRIV, and Fc were preincubated with a 20-fold molar excess of GST-RAP to inhibit ligand binding. Preparations were trypsin-digested, and the resulting peptides were identified by mass spectrometry using an LTQ-Orbitrap. As an additional control, fusion proteins also were analyzed without incubation with myelin extracts to identify ligands derived from CHO-K1 cells, which may co-purify with the CCRs. Using the described method, 72 proteins were identified as ligands for CCRII and CCRIV (supplemental Table 1). As expected, LRP1 peptides were present only when CCRs were analyzed and not Fc. LRP1 peptide abundance was not affected by the presence of myelin protein or by a large excess of GST-

RAP, indicating that these reagents did not influence CCR-binding to protein A-agarose. LRP1 partners identified in our screens were separated into two categories: myelin-specific LRP1 ligands (Table 1 and Fig. 2A) and CHO-K1 cell proteins co-purifying with CCRs (Table 2 and Fig. 2B). When CCRII and CCRIV were used to identify myelin-specific LRP1 ligands (Table 1 and Fig. 2A), we confirmed the binding of MBP and myelin-associated glycoprotein, two proteins that we have previously reported as ligands for LRP1 (4, 14). The myelin proteins, CNP and PLP, also were identified as ligands for LRP1 using our screen.

Surprisingly, myelin-specific CCR partners included many intracellular proteins. We identified members of the septin family (septins 2, 4, 7, and 8) and microtubule-associated proteins, Mtap1a and Mtap1b, as novel LRP1 ligands (Table 1 and Fig. 2A). As shown in Table 2 and in Fig. 2B, 10 proteins co-purified at significant levels with CCRII and CCRIV when the fusion proteins were expressed in CHO-K1 cells. This list includes known LRP1 ligands such as RAP, matrix metalloproteinase-9, and tissue inhibitor of metalloproteinase 2 (37, 38) together with previously unidentified LRP1 ligands, such as the proteases matrix metalloproteinase-19 and legumain, and the extracellular matrix proteins SPARC and collagen 5 (col5a2). As anticipated, following GST-RAP treatment, the spectral counts for RAP binding to CCRII and CCRIV increased from 10 to 71 and from 15.2 to 46.2, respectively. This result shows that exogenous RAP can efficiently bind to the CCRs.

In both categories of LRP1 ligands, comparable binding to CCRII and CCRIV was most frequently observed. However, we were also able to identify proteins that bind specifically to CCRII or CCRIV, but not both. Collagen 5 (Col5a2), PAD2 or Padi2, and MYO18 (Myo18a) bind only to CCRII, whereas legumain, tissue inhibitor of metalloproteinase 2, and FHL1 (four and a half LIM domains 1) bind only to CCRIV (Fig. 2B). Taken together, our results suggest that the binding sites for a variety of LRP1 ligands reside within a specific domain of LRP1, allow-

LRP1 Ligands in CNS Myelin

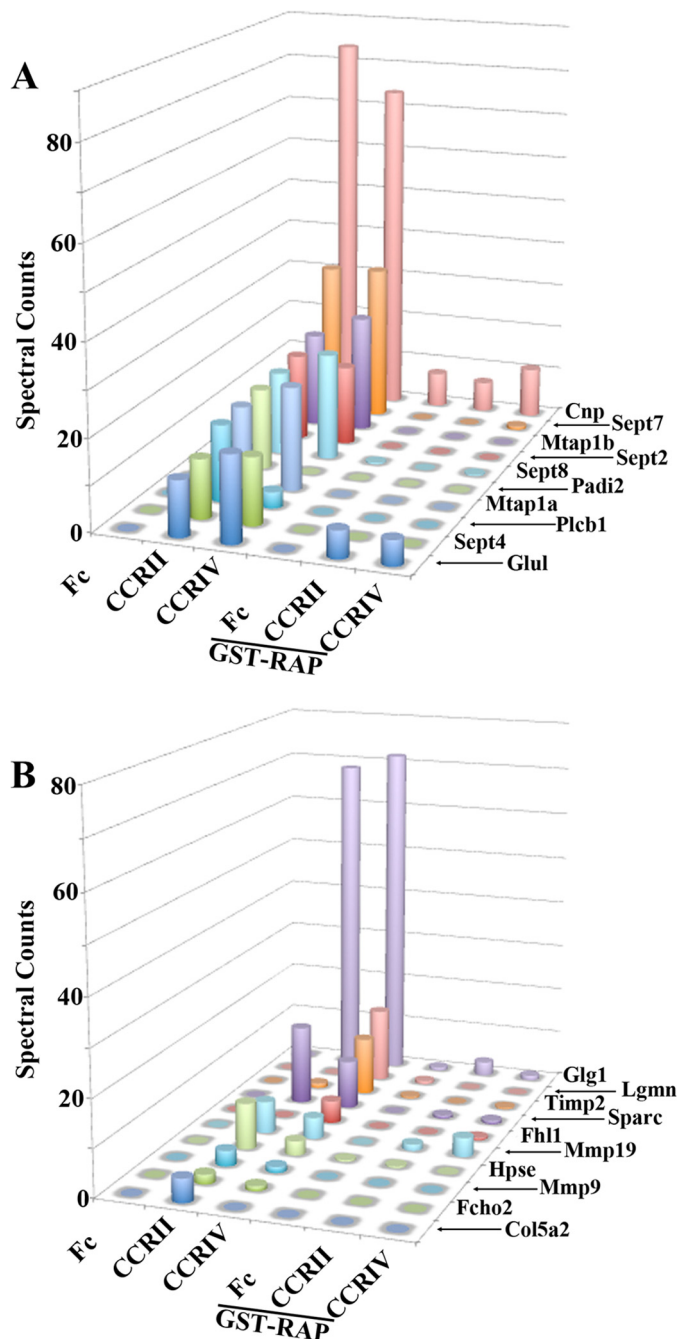


FIGURE 2. Identification of LRP1 CCR ligands. *A*, myelin proteins interacting with LRP1 CCRs were as follows: *Cnp*, CNP; *Sept7*, septin-7; *Mtap1b*, microtubule-associated protein-1b; *Sept2*, septin-2; *Sept8*, septin-8; *Padi2*, PAD2; *Mtap1a*, microtubule-associated protein-1a; *Plcb1*, phosphatidylinositol-bisphosphate phosphodiesterase β -1; *Sept4*, septin-4; *Glul*, glutamine synthetase. *B*, endogenous proteins associating with LRP1 CCR were as follows: *Glg1*, Golgi glycoprotein-1; *Lgmn*, legumain; *Timp2*, tissue inhibitor of metalloproteinase-2; *Sparc*, secreted protein acidic and rich in cysteine; *Fhl1*, four and a half LIM domains protein 1; *Mmp19*, matrix metalloproteinase-19; *Hpse*, heparanase; *Mmp9*, matrix metalloproteinase-9; *Fcho2*, FCH domain only protein-2; *Col5a2*, collagen 5.

ing inhibitor design for targeted disruption of specific LRP1-ligand interactions.

PAD2 and CNP Are Novel LRP1 Ligands in Myelin—To validate the results obtained using proteomics we chose a candidate approach. We selected two myelin-specific proteins, CNP and PAD2, as targets for validation, due to the proposed

involvement of these proteins in neurodegeneration and MS. CNP is a major protein component of myelin, an early marker of oligodendrocyte myelination (39), and a potential auto-antigen in MS (20, 21). The proposed function of CNP is to mediate the compaction of myelin by organizing the tubulin network (40). PAD2 is a member of the PAD family of Ca^{2+} -dependent enzymes, which catalyze the post-translational modification of protein arginines, in a process called deimination or citrullination (24). PAD2 expression and the level of citrullination correlate with active disease in both human MS and the animal models of MS (25–30).

We first confirmed binding of PAD2 and CNP to CCRII and CCRIV by immunoblot analysis. As shown in Fig. 3A, PAD2 in whole CNS myelin interacted with CCRII, but not with CCRIV or Fc, confirming the results of our proteomic analysis (Fig. 3A). CNP bound to both CCRII and CCRIV but not the control protein Fc (Fig. 3B). GST-RAP treatment completely inhibited association of both PAD2 and CNP with the CCRs (Fig. 3).

We next determined whether recombinant PAD2 and CNP bind to full-length LRP1. We expressed PAD2 as a His-tagged fusion protein and CNP as a GST-tagged fusion protein in bacteria, as described under “Experimental Procedures.” Protein preparations were first tested for purity by SDS-PAGE. As shown in Fig. 4, recombinant PAD2 and CNP migrated as single bands with an apparent size of 80 and 60 kDa, respectively, as anticipated (Fig. 4A). Binding of PAD2-His and GST-CNP to LRP1 was then evaluated using an ELISA format. Purified LRP1, fibronectin, and BSA were immobilized in microtiter plates. Recombinant PAD2-His bound to LRP1, but did not bind to purified fibronectin or BSA under the same conditions (Fig. 4B).

To study binding of LRP1 to CNP, BSA, GST, GST-CNP, and GST-RAP were immobilized in microtiter plates. Shed LRP1, which was purified from human plasma, was then incubated with the immobilized proteins. Binding of shed LRP1 to GST-CNP wells was significantly increased compared with binding to BSA or GST alone (Fig. 4C). Shed LRP-1 binding to immobilized GST-RAP was used as a positive control.

LRP1 Is Citrullinated by PAD2—Protein citrullination converts positively charged arginine residues into the neutral residue, citrulline, which can substantially alter protein structure and function (23). To test whether LRP1 is a target for PAD2-mediated citrullination, we performed *in vitro* citrullination assays. RAW 264.7 cell protein extracts were incubated with or without PAD2 in the presence or absence of Ca^{2+} . LRP1 was then recovered by affinity precipitation with GST-RAP, and samples were subjected to immunoblot analysis. As is shown in Fig. 5A, when cell extracts were incubated with PAD2 in the presence of Ca^{2+} , LRP1 citrullination was readily detected. As expected, LRP1 was precipitated under all conditions. Other proteins also were citrullinated by PAD2, as determined by immunoblotting for citrullinated proteins in the RAW 264.7 cell extracts. As a control, we determined that levels of LRP1 and Grp78 were present in equal quantity in the initial cell extracts incubated with PAD2.

Next, we examined whether LRP1 can be citrullinated in whole brain extracts (Fig. 5B). Protein extracts from mouse brain were prepared and supplemented with Ca^{2+} alone, or

TABLE 2

Proteins co-purifying with CCRII and CCRIV in CHO-K1 cells

The gene products below were identified by tandem mass spectrometry as partners for LRP1 CCRs with (+) or without (–) RAP. Mean spectral counts and S.D. are shown ($n = 3$).

Gene name	Fc	CCRII	CCRIV	Fc	CCRII	CCRIV
RAP	–	–	–	+	+	+
<i>Lrp1</i>	0 ± 0	29.2 ± 0.1	75 ± 0.2	3.3 ± 1.7	22.6 ± 0.1	58.5 ± 0.3
<i>Glg1</i>	0 ± 0	68.5 ± 0.1	71.7 ± 0.2	0.7 ± 1.7	3 ± 0.5	1 ± 0.8
<i>Lgmn</i>	0 ± 0	0 ± 0	15.7 ± 0.3	0.7 ± 0.9	0 ± 0	0 ± 0
<i>Lrpap1</i>	0.4 ± 1.4	10 ± 0.2	15.2 ± 0.1	3 ± 1.7	71 ± 0.2	46.2 ± 0.2
<i>Timp2</i>	0 ± 0	1 ± 0.8	12.2 ± 0.3	0.30 ± 1.7	0 ± 0	0.20 ± 2
<i>Sparc</i>	0 ± 0	16.7 ± 0.1	10.2 ± 0.3	0 ± 0	0.7 ± 0.9	0.7 ± 1.3
<i>Fhl1</i>	0 ± 0	0 ± 0	4.7 ± 0.5	0 ± 0	0 ± 0	0.5 ± 2
<i>Mmp19</i>	0 ± 0	6.7 ± 0.1	4.5 ± 0.3	0 ± 0	1.3 ± 0.4	4 ± 0.3
<i>Hpse</i>	0 ± 0	9.7 ± 0.4	3 ± 0.3	0.3 ± 1.7	0.3 ± 1.7	0 ± 0
<i>Mmp9</i>	0 ± 0	3.2 ± 0.5	1.2 ± 0.8	0 ± 0	0 ± 0	0 ± 0
<i>Fcho2</i>	0 ± 0	2 ± 0	1 ± 0.8	0 ± 0	0 ± 0	0 ± 0
<i>Col5a2</i>	0 ± 0	5 ± 0.76	0 ± 0	0 ± 0	0 ± 0	0 ± 0

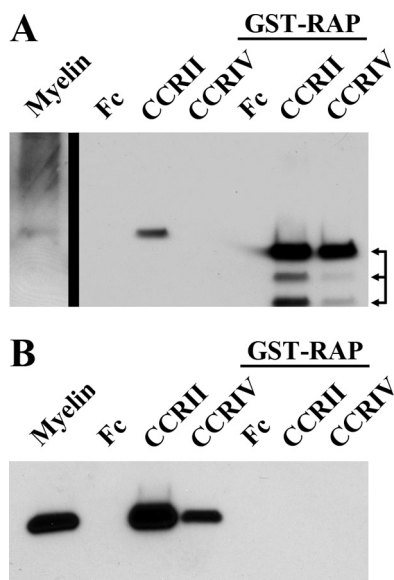


FIGURE 3. **PAD2 and CNP bind to specific CCRs.** Purified myelin protein extracts were incubated with Fc, CCRII, and CCRIV in the presence or absence of GST-RAP as described under “Experimental Procedures.” Fc and CCR were recovered with protein A-agarose beads. Samples and myelin extracts were analyzed by immunoblot to detect PAD2 (A) and CNP (B). The vertical line was used to highlight a longer exposure of the same membrane to show expression of PAD2 in myelin extract. Arrows indicate GST-RAP recognized by the anti-PAD2 mouse serum developed against a GST-PAD2 fusion protein.

with recombinant PAD2 and Ca^{2+} . LRP1 was recovered by affinity precipitation with GST-RAP and protein citrullination was examined. As is shown in Fig. 5B, in the absence of added Ca^{2+} , we did not detect citrullination of LRP1. However, when we added Ca^{2+} to the brain extracts, to activate endogenous PAD, LRP1 citrullination was observed. Because PAD2 is the only member of the PAD family expressed in the healthy CNS, it is reasonable to conclude that endogenous PAD2 citrullinates LRP1 (24). Adding recombinant PAD2 to mouse brain extracts, in the presence of Ca^{2+} , induced robust LRP1 citrullination. (Fig. 5B).

In the CNS extracts, LRP1 was one of many proteins that are citrullinated by PAD2, as determined by immunoblot analysis for citrullinated proteins in protein extracts (Fig. 5B). Next, we sought to determine whether extracellular PAD2 can citrullinate cell surface proteins. LRP1-positive and -deficient fibroblasts were treated with recombinant PAD2 for 6 h at 37 °C.

Cell surface proteins were labeled with membrane impermeable biotin and recovered by streptavidin affinity precipitation. Affinity precipitates were then analyzed by immunoblot for the presence of citrullination and LRP1. As is shown in Fig. 6A, PAD2 induces a robust citrullination of cell surface proteins. Furthermore, cell surface citrullination is increased in LRP1 positive cells (Fig. 6A). LRP1 was only detected in LRP1 positive cells, as expected.

We further tested whether PAD2-mediated citrullination of cell surface proteins affects the endocytic function of LRP1. LRP1-positive and -deficient fibroblasts, previously treated with recombinant PAD2 for 3 h at 37 °C, were incubated with GFP-RAP for 3 h (Fig. 6B). After extensive washing, GFP fluorescence was assessed by flow cytometry as a measure of LRP1-mediated endocytosis. No fluorescence was detected with LRP1-deficient cells, as expected (Fig. 6B). PAD2 treatment induces a small but significant decrease ($12 \pm 2\%$, $n = 4$) in GFP-RAP association with LRP1-positive cells. Therefore, our data suggests that citrullination of cell surface proteins by PAD2 can decrease the endocytic function of LRP1.

LRP1 Is a Phagocytic Receptor for Necrotic Cells—Multiple LRP1-specific ligands identified in our proteomic screen are myelin-enriched cytoplasmic proteins, including components of the cytoskeleton. We thus hypothesized that LRP1 could be a novel receptor involved in the clearance of necrotic cells and cellular debris. To test this hypothesis, we prepared two types of necrotic cells by heat shock treatment: the T cell-like Jurkat cell line and the oligodendrocyte cell line N20.1 (34). Four hours post induction of necrosis, >95% of the cells are trypan blue-positive, indicating the loss of plasma membrane integrity (data not shown). Furthermore, necrotic Jurkat cells were 95% positive for both annexin-5 and 7-amino-actinomycin D when analyzed by flow cytometry (Fig. 7A). Finally, necrotic N20.1 cells showed ruffling of the plasma membrane when compared with live cells by phase contrast microscopy (Fig. 7B).

Necrotic Jurkat cells were labeled with CypHer5, a pH-sensitive fluorescent dye (41), and added to CFSE-labeled LRP1 positive and deficient fibroblasts. After 2 h of incubation at 37 °C, engulfment of necrotic cells was analyzed by flow cytometry. As shown in Fig. 7, LRP1-positive cells are phagocytosing necrotic Jurkat cells more efficiently than LRP1-deficient cells (2.7-fold increase, $p < 0.0001$, $n = 3$; Fig. 7, C and D). On the

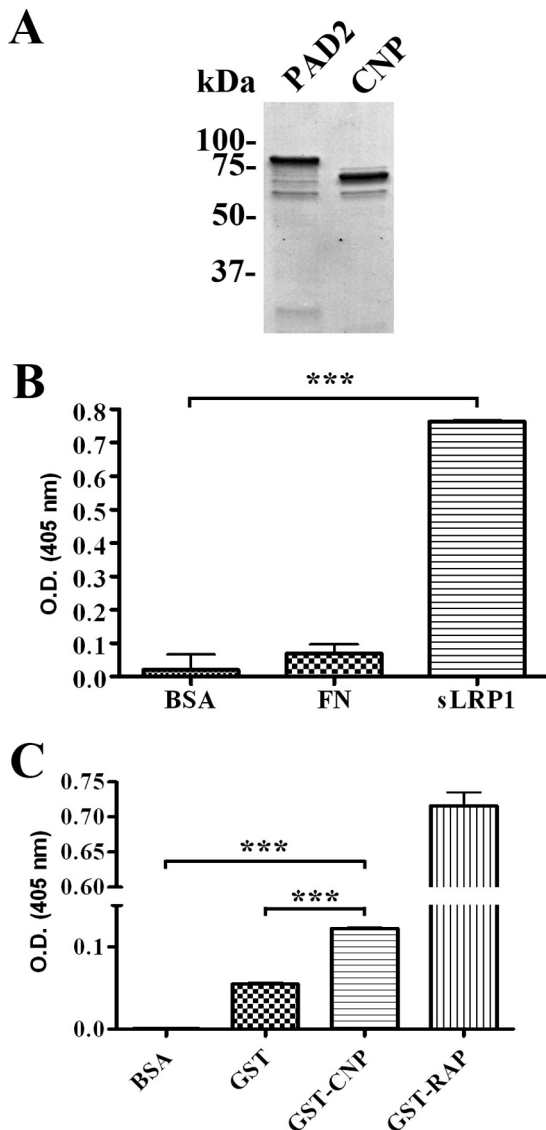


FIGURE 4. PAD2 and CNP interact with full-length LRP1. A, PAD2-His and GST-CNP were expressed as fusion proteins in bacteria and subjected to SDS-PAGE with Coomassie staining. B, BSA, FN (Fibronectin), and LRP1 were adsorbed onto plastic wells and incubated with purified PAD2-His. PAD2 binding to the immobilized phase was detected in an ELISA format, using anti-PAD2 serum, as described under "Experimental Procedures." $***, p < 0.001$. C, BSA, GST, GST-CNP, and GST-RAP were adsorbed onto plastic wells as described under "Experimental Procedures" and incubated with soluble human LRP1. LRP1 binding to the immobilized phase was detected in an ELISA format, using LRP1 α -chain-specific antibody 8G1. $***, p < 0.001$.

other hand, engulfment of live Jurkat cells was not significantly different between LRP1-positive and -deficient fibroblasts. In a complimentary approach, when LRP1-positive fibroblasts were pretreated with an LRP1 antagonist (GST-RAP), engulfment of necrotic cells was inhibited to the levels observed in LRP1-deficient cells (supplemental Fig. 1A). To next examine the function of LRP1 in the phagocytosis of CNS myelin debris, we repeated necrotic cell internalization experiments using the microglial cell line BV2 as model phagocytes and the oligodendrocyte cell line N20.1 as model necrotic cells (34, 42). When BV2 were pretreated with GST-RAP, phagocytosis of necrotic oligodendrocytes was inhibited by 35% ($p < 0.001, n = 6$; Fig. 7, E and F), whereas no significant difference was detected with

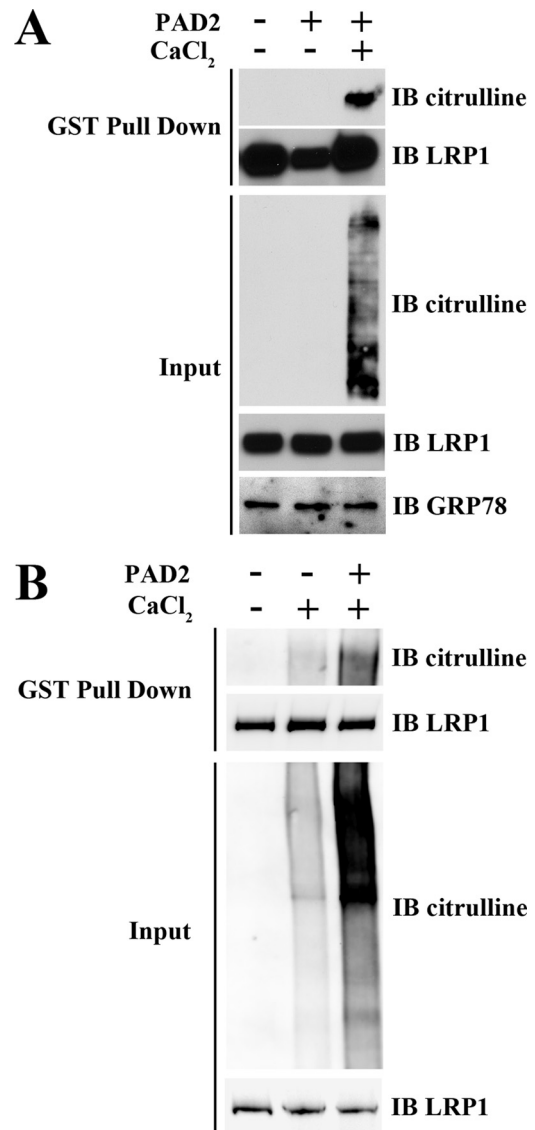


FIGURE 5. LRP1 is a substrate for PAD2-mediated citrullination. A, RAW264.7 cell extracts were incubated with or without purified PAD2 and CaCl₂, as described under "Experimental Procedures." LRP1 was then purified using GST-RAP pull-down. Samples and input were analyzed by immunoblotting (IB) using LRP1 α -chain-specific antibody or with an antibody specific for citrullinated proteins. Grp78 immunoblot was used as a control of protein load. B, brain protein extract was incubated with or without CaCl₂, or with CaCl₂ and purified PAD2, as described under "Experimental Procedures." LRP1 was then purified using GST-RAP pull-down. Samples and input were analyzed by immunoblotting using LRP1 α -chain-specific antibody or with an antibody specific for citrullinated proteins.

live oligodendrocytes following GST or GST-RAP treatment. Finally, endocytosis of necrotic oligodendrocytes was also inhibited in LRP1-deficient fibroblasts (supplemental Fig. 1B).

Together, our results demonstrate that LRP1 binds intracellular proteins present in myelin. We also describe a new function for LRP1 as a phagocytic receptor for necrotic cells and cellular debris that could be present in the CNS.

DISCUSSION

Proper clearance of dead cells is critical for tissue homeostasis. Defects in apoptotic cell clearance can lead to secondary necrosis and release of cellular components into the extracellu-

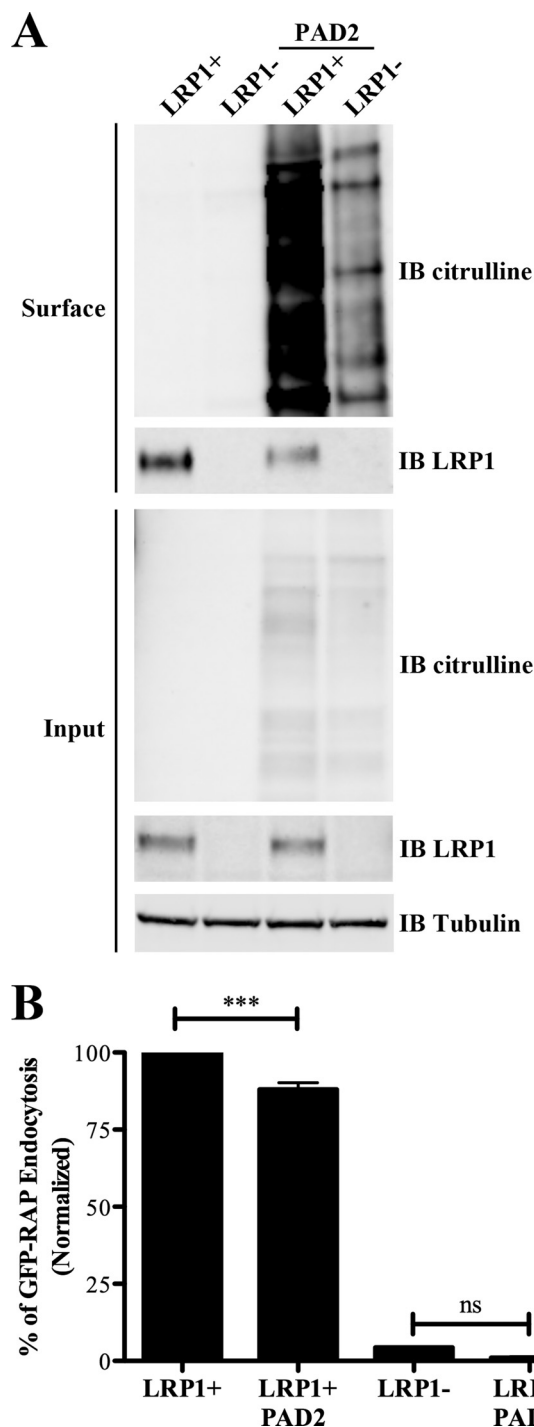


FIGURE 6. Cell surface protein citrullination blocks GFP-RAP endocytosis. *A*, LRP1-positive or -negative fibroblasts were incubated with or without purified PAD2, as described under "Experimental Procedures." Cell surface proteins were labeled with membrane impermeable biotin and recovered by streptavidin affinity purification. Samples and input were analyzed by immunoblotting using LRP1 β -chain-specific antibody or with an antibody specific for citrullinated proteins. Tubulin immunoblot (*IB*) was used as a control of protein load. *B*, LRP1-positive or -negative fibroblasts were pretreated with or without purified PAD2 and then treated with GFP-RAP for 3 h. After washing, cell-associated GFP fluorescence was analyzed by flow cytometry. Results are normalized to the difference of mean GFP-RAP fluorescence between treated LRP1-positive cells and untreated LRP1-positive cells ($n = 4$; ***, $p < 0.001$). *ns*, not significant.

lar environment, generating an inflammatory stimulus that could lead to the development of autoimmune diseases, including MS (3, 43).

LRP1 was recently reported to function as a phagocytic receptor for apoptotic cells and myelin debris (4–6). Although LRP1 was originally described as a scavenger receptor for extracellular proteins (9), it is now clear that LRP1 function is more complex than just mediating endocytosis (9). LRP1 can regulate cell signaling events and functions in inflammation and neurogenesis (12, 44).

The goal of the present study was to characterize LRP1 ligands present in CNS myelin. The LRP1 ligand-binding domains CCR2 and CCR4 were prepared as fusion proteins and used in an affinity-based proteomics screen. Using this approach, we identified >70 ligands for LRP1. These ligands could be separated into two categories based on their cellular localization: extracellular and intracellular proteins. Some of the proteins were identified because of their ability to co-purify with the CCRs during expression and purification (Table 2 and Fig. 2*B*). This category included known ligands for LRP1, such as RAP, matrix metalloproteinase-9, and tissue inhibitor of metalloproteinase 2 (16, 37, 38). The most abundant LRP1 ligand discovered in the extracellular protein category is a member of the FGF receptor family: Golgi glycoprotein 1 (GLG1)/cysteine-rich fibroblast growth factor receptor/E-selectin ligand 1. GLG1 function remains elusive but studies using GLG1 knock-out mice suggest a role during development as an FGF18 receptor (45). Furthermore, GLG1 is an E-selectin ligand involved in leukocyte extravasation during inflammation (46). By mediating the removal of GLG1 from extracellular spaces, LRP1 may modulate leukocyte migration.

We also identified membrane bound myelin-specific proteins during our screen. We confirmed the interaction of MBP and myelin-associated glycoprotein with LRP1 (Table 1 and supplemental Table 1) (4, 14) and also detected PLP1 as LRP1 ligands (Table 1). The most surprising result we obtained by proteomics screening was the identification of numerous intracellular LRP1 ligands in myelin (Table 1). These included cytoskeleton proteins such as septin 2, 4, 7, and 8; MTAP1a and 1b; and ROCK. MTAP and septins are known components of myelin (47–49). As myelin wraps multiple times around the axon, the formation and maintenance of the myelin sheath is dependent on the cytoskeleton, probably explaining the abundance of cytoskeletal proteins in myelin preparations (50).

We selected two intracellular proteins as candidates for validation as LRP1 binding partners: CNP and PAD2. CNP is a major component of myelin, with a potential role in myelin formation and compaction (40). Clearance of CNP by LRP1 may be critical because it has been identified as a potential auto-antigen in MS (21), and auto-reactive populations of CNP-specific T cells were identified in MS patients with active disease (20). Similarly, PAD2 is a common component of the CNS myelin (24), and its up-regulation is thought to be an early marker of demyelinating disease due to the reduced stability of the citrullinated protein components of the myelin sheath (25). We demonstrate here that LRP1 is a potential regulator of

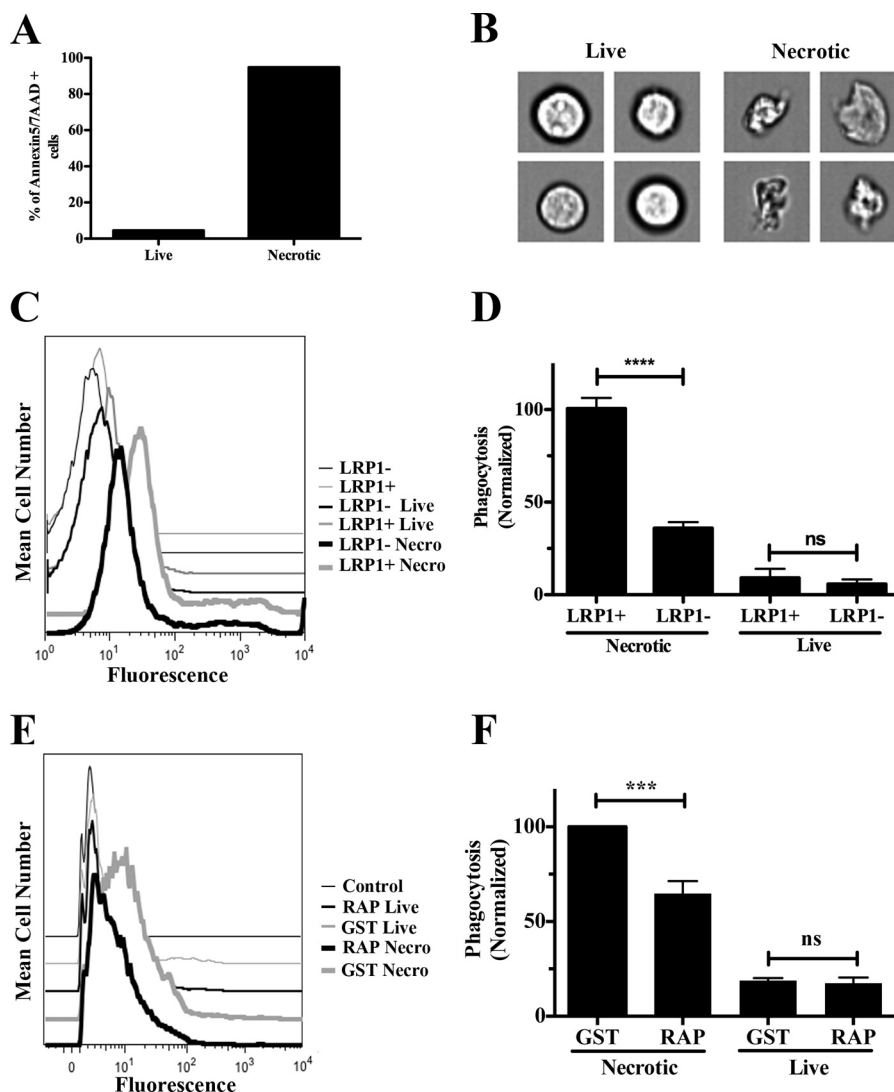


FIGURE 7. LRP1 is a phagocytic receptor for necrotic cells. *A*, annexin 5/7-aminocoumarin D (7AAD) staining of live and necrotic Jurkat cells. *B*, phase contrast microscopy of live and necrotic N20.1 cells. *C*, CFSE-labeled LRP1 positive or negative fibroblasts were incubated with live or necrotic CypHer-labeled Jurkat cells for 2 h. After washing, fibroblast-associated CypHer fluorescence was analyzed by flow cytometry. *D*, results are normalized to the difference of CypHer median fluorescence between LRP1-positive cells incubated with necrotic cells and untreated LRP1-positive cells (a representative of two independent experiments is shown; ****, $p < 0.0001$). *E*, BV2 cells were incubated with live or necrotic CypHer-labeled N20.1 cells for 30 min. After washing, BV2 were stained with CD11b-Alexa Fluor 488 antibody and BV2-associated CypHer fluorescence was analyzed by flow cytometry. *F*, results are normalized to the difference of CypHer median fluorescence between GST treated cells incubated with necrotic cells and untreated BV2 cells (a representative of six independent experiments is shown). ***, $p < 0.001$. ns, not significant.

demyelination via interaction with CNP and PAD2. Furthermore, LRP1 can itself be post-translationally modified, at least *in vitro*, by endogenous PAD2 present in brain extract. We also demonstrate that LRP1 function in endocytosis is regulated by extracellular PAD2-mediated citrullination. Whether PAD2-mediated citrullination affects endocytosis of only a subset, or all LRP1 ligands, remains to be determined.

Finally, we demonstrate here for the first time a new function for LRP1 in clearing necrotic debris. LRP1 has been previously described as a phagocytic receptor for apoptotic cells (5, 6). In this study, we demonstrate that LRP1 function was required for optimal engulfment by both non-professional (fibroblasts) and CNS professional (microglia) phagocytes of necrotic T cells and necrotic oligodendrocytes. Removal of dead and dying oligodendrocytes and infiltrating or resident activated lymphocytes could be of critical importance in neuroinflammatory states

such as MS, as a means of removal of potential auto-antigens and danger signals.

In conclusion, our study demonstrates that LRP1 specifically associates with numerous proteins in myelin and is a novel phagocytic receptor for necrotic cells. To our knowledge, we are the first to describe that LRP1 can interact with a variety of cytoplasmic proteins through the extracellular domain. Our results strongly indicate that the function of LRP1 extends beyond regulation of extracellular matrix and cell surface proteins and is consistent with the proposed function of LRP1 in mediating the removal of apoptotic cells and necrotic debris during inflammatory diseases of the CNS, including MS. Further elucidation of the mechanisms by which LRP1 may regulate inflammatory diseases could pave the way for the development of therapeutic treatments, perhaps based on CCR2 and CCR4, which would be utilized to inhibit inflammation and the autoimmune response.

REFERENCES

- Compston, A., and Coles, A. (2008) Multiple sclerosis. *Lancet* **372**, 1502–1517
- Barnett, M. H., and Prineas, J. W. (2004) Relapsing and remitting multiple sclerosis: pathology of the newly forming lesion. *Ann. Neurol.* **55**, 458–468
- Botto, M., Dell'Agnola, C., Bygrave, A. E., Thompson, E. M., Cook, H. T., Petry, F., Loos, M., Pandolfi, P. P., and Walport, M. J. (1998) Homozygous C1q deficiency causes glomerulonephritis associated with multiple apoptotic bodies. *Nat. Genet.* **19**, 56–59
- Gaultier, A., Wu, X., Le Moan, N., Takimoto, S., Mukandala, G., Akassoglou, K., Campana, W. M., and Gonias, S. L. (2009) Low-density lipoprotein receptor-related protein 1 is an essential receptor for myelin phagocytosis. *J. Cell Sci.* **122**, 1155–1162
- Gardai, S. J., McPhillips, K. A., Frasca, S. C., Janssen, W. J., Starefeldt, A., Murphy-Ullrich, J. E., Bratton, D. L., Oldenborg, P. A., Michalak, M., and Henson, P. M. (2005) Cell-surface calreticulin initiates clearance of viable or apoptotic cells through trans-activation of LRP on the phagocyte. *Cell* **123**, 321–334
- Ogden, C. A., deCathelineau, A., Hoffmann, P. R., Bratton, D., Ghebrehewet, B., Fadok, V. A., and Henson, P. M. (2001) C1q and mannose binding lectin engagement of cell surface calreticulin and CD91 initiates macrophocytosis and uptake of apoptotic cells. *J. Exp. Med.* **194**, 781–795
- Herz, J., Hamann, U., Rogne, S., Myklebost, O., Gausepohl, H., and Stanley, K. K. (1988) Surface location and high affinity for calcium of a 500-kD liver membrane protein closely related to the LDL-receptor suggest a physiological role as lipoprotein receptor. *EMBO J.* **7**, 4119–4127
- Strickland, D. K., Ashcom, J. D., Williams, S., Burgess, W. H., Migliorini, M., and Argraves, W. S. (1990) Sequence identity between the α 2-macroglobulin receptor and low density lipoprotein receptor-related protein suggests that this molecule is a multifunctional receptor. *J. Biol. Chem.* **265**, 17401–17404
- Lillis, A. P., Van Duyn, L. B., Murphy-Ullrich, J. E., and Strickland, D. K. (2008) LDL receptor-related protein 1: unique tissue-specific functions revealed by selective gene knockout studies. *Physiol. Rev.* **88**, 887–918
- Gonias, S. L., Wu, L., and Salicioni, A. M. (2004) Low density lipoprotein receptor-related protein: regulation of the plasma membrane proteome. *Thromb. Haemost.* **91**, 1056–1064
- Gonias, S. L., Gaultier, A., and Jo, M. (2011) Regulation of the urokinase receptor (uPAR) by LDL receptor-related protein-1 (LRP1). *Curr. Pharm. Des.* **17**, 1962–1969
- Gaultier, A., Arandjelovic, S., Niessen, S., Overton, C. D., Linton, M. F., Fazio, S., Campana, W. M., Cravatt, B. F., 3rd, and Gonias, S. L. (2008) Regulation of tumor necrosis factor receptor-1 and the IKK-NF- κ B pathway by LDL receptor-related protein explains the antiinflammatory activity of this receptor. *Blood* **111**, 5316–5325
- Zurhove, K., Nakajima, C., Herz, J., Bock, H. H., and May, P. (2008) γ -Secretase limits the inflammatory response through the processing of LRP1. *Sci. Signal* **1**, ra15
- Stiles, T. L., Dickendeshner, T. L., Gaultier, A., Fernandez-Castaneda, A., Mantuano, E., Giger, R. J., and Gonias, S. L. (2012) LDL Receptor-related Protein-1 is a sialic acid-independent receptor for myelin-associated glycoprotein (MAG) that functions in neurite outgrowth inhibition by MAG and CNS myelin. *J. Cell Sci.* [Epub ahead of print]
- Neels, J. G., van Den Berg, B. M., Lookene, A., Olivecrona, G., Pannekoek, H., and van Zonneveld, A. J. (1999) The second and fourth cluster of class A cysteine-rich repeats of the low density lipoprotein receptor-related protein share ligand-binding properties. *J. Biol. Chem.* **274**, 31305–31311
- Herz, J., Goldstein, J. L., Strickland, D. K., Ho, Y. K., and Brown, M. S. (1991) 39-kDa protein modulates binding of ligands to low density lipoprotein receptor-related protein/ α 2-macroglobulin receptor. *J. Biol. Chem.* **266**, 21232–21238
- Lee, J., Gravel, M., Zhang, R., Thibault, P., and Braun, P. E. (2005) Process outgrowth in oligodendrocytes is mediated by CNP, a novel microtubule assembly myelin protein. *J. Cell Biol.* **170**, 661–673
- Kozlov, G., Lee, J., Elias, D., Gravel, M., Gutierrez, P., Ekiel, I., Braun, P. E., and Gehring, K. (2003) Structural evidence that brain cyclic nucleotide phosphodiesterase is a member of the 2H phosphodiesterase superfamily. *J. Biol. Chem.* **278**, 46021–46028
- Lappe-Siefke, C., Goebbels, S., Gravel, M., Nicksch, E., Lee, J., Braun, P. E., Griffiths, I. R., and Nave, K. A. (2003) Disruption of Cnp1 uncouples oligodendroglial functions in axonal support and myelination. *Nat. Genet.* **33**, 366–374
- Muraro, P. A., Kalbus, M., Afshar, G., McFarland, H. F., and Martin, R. (2002) T cell response to 2',3'-cyclic nucleotide 3'-phosphodiesterase (CNPase) in multiple sclerosis patients. *J. Neuroimmunol.* **130**, 233–242
- Rötsner, M., Muraro, P. A., Riethmüller, A., Kalbus, M., Sappeler, G., Thompson, R. J., Lichtenfels, R., Sommer, N., McFarland, H. F., and Martin, R. (1997) 2',3'-cyclic nucleotide 3'-phosphodiesterase: a novel candidate autoantigen in demyelinating diseases. *J. Neuroimmunol.* **75**, 28–34
- Lamensa, J. W., and Moscarello, M. A. (1993) Deimination of human myelin basic protein by a peptidylarginine deiminase from bovine brain. *J. Neurochem.* **61**, 987–996
- Vossenaar, E. R., Zendman, A. J., van Venrooij, W. J., and Pruijn, G. J. (2003) PAD, a growing family of citrullinating enzymes: genes, features and involvement in disease. *BioEssays* **25**, 1106–1118
- Wood, D. D., Ackerley, C. A., Brand, B. v., Zhang, L., Raijmakers, R., Mastronardi, F. G., and Moscarello, M. A. (2008) Myelin localization of peptidylarginine deiminases 2 and 4: comparison of PAD2 and PAD4 activities. *Lab. Invest.* **88**, 354–364
- Moscarello, M. A., Wood, D. D., Ackerley, C., and Boulias, C. (1994) Myelin in multiple sclerosis is developmentally immature. *J. Clin. Invest.* **94**, 146–154
- Wood, D. D., Bilbao, J. M., O'Connors, P., and Moscarello, M. A. (1996) Acute multiple sclerosis (Marburg type) is associated with developmentally immature myelin basic protein. *Ann. Neurol.* **40**, 18–24
- Kim, J. K., Mastronardi, F. G., Wood, D. D., Lubman, D. M., Zand, R., and Moscarello, M. A. (2003) Multiple sclerosis: an important role for post-translational modifications of myelin basic protein in pathogenesis. *Mol. Cell Proteomics* **2**, 453–462
- Musse, A. A., and Harauz, G. (2007) Molecular “negativity” may underlie multiple sclerosis: Role of the myelin basic protein family in the pathogenesis of MS. *Neurobiology of Multiple Sclerosis* **79**, 149–172
- Mastronardi, F. G., Noor, A., Wood, D. D., Paton, T., and Moscarello, M. A. (2007) Peptidyl argininedeiminase 2 CpG island in multiple sclerosis white matter is hypomethylated. *J. Neurosci. Res.* **85**, 2006–2016
- Musse, A. A., Li, Z., Ackerley, C. A., Bienzle, D., Lei, H., Poma, R., Harauz, G., Moscarello, M. A., and Mastronardi, F. G. (2008) Peptidylarginine deiminase 2 (PAD2) overexpression in transgenic mice leads to myelin loss in the central nervous system. *Dis. Model Mech.* **1**, 229–240
- Savill, J., and Fadok, V. (2000) Corpse clearance defines the meaning of cell death. *Nature* **407**, 784–788
- Stern, M., Savill, J., and Haslett, C. (1996) Human monocyte-derived macrophage phagocytosis of senescent eosinophils undergoing apoptosis. Mediation by α v β 3/CD36/thrombospondin recognition mechanism and lack of phagocytic response. *Am. J. Pathol.* **149**, 911–921
- Gorovoy, M., Gaultier, A., Campana, W. M., Firestein, G. S., and Gonias, S. L. (2010) Inflammatory mediators promote production of shed LRP1/CD91, which regulates cell signaling and cytokine expression by macrophages. *J. Leukoc. Biol.* **88**, 769–778
- Studzinski, D. M., and Benjamins, J. A. (2003) Regulation of CNS glial phenotypes in N20.1 cells. *J. Neurosci. Res.* **73**, 31–41
- Norton, W. T., and Poduslo, S. E. (1973) Myelination in rat brain: method of myelin isolation. *J. Neurochem.* **21**, 749–757
- Gaultier, A., Simon, G., Niessen, S., Dix, M., Takimoto, S., Cravatt, B. F., 3rd, and Gonias, S. L. (2010) LDL receptor-related protein 1 regulates the abundance of diverse cell-signaling proteins in the plasma membrane proteome. *J. Proteome Res.* **9**, 6689–6695
- Emonard, H., Bellon, G., Troeberg, L., Berton, A., Robinet, A., Henriot, P., Marbaix, E., Kirkegaard, K., Patthy, L., Eeckhout, Y., Nagase, H., Hornebeck, W., and Courtroy, P. J. (2004) Low density lipoprotein receptor-related protein mediates endocytic clearance of pro-MMP-2/TIMP-2 complex through a thrombospondin-independent mechanism. *J. Biol. Chem.* **279**, 54944–54951
- Hahn-Dantona, E., Ruiz, J. F., Bornstein, P., and Strickland, D. K. (2001)

- The low density lipoprotein receptor-related protein modulates levels of matrix metalloproteinase 9 (MMP-9) by mediating its cellular catabolism. *J. Biol. Chem.* **276**, 15498–15503
39. Gravel, M., Peterson, J., Yong, V. W., Kottis, V., Trapp, B., and Braun, P. E. (1996) Overexpression of 2',3'-cyclic nucleotide 3'-phosphodiesterase in transgenic mice alters oligodendrocyte development and produces aberrant myelination. *Mol. Cell Neurosci.* **7**, 453–466
 40. Bifulco, M., Laezza, C., Stingo, S., and Wolff, J. (2002) 2',3'-Cyclic nucleotide 3'-phosphodiesterase: a membrane-bound, microtubule-associated protein and membrane anchor for tubulin. *Proc. Natl. Acad. Sci. U.S.A.* **99**, 1807–1812
 41. Adie, E. J., Francis, M. J., Davies, J., Smith, L., Marengi, A., Hather, C., Hadingham, K., Michael, N. P., Milligan, G., and Game, S. (2003) CypHer 5: a generic approach for measuring the activation and trafficking of G protein-coupled receptors in live cells. *Assay Drug Dev. Technol.* **1**, 251–259
 42. Henn, A., Lund, S., Hedtjam, M., Porzgen, P., and Leist, M. (2009) The suitability of BV2 cells as alternative model system for primary microglia cultures or animal experiments of brain inflammation. *ALTEX* **26**, 83–94
 43. Elliott, M. R., and Ravichandran, K. S. (2010) Clearance of apoptotic cells: implications in health and disease. *J. Cell Biol.* **189**, 1059–1070
 44. Mantuano, E., Inoue, G., Li, X., Takahashi, K., Gaultier, A., Gonias, S. L., and Campana, W. M. (2008) The hemopexin domain of matrix metalloproteinase-9 activates cell signaling and promotes migration of schwann cells by binding to low-density lipoprotein receptor-related protein. *J. Neurosci.* **28**, 11571–11582
 45. Miyaoka, Y., Tanaka, M., Imamura, T., Takada, S., and Miyajima, A. (2010) A novel regulatory mechanism for Fgf18 signaling involving cysteine-rich FGF receptor (Cfr) and δ -like protein (Dlk). *Development* **137**, 159–167
 46. Hidalgo, A., Peired, A. J., Wild, M. K., Vestweber, D., and Frenette, P. S. (2007) Complete identification of E-selectin ligands on neutrophils reveals distinct functions of PSGL-1, ESL-1, and CD44. *Immunity* **26**, 477–489
 47. Garner, C. C., Garner, A., Huber, G., Kozak, C., and Matus, A. (1990) Molecular cloning of microtubule-associated protein 1 (MAP1A) and microtubule-associated protein 5 (MAP1B): identification of distinct genes and their differential expression in developing brain. *J. Neurochem.* **55**, 146–154
 48. Buser, A. M., Erne, B., Werner, H. B., Nave, K. A., and Schaeren-Wiemers, N. (2009) The septin cytoskeleton in myelinating glia. *Mol. Cell Neurosci.* **40**, 156–166
 49. Hall, P. A., and Russell, S. E. (2012) Mammalian septins: dynamic heteromers with roles in cellular morphogenesis and compartmentalization. *The Journal of pathology* **226**, 287–299
 50. Bauer, N. G., Richter-Landsberg, C., and Ffrench-Constant, C. (2009) Role of the oligodendroglial cytoskeleton in differentiation and myelination. *Glia* **57**, 1691–1705

References

- ABOUL-ENEIN, F. & LASSMANN, H. 2005. Mitochondrial damage and histotoxic hypoxia: a pathway of tissue injury in inflammatory brain disease? *Acta Neuropathol*, 109, 49-55.
- ADIE, E. J., FRANCIS, M. J., DAVIES, J., SMITH, L., MARENCHI, A., HATHER, C., HADINGHAM, K., MICHAEL, N. P., MILLIGAN, G. & GAME, S. 2003. CypHer 5: a generic approach for measuring the activation and trafficking of G protein-coupled receptors in live cells. *Assay Drug Dev Technol*, 1, 251-9.
- AJAMI, B., BENNETT, J. L., KRIEGER, C., MCNAGNY, K. M. & ROSSI, F. M. 2011. Infiltrating monocytes trigger EAE progression, but do not contribute to the resident microglia pool. *Nat Neurosci*, 14, 1142-9.
- ANDREWS, T., ZHANG, P. & BHAT, N. R. 1998. TNFalpha potentiates IFNgamma-induced cell death in oligodendrocyte progenitors. *J Neurosci Res*, 54, 574-83.
- ARANOW, C. 2011. Vitamin D and the immune system. *J Investig Med*, 59, 881-6.
- ARNETT, H. A., FANCY, S. P., ALBERTA, J. A., ZHAO, C., PLANT, S. R., KAING, S., RAINE, C. S., ROWITCH, D. H., FRANKLIN, R. J. & STILES, C. D. 2004. bHLH transcription factor Olig1 is required to repair demyelinated lesions in the CNS. *Science*, 306, 2111-5.
- ARNETT, H. A., MASON, J., MARINO, M., SUZUKI, K., MATSUSHIMA, G. K. & TING, J. P. 2001. TNF alpha promotes proliferation of oligodendrocyte progenitors and remyelination. *Nat Neurosci*, 4, 1116-22.
- ASCHERIO, A., MUNGER, K. L., WHITE, R., KOCHERT, K., SIMON, K. C., POLMAN, C. H., FREEDMAN, M. S., HARTUNG, H. P., MILLER, D. H., MONTALBAN, X., EDAN, G., BARKHOF, F., PLEIMES, D., RADU, E. W., SANDBRINK, R., KAPPOS, L. & POHL, C. 2014. Vitamin D as an early predictor of multiple sclerosis activity and progression. *JAMA Neurol*, 71, 306-14.
- AUDERSET, L., CULLEN, C. L. & YOUNG, K. M. 2016. Low Density Lipoprotein-Receptor Related Protein 1 Is Differentially Expressed by Neuronal and Glial Populations in the Developing and Mature Mouse Central Nervous System. *PLoS One*, 11, e0155878.
- BACK, S. A., TUOHY, T. M., CHEN, H., WALLINGFORD, N., CRAIG, A., STRUVE, J., LUO, N. L., BANINE, F., LIU, Y., CHANG, A., TRAPP, B. D., BEBO, B. F., JR., RAO, M. S. & SHERMAN, L. S. 2005. Hyaluronan accumulates in demyelinated lesions and inhibits oligodendrocyte progenitor maturation. *Nat Med*, 11, 966-72.
- BAECHER-ALLAN, C., KASKOW, B. J. & WEINER, H. L. 2018. Multiple Sclerosis: Mechanisms and Immunotherapy. *Neuron*, 97, 742-768.
- BAER, A. S., SYED, Y. A., KANG, S. U., MITTEREGGER, D., VIG, R., FFRENCH-CONSTANT, C., FRANKLIN, R. J. M., ALTMANN, F., LUBEC, G. & KOTTER, M. R. 2009. Myelin-mediated inhibition of oligodendrocyte precursor differentiation can be overcome by pharmacological modulation of Fyn-RhoA and protein kinase C signalling. *Brain*, 132, 465-481.
- BARNETT, M. H. & PRINEAS, J. W. 2004. Relapsing and remitting multiple sclerosis: pathology of the newly forming lesion. *Ann Neurol*, 55, 458-68.

- BASU, S., BINDER, R. J., RAMALINGAM, T. & SRIVASTAVA, P. K. 2001. CD91 is a common receptor for heat shock proteins gp96, hsp90, hsp70, and calreticulin. *Immunity*, 14, 303-13.
- BAUER, N. G., RICHTER-LANDSBERG, C. & FFRENCH-CONSTANT, C. 2009. Role of the oligodendroglial cytoskeleton in differentiation and myelination. *Glia*, 57, 1691-705.
- BEHJATI, S. & FRANK, M. H. 2009. The effects of tamoxifen on immunity. *Curr Med Chem*, 16, 3076-80.
- BELBASIS, L., BELLOU, V., EVANGELOU, E., IOANNIDIS, J. P. & TZOULAKI, I. 2015. Environmental risk factors and multiple sclerosis: an umbrella review of systematic reviews and meta-analyses. *Lancet Neurol*, 14, 263-73.
- BIFULCO, M., LAZZA, C., STINGO, S. & WOLFF, J. 2002. 2',3'-Cyclic nucleotide 3'-phosphodiesterase: a membrane-bound, microtubule-associated protein and membrane anchor for tubulin. *Proc Natl Acad Sci U S A*, 99, 1807-12.
- BINDER, R. J., HAN, D. K. & SRIVASTAVA, P. K. 2000. CD91: a receptor for heat shock protein gp96. *Nat Immunol*, 1, 151-5.
- BINDER, R. J. & SRIVASTAVA, P. K. 2004. Essential role of CD91 in re-presentation of gp96-chaperoned peptides. *Proc Natl Acad Sci U S A*, 101, 6128-33.
- BOTTO, M., DELL'AGNOLA, C., BYGRAVE, A. E., THOMPSON, E. M., COOK, H. T., PETRY, F., LOOS, M., PANDOLFI, P. P. & WALPORT, M. J. 1998. Homozygous C1q deficiency causes glomerulonephritis associated with multiple apoptotic bodies. *Nat Genet*, 19, 56-9.
- BRIFAULT, C., GILDER, A. S., LAUDATI, E., BANKI, M. & GONIAS, S. L. 2017. Shedding of membrane-associated LDL receptor-related protein-1 from microglia amplifies and sustains neuroinflammation. *J Biol Chem*, 292, 18699-18712.
- BUSER, A. M., ERNE, B., WERNER, H. B., NAVE, K. A. & SCHAEEREN-WIEMERS, N. 2009. The septin cytoskeleton in myelinating glia. *Mol Cell Neurosci*, 40, 156-66.
- BUTOVSKY, O., LANDA, G., KUNIS, G., ZIV, Y., AVIDAN, H., GREENBERG, N., SCHWARTZ, A., SMIRNOV, I., POLLACK, A., JUNG, S. & SCHWARTZ, M. 2006. Induction and blockage of oligodendrogenesis by differently activated microglia in an animal model of multiple sclerosis. *J Clin Invest*, 116, 905-15.
- BUTTI, E., BACIGALUPPI, M., CHAABANE, L., RUFFINI, F., BRAMBILLA, E., BERERA, G., MONTONATI, C., QUATTRINI, A. & MARTINO, G. 2019. Neural Stem Cells of the Subventricular Zone Contribute to Neuroprotection of the Corpus Callosum after Cuprizone-Induced Demyelination. *J Neurosci*, 39, 5481-5492.
- CANTUTI-CASTELVETRI, L., FITZNER, D., BOSCH-QUERALT, M., WEIL, M. T., SU, M., SEN, P., RUHWEDEL, T., MITKOVSKI, M., TRENDELENBURG, G., LUTJOHANN, D., MOBIUS, W. & SIMONS, M. 2018. Defective cholesterol clearance limits remyelination in the aged central nervous system. *Science*, 359, 684-688.
- CHANG, A., STAUGAITIS, S. M., DUTTA, R., BATT, C. E., EASLEY, K. E., CHOMYK, A. M., YONG, V. W., FOX, R. J., KIDD, G. J. & TRAPP, B. D. 2012. Cortical remyelination: a new target for repair therapies in multiple sclerosis. *Ann Neurol*, 72, 918-26.

- CHANG, A., TOURTELLOTTE, W. W., RUDICK, R. & TRAPP, B. D. 2002. Premyelinating oligodendrocytes in chronic lesions of multiple sclerosis. *N Engl J Med*, 346, 165-73.
- CHARLES, P., HERNANDEZ, M. P., STANKOFF, B., AIGROT, M. S., COLIN, C., ROUGON, G., ZALC, B. & LUBETZKI, C. 2000. Negative regulation of central nervous system myelination by polysialylated-neural cell adhesion molecule. *Proc Natl Acad Sci U S A*, 97, 7585-90.
- CHARLES, P., REYNOLDS, R., SEILHEAN, D., ROUGON, G., AIGROT, M. S., NIEZGODA, A., ZALC, B. & LUBETZKI, C. 2002. Re-expression of PSA-NCAM by demyelinated axons: an inhibitor of remyelination in multiple sclerosis? *Brain*, 125, 1972-9.
- CHAUDHURI, A. & BEHAN, P. O. 2004. Multiple sclerosis is not an autoimmune disease. *Arch Neurol*, 61, 1610-2.
- CHEW, L. J., KING, W. C., KENNEDY, A. & GALLO, V. 2005. Interferon-gamma inhibits cell cycle exit in differentiating oligodendrocyte progenitor cells. *Glia*, 52, 127-43.
- CHUANG, T. Y., GUO, Y., SEKI, S. M., ROSEN, A. M., JOHANSON, D. M., MANDELL, J. W., LUCCHINETTI, C. F. & GAULTIER, A. 2016. LRP1 expression in microglia is protective during CNS autoimmunity. *Acta Neuropathol Commun*, 4, 68.
- COMPSTON, A. & COLES, A. 2002. Multiple sclerosis. *Lancet*, 359, 1221-31.
- COMPSTON, A. & COLES, A. 2008. Multiple sclerosis. *Lancet*, 372, 1502-17.
- DAI, J., BERCURY, K. K., AHRENDSEN, J. T. & MACKLIN, W. B. 2015. Olig1 function is required for oligodendrocyte differentiation in the mouse brain. *J Neurosci*, 35, 4386-402.
- DENDROU, C. A., FUGGER, L. & FRIESE, M. A. 2015. Immunopathology of multiple sclerosis. *Nat Rev Immunol*, 15, 545-58.
- DENKER, S. P., JI, S., DINGMAN, A., LEE, S. Y., DERUGIN, N., WENDLAND, M. F. & VEXLER, Z. S. 2007. Macrophages are comprised of resident brain microglia not infiltrating peripheral monocytes acutely after neonatal stroke. *J Neurochem*, 100, 893-904.
- EL WALY, B., MACCHI, M., CAYRE, M. & DURBEC, P. 2014. Oligodendrogenesis in the normal and pathological central nervous system. *Front Neurosci*, 8, 145.
- ELLIOTT, M. R. & RAVICHANDRAN, K. S. 2010. Clearance of apoptotic cells: implications in health and disease. *J Cell Biol*, 189, 1059-70.
- EMERY, B. & DUGAS, J. C. 2013. Purification of oligodendrocyte lineage cells from mouse cortices by immunopanning. *Cold Spring Harb Protoc*, 2013, 854-68.
- EMONARD, H., BELLON, G., TROEBERG, L., BERTON, A., ROBINET, A., HENRIET, P., MARBAIX, E., KIRKEGAARD, K., PATTHY, L., EECKHOUT, Y., NAGASE, H., HORNEBECK, W. & COURTOY, P. J. 2004. Low density lipoprotein receptor-related protein mediates endocytic clearance of pro-MMP-2.TIMP-2 complex through a thrombospondin-independent mechanism. *J Biol Chem*, 279, 54944-51.
- FALCAO, A. M., VAN BRUGGEN, D., MARQUES, S., MEIJER, M., JAKEL, S., AGIRRE, E., SAMUDYATA, FLORIDDIA, E. M., VANICHKINA, D. P., FFRENCH-CONSTANT, C., WILLIAMS, A., GUERREIRO-CACAIS, A. O. & CASTELO-BRANCO, G. 2018a. Disease-specific oligodendrocyte lineage cells arise in multiple sclerosis. *Nat Med*.

- FALCAO, A. M., VAN BRUGGEN, D., MARQUES, S., MEIJER, M., JAKEL, S., AGIRRE, E., SAMUDYATA, FLORIDDIA, E. M., VANICHKINA, D. P., FFRENCH-CONSTANT, C., WILLIAMS, A., GUERREIRO-CACAIS, A. O. & CASTELO-BRANCO, G. 2018b. Disease-specific oligodendrocyte lineage cells arise in multiple sclerosis. *Nat Med*, 24, 1837-1844.
- FELDHAUS, B., DIETZEL, I. D., HEUMANN, R. & BERGER, R. 2004. Effects of interferon-gamma and tumor necrosis factor-alpha on survival and differentiation of oligodendrocyte progenitors. *J Soc Gynecol Investig*, 11, 89-96.
- FERNANDEZ-CASTANEDA, A., ARANDJELOVIC, S., STILES, T. L., SCHLOBACH, R. K., MOWEN, K. A., GONIAS, S. L. & GAULTIER, A. 2013. Identification of the low density lipoprotein (LDL) receptor-related protein-1 interactome in central nervous system myelin suggests a role in the clearance of necrotic cell debris. *J Biol Chem*, 288, 4538-48.
- FERNANDEZ-CASTANEDA, A. & GAULTIER, A. 2016. Adult oligodendrocyte progenitor cells - Multifaceted regulators of the CNS in health and disease. *Brain Behav Immun*, 57, 1-7.
- FORD, M. L. & EVAVOLD, B. D. 2005. Specificity, magnitude, and kinetics of MOG-specific CD8+ T cell responses during experimental autoimmune encephalomyelitis. *Eur J Immunol*, 35, 76-85.
- FRANKLIN, R. J. 2002. Why does remyelination fail in multiple sclerosis? *Nat Rev Neurosci*, 3, 705-14.
- GAO, X., GILLIG, T. A., YE, P., D'ERCOLE, A. J., MATSUSHIMA, G. K. & POPKO, B. 2000. Interferon-gamma protects against cuprizone-induced demyelination. *Mol Cell Neurosci*, 16, 338-49.
- GARDAI, S. J., MCPHILLIPS, K. A., FRASCH, S. C., JANSSEN, W. J., STAREFELDT, A., MURPHY-ULLRICH, J. E., BRATTON, D. L., OLDBORG, P. A., MICHALAK, M. & HENSON, P. M. 2005. Cell-surface calreticulin initiates clearance of viable or apoptotic cells through trans-activation of LRP on the phagocyte. *Cell*, 123, 321-34.
- GARNER, C. C., GARNER, A., HUBER, G., KOZAK, C. & MATUS, A. 1990. Molecular cloning of microtubule-associated protein 1 (MAP1A) and microtubule-associated protein 5 (MAP1B): identification of distinct genes and their differential expression in developing brain. *J Neurochem*, 55, 146-54.
- GAULTIER, A., ARANDJELOVIC, S., NIESSEN, S., OVERTON, C. D., LINTON, M. F., FAZIO, S., CAMPANA, W. M., CRAVATT, B. F., 3RD & GONIAS, S. L. 2008. Regulation of tumor necrosis factor receptor-1 and the IKK-NF-kappaB pathway by LDL receptor-related protein explains the antiinflammatory activity of this receptor. *Blood*, 111, 5316-25.
- GAULTIER, A., HOLLISTER, M., REYNOLDS, I., HSIEH, E. H. & GONIAS, S. L. 2010a. LRP1 regulates remodeling of the extracellular matrix by fibroblasts. *Matrix Biol*, 29, 22-30.
- GAULTIER, A., SIMON, G., NIESSEN, S., DIX, M., TAKIMOTO, S., CRAVATT, B. F., 3RD & GONIAS, S. L. 2010b. LDL receptor-related protein 1 regulates the abundance of diverse cell-signaling proteins in the plasma membrane proteome. *J Proteome Res*, 9, 6689-95.

- GAULTIER, A., WU, X., LE MOAN, N., TAKIMOTO, S., MUKANDALA, G., AKASSOGLU, K., CAMPANA, W. M. & GONIAS, S. L. 2009. Low-density lipoprotein receptor-related protein 1 is an essential receptor for myelin phagocytosis. *J Cell Sci*, 122, 1155-62.
- GAUTIER, H. O., EVANS, K. A., VOLBRACHT, K., JAMES, R., SITNIKOV, S., LUNDGAARD, I., JAMES, F., LAO-PEREGRIN, C., REYNOLDS, R., FRANKLIN, R. J. & KARADOTTIR, R. T. 2015. Neuronal activity regulates remyelination via glutamate signalling to oligodendrocyte progenitors. *Nat Commun*, 6, 8518.
- EGINAT, J., PARONI, M., PAGANI, M., GALIMBERTI, D., DE FRANCESCO, R., SCARPINI, E. & ABRIGNANI, S. 2017. The Enigmatic Role of Viruses in Multiple Sclerosis: Molecular Mimicry or Disturbed Immune Surveillance? *Trends Immunol*, 38, 498-512.
- GIBSON, E. M., PURGER, D., MOUNT, C. W., GOLDSTEIN, A. K., LIN, G. L., WOOD, L. S., INEMA, I., MILLER, S. E., BIERI, G., ZUCHERO, J. B., BARRES, B. A., WOO, P. J., VOGEL, H. & MONJE, M. 2014. Neuronal activity promotes oligodendrogenesis and adaptive myelination in the mammalian brain. *Science*, 344, 1252304.
- GOLDBERG, J., DANIEL, M., VAN HEUVEL, Y., VICTOR, M., BEYER, C., CLARNER, T. & KIPP, M. 2013. Short-term cuprizone feeding induces selective amino acid deprivation with concomitant activation of an integrated stress response in oligodendrocytes. *Cell Mol Neurobiol*, 33, 1087-98.
- GOLDMANN, T., WIEGHOFER, P., MULLER, P. F., WOLF, Y., VAROL, D., YONA, S., BRENDENCKE, S. M., KIERDORF, K., STASZEWSKI, O., DATTA, M., LUEDDE, T., HEIKENWALDER, M., JUNG, S. & PRINZ, M. 2013. A new type of microglia gene targeting shows TAK1 to be pivotal in CNS autoimmune inflammation. *Nat Neurosci*, 16, 1618-26.
- GONG, S., ZHENG, C., DOUGHTY, M. L., LOSOS, K., DIDKOVSKY, N., SCHAMBRA, U. B., NOWAK, N. J., JOYNER, A., LEBLANC, G., HATTEN, M. E. & HEINTZ, N. 2003. A gene expression atlas of the central nervous system based on bacterial artificial chromosomes. *Nature*, 425, 917-25.
- GONIAS, S. L. & CAMPANA, W. M. 2014. LDL receptor-related protein-1: a regulator of inflammation in atherosclerosis, cancer, and injury to the nervous system. *Am J Pathol*, 184, 18-27.
- GONIAS, S. L., GAULTIER, A. & JO, M. 2011. Regulation of the Urokinase Receptor (uPAR) by LDL Receptor-related Protein-1 (LRP1). *Curr Pharm Des*, 17, 1962-9.
- GONIAS, S. L., WU, L. & SALICIONI, A. M. 2004. Low density lipoprotein receptor-related protein: regulation of the plasma membrane proteome. *Thromb Haemost*, 91, 1056-64.
- GONZALEZ, G. A., HOFER, M. P., SYED, Y. A., AMARAL, A. I., RUNDLE, J., RAHMAN, S., ZHAO, C. & KOTTER, M. R. 2016. Tamoxifen accelerates the repair of demyelinated lesions in the central nervous system. *Sci Rep*, 6, 31599.
- GOROVOY, M., GAULTIER, A., CAMPANA, W. M., FIRESTEIN, G. S. & GONIAS, S. L. 2010. Inflammatory mediators promote production of shed LRP1/CD91, which regulates cell signaling and cytokine expression by macrophages. *J Leukoc Biol*, 88, 769-78.

- GRAVEL, M., PETERSON, J., YONG, V. W., KOTTIS, V., TRAPP, B. & BRAUN, P. E. 1996. Overexpression of 2',3'-cyclic nucleotide 3'-phosphodiesterase in transgenic mice alters oligodendrocyte development and produces aberrant myelination. *Mol Cell Neurosci*, 7, 453-66.
- GULCHER, J. R., VARTANIAN, T. & STEFANSSON, K. 1994. Is multiple sclerosis an autoimmune disease? *Clin Neurosci*, 2, 246-52.
- HAHN-DANTONA, E., RUIZ, J. F., BORNSTEIN, P. & STRICKLAND, D. K. 2001. The low density lipoprotein receptor-related protein modulates levels of matrix metalloproteinase 9 (MMP-9) by mediating its cellular catabolism. *J Biol Chem*, 276, 15498-503.
- HALL, P. A. & RUSSELL, S. E. 2012. Mammalian septins: dynamic heteromers with roles in cellular morphogenesis and compartmentalization. *J Pathol*, 226, 287-99.
- HART, J. P., GUNN, M. D. & PIZZO, S. V. 2004. A CD91-positive subset of CD11c+ blood dendritic cells: characterization of the APC that functions to enhance adaptive immune responses against CD91-targeted antigens. *J Immunol*, 172, 70-8.
- HARTUNG, H. P., JUNG, S., STOLL, G., ZIELASEK, J., SCHMIDT, B., ARCHELOS, J. J. & TOYKA, K. V. 1992. Inflammatory mediators in demyelinating disorders of the CNS and PNS. *Journal of Neuroimmunology*, 40, 197-210.
- HENN, A., LUND, S., HEDTJARN, M., SCHRATTENHOLZ, A., PORZGEN, P. & LEIST, M. 2009. The Suitability of BV2 Cells as Alternative Model System for Primary Microglia Cultures or for Animal Experiments Examining Brain Inflammation. *Altex-Alternativen Zu Tierexperimenten*, 26, 83-94.
- HERZ, J., GOLDSTEIN, J. L., STRICKLAND, D. K., HO, Y. K. & BROWN, M. S. 1991. 39-kDa protein modulates binding of ligands to low density lipoprotein receptor-related protein/alpha 2-macroglobulin receptor. *J Biol Chem*, 266, 21232-8.
- HERZ, J., HAMANN, U., ROGNE, S., MYKLEBOST, O., GAUSEPOHL, H. & STANLEY, K. K. 1988. Surface location and high affinity for calcium of a 500-kd liver membrane protein closely related to the LDL-receptor suggest a physiological role as lipoprotein receptor. *Embo J*, 7, 4119-27.
- HIDALGO, A., PEIRED, A. J., WILD, M. K., VESTWEBER, D. & FRENETTE, P. S. 2007. Complete identification of E-selectin ligands on neutrophils reveals distinct functions of PSGL-1, ESL-1, and CD44. *Immunity*, 26, 477-89.
- HOLLENBACH, J. A. & OKSENBERG, J. R. 2015. The immunogenetics of multiple sclerosis: A comprehensive review. *J Autoimmun*, 64, 13-25.
- HUANG, J. K., FANCY, S. P., ZHAO, C., ROWITCH, D. H., FFRENCH-CONSTANT, C. & FRANKLIN, R. J. 2011. Myelin regeneration in multiple sclerosis: targeting endogenous stem cells. *Neurotherapeutics*, 8, 650-8.
- HUGHES, E. G., KANG, S. H., FUKAYA, M. & BERGLES, D. E. 2013. Oligodendrocyte progenitors balance growth with self-repulsion to achieve homeostasis in the adult brain. *Nat Neurosci*, 16, 668-76.
- HUSEBY, E. S., LIGGITT, D., BRABB, T., SCHNABEL, B., OHLEN, C. & GOVERMAN, J. 2001. A pathogenic role for myelin-specific CD8(+) T cells in a model for multiple sclerosis. *J Exp Med*, 194, 669-76.
- INTERNATIONAL MULTIPLE SCLEROSIS GENETICS, C., BEECHAM, A. H., PATSOPOULOS, N. A., XIFARA, D. K., DAVIS, M. F., KEMPPINEN, A.,

- COTSAPAS, C., SHAH, T. S., SPENCER, C., BOOTH, D., GORIS, A., OTURAI, A., SAARELA, J., FONTAINE, B., HEMMER, B., MARTIN, C., ZIPP, F., D'ALFONSO, S., MARTINELLI-BONESCHI, F., TAYLOR, B., HARBO, H. F., KOCKUM, I., HILLERT, J., OLSSON, T., BAN, M., OKSENBERG, J. R., HINTZEN, R., BARCELLOS, L. F., WELLCOME TRUST CASE CONTROL, C., INTERNATIONAL, I. B. D. G. C., AGLIARDI, C., ALFREDSSON, L., ALIZADEH, M., ANDERSON, C., ANDREWS, R., SONDERGAARD, H. B., BAKER, A., BAND, G., BARANZINI, S. E., BARIZZONE, N., BARRETT, J., BELLENGUEZ, C., BERGAMASCHI, L., BERNARDINELLI, L., BERTHELE, A., BIBERACHER, V., BINDER, T. M., BLACKBURN, H., BOMFIM, I. L., BRAMBILLA, P., BROADLEY, S., BROCHET, B., BRUNDIN, L., BUCK, D., BUTZKUEVEN, H., CAILLIER, S. J., CAMU, W., CARPENTIER, W., CAVALLA, P., CELIUS, E. G., COMAN, I., COMI, G., CORRADO, L., COSEMANS, L., COURNU-REBEIX, I., CREE, B. A., CUSI, D., DAMOTTE, V., DEFER, G., DELGADO, S. R., DELOUKAS, P., DI SAPIO, A., DILTNEY, A. T., DONNELLY, P., DUBOIS, B., DUDDY, M., EDKINS, S., ELOVAARA, I., ESPOSITO, F., EVANGELOU, N., FIDDES, B., FIELD, J., FRANKE, A., FREEMAN, C., FROHLICH, I. Y., GALIMBERTI, D., GIEGER, C., GOURRAUD, P. A., GRAETZ, C., GRAHAM, A., GRUMMEL, V., GUASCHINO, C., HADJIXENOFONTOS, A., HAKONARSON, H., HALFPENNY, C., HALL, G., HALL, P., HAMSTEN, A., HARLEY, J., HARROWER, T., et al. 2013. Analysis of immune-related loci identifies 48 new susceptibility variants for multiple sclerosis. *Nat Genet*, 45, 1353-60.
- INTERNATIONAL MULTIPLE SCLEROSIS GENETICS, C., HAFLER, D. A., COMPSTON, A., SAWCER, S., LANDER, E. S., DALY, M. J., DE JAGER, P. L., DE BAKKER, P. I., GABRIEL, S. B., MIREL, D. B., IVINSON, A. J., PERICAK-VANCE, M. A., GREGORY, S. G., RIOUX, J. D., MCCAULEY, J. L., HAINES, J. L., BARCELLOS, L. F., CREE, B., OKSENBERG, J. R. & HAUSER, S. L. 2007. Risk alleles for multiple sclerosis identified by a genomewide study. *N Engl J Med*, 357, 851-62.
- IRVINE, K. A. & BLAKEMORE, W. F. 2008. Remyelination protects axons from demyelination-associated axon degeneration. *Brain*, 131, 1464-77.
- KANG, Z., WANG, C., ZEPP, J., WU, L., SUN, K., ZHAO, J., CHANDRASEKHARAN, U., DICORLETO, P. E., TRAPP, B. D., RANSOHOFF, R. M. & LI, X. 2013. Act1 mediates IL-17-induced EAE pathogenesis selectively in NG2+ glial cells. *Nat Neurosci*, 16, 1401-8.
- KIM, J. K., MASTRONARDI, F. G., WOOD, D. D., LUBMAN, D. M., ZAND, R. & MOSCARELLO, M. A. 2003. Multiple sclerosis - An important role for post-translational modifications of myelin basic protein in pathogenesis. *Molecular & Cellular Proteomics*, 2, 453-462.
- KIPP, M., CLARNER, T., DANG, J., COPRAY, S. & BEYER, C. 2009. The cuprizone animal model: new insights into an old story. *Acta Neuropathol*, 118, 723-36.
- KIRBY, L., JIN, J., CARDONA, J. G., SMITH, M. D., MARTIN, K. A., WANG, J., STRASBURGER, H., HERBST, L., ALEXIS, M., KARNELL, J., DAVIDSON, T., DUTTA, R., GOVERMAN, J., BERGLES, D. & CALABRESI, P. A. 2019. Oligodendrocyte precursor cells present antigen and are cytotoxic targets in inflammatory demyelination. *Nat Commun*, 10, 3887.

- KIRBY, L., JIN, J., GONZALEZ-CARDONA, J., SMITH, M., MARTIN, K., WANG, J., STRASBURGER, H., HERBST, L., ALEXIS, M., KARNELL, J., DAVIDSON, T., DUTTA, R., GOVERMAN, J., BERGLES, D. E. & CALABRESI, P. A. 2018a. Oligodendrocyte Precursor Cells Are Co-Opted by the Immune System to Cross-Present Antigen and Mediate Cytotoxicity. *bioRxiv*, 461434.
- KIRBY, L. A., JIN, J., GONZALEZ-CARDONA, J., SMYITH, M., MARTIN, K., WANG, J., STRASBURGER, H., HERBST, L., ALEXIS, M., KARNELI, J., DAVIDSON, T. S., DUTTA, R., GOVERMAN, J. M., BERGLES, D. E. & CALABRESI, P. A. 2018b. Oligodendrocyte Precursor Cells Are Co-Opted by the Immune System to Cross-Present Antigen and Mediate Cytotoxicity. *bioRxiv*, 461434.
- KOTTER, M. R., LI, W. W., ZHAO, C. & FRANKLIN, R. J. 2006. Myelin impairs CNS remyelination by inhibiting oligodendrocyte precursor cell differentiation. *J Neurosci*, 26, 328-32.
- KOTTER, M. R., SETZU, A., SIM, F. J., VAN ROOIJEN, N. & FRANKLIN, R. J. 2001. Macrophage depletion impairs oligodendrocyte remyelination following lysolecithin-induced demyelination. *Glia*, 35, 204-12.
- KOZLOV, G., LEE, J., ELIAS, D., GRAVEL, M., GUTIERREZ, P., EKIEL, I., BRAUN, P. E. & GEHRING, K. 2003. Structural evidence that brain cyclic nucleotide phosphodiesterase is a member of the 2H phosphodiesterase superfamily. *Journal of Biological Chemistry*, 278, 46021-46028.
- KUHLMANN, T., MIRON, V., CUI, Q., WEGNER, C., ANTEL, J. & BRUCK, W. 2008. Differentiation block of oligodendroglial progenitor cells as a cause for remyelination failure in chronic multiple sclerosis. *Brain*, 131, 1749-58.
- LAMENSA, J. W. & MOSCARELLO, M. A. 1993. Deimination of human myelin basic protein by a peptidylarginine deiminase from bovine brain. *J Neurochem*, 61, 987-96.
- LAPPE-SIEFKE, C., GOEBBELS, S., GRAVEL, M., NICKSCH, E., LEE, J., BRAUN, P. E., GRIFFITHS, I. R. & NAVE, K. A. 2003. Disruption of Cnp1 uncouples oligodendroglial functions in axonal support and myelination. *Nat Genet*, 33, 366-74.
- LAU, L. W., KEOUGH, M. B., HAYLOCK-JACOBS, S., CUA, R., DORING, A., SLOKA, S., STIRLING, D. P., RIVEST, S. & YONG, V. W. 2012. Chondroitin sulfate proteoglycans in demyelinated lesions impair remyelination. *Ann Neurol*, 72, 419-32.
- LEE, J., GRAVEL, M., ZHANG, R. L., THIBAUT, P. & BRAUN, P. E. 2005. Process outgrowth in oligodendrocytes is mediated by CNP, a novel microtubule assembly myelin protein. *Journal of Cell Biology*, 170, 661-673.
- LEVIN, L. I., MUNGER, K. L., RUBERTONE, M. V., PECK, C. A., LENNETTE, E. T., SPIEGELMAN, D. & ASCHERIO, A. 2005. Temporal relationship between elevation of epstein-barr virus antibody titers and initial onset of neurological symptoms in multiple sclerosis. *JAMA*, 293, 2496-500.
- LILLIS, A. P., VAN DUYN, L. B., MURPHY-ULLRICH, J. E. & STRICKLAND, D. K. 2008. LDL Receptor-Related Protein 1: Unique Tissue-Specific Functions Revealed by Selective Gene Knockout Studies. *Physiol Rev*, 88, 887-918.

- LIN, J. P., MIRONOVA, Y. A., SHRAGER, P. & GIGER, R. J. 2017. LRP1 regulates peroxisome biogenesis and cholesterol homeostasis in oligodendrocytes and is required for proper CNS myelin development and repair. *Elife*, 6.
- LIN, W., BAILEY, S. L., HO, H., HARDING, H. P., RON, D., MILLER, S. D. & POPKO, B. 2007. The integrated stress response prevents demyelination by protecting oligodendrocytes against immune-mediated damage. *J Clin Invest*, 117, 448-56.
- LIN, W., KEMPER, A., DUPREE, J. L., HARDING, H. P., RON, D. & POPKO, B. 2006. Interferon-gamma inhibits central nervous system remyelination through a process modulated by endoplasmic reticulum stress. *Brain*, 129, 1306-18.
- LOSSIUS, A., JOHANSEN, J. N., VARTDAL, F., ROBINS, H., JURATE SALTYTE, B., HOLMOY, T. & OLWEUS, J. 2014. High-throughput sequencing of TCR repertoires in multiple sclerosis reveals intrathecal enrichment of EBV-reactive CD8+ T cells. *Eur J Immunol*, 44, 3439-52.
- LU, Q. R., SUN, T., ZHU, Z., MA, N., GARCIA, M., STILES, C. D. & ROWITCH, D. H. 2002. Common developmental requirement for Olig function indicates a motor neuron/oligodendrocyte connection. *Cell*, 109, 75-86.
- LUCCHINETTI, C., BRUCK, W., PARISI, J., SCHEITHAUER, B., RODRIGUEZ, M. & LASSMANN, H. 2000. Heterogeneity of multiple sclerosis lesions: implications for the pathogenesis of demyelination. *Ann Neurol*, 47, 707-17.
- MALLUCCI, G., PERUZZOTTI-JAMETTI, L., BERNSTOCK, J. D. & PLUCHINO, S. 2015. The role of immune cells, glia and neurons in white and gray matter pathology in multiple sclerosis. *Prog Neurobiol*.
- MANTUANO, E., BRIFAUULT, C., LAM, M. S., AZMOON, P., GILDER, A. S. & GONIAS, S. L. 2016. LDL receptor-related protein-1 regulates NFkappaB and microRNA-155 in macrophages to control the inflammatory response. *Proc Natl Acad Sci U S A*, 113, 1369-74.
- MANTUANO, E., INOUE, G., LI, X., TAKAHASHI, K., GAULTIER, A., GONIAS, S. L. & CAMPANA, W. M. 2008. The hemopexin domain of matrix metalloproteinase-9 activates cell signaling and promotes migration of schwann cells by binding to low-density lipoprotein receptor-related protein. *J Neurosci*, 28, 11571-82.
- MARCUS, J., HONIGBAUM, S., SHROFF, S., HONKE, K., ROSENBLUTH, J. & DUPREE, J. L. 2006. Sulfatide is essential for the maintenance of CNS myelin and axon structure. *Glia*, 53, 372-81.
- MASTRONARDI, F. G., NOOR, A., WOOD, D. D., PATON, T. & MOSCARELLO, M. A. 2007. Peptidyl argininedeiminase 2 CpG island in multiple sclerosis white matter is hypomethylated. *Journal of Neuroscience Research*, 85, 2006-2016.
- MAY, P., ROHLMANN, A., BOCK, H. H., ZURHOVE, K., MARTH, J. D., SCHOMBURG, E. D., NOEBELS, J. L., BEFFERT, U., SWEATT, J. D., WEEBER, E. J. & HERZ, J. 2004. Neuronal LRP1 functionally associates with postsynaptic proteins and is required for normal motor function in mice. *Mol Cell Biol*, 24, 8872-83.
- MILO, R. & KAHANA, E. 2010. Multiple sclerosis: geoeidemiology, genetics and the environment. *Autoimmun Rev*, 9, A387-94.
- MIYAOKA, Y., TANAKA, M., IMAMURA, T., TAKADA, S. & MIYAJIMA, A. 2010. A novel regulatory mechanism for Fgf18 signaling involving cysteine-rich FGF receptor (Cfr) and delta-like protein (Dlk). *Development*, 137, 159-67.

- MOSCARELLO, M. A., WOOD, D. D., ACKERLEY, C. & BOULIAS, C. 1994. Myelin in Multiple-Sclerosis Is Developmentally Immature. *Journal of Clinical Investigation*, 94, 146-154.
- MURARO, P. A., KALBUS, M., AFSHAR, G., MCFARLAND, H. F. & MARTIN, R. 2002. T cell response to 2',3'-cyclic nucleotide 3'-phosphodiesterase (CNPase) in multiple sclerosis patients. *J Neuroimmunol*, 130, 233-42.
- MUSSE, A. A. & HARAUZ, G. 2007. Molecular "negativity" may underlie multiple sclerosis: Role of the myelin basic protein family in the pathogenesis of MS. *Neurobiology of Multiple Sclerosis*, 79, 149-172.
- MUSSE, A. A., LI, Z., ACKERLEY, C. A., BIENZLE, D., LEI, H., POMA, R., HARAUZ, G., MOSCARELLO, M. A. & MASTRONARDI, F. G. 2008. Peptidylarginine deiminase 2 (PAD2) overexpression in transgenic mice leads to myelin loss in the central nervous system. *Dis Model Mech*, 1, 229-40.
- NA, S. Y., CAO, Y., TOBEN, C., NITSCHKE, L., STADELMANN, C., GOLD, R., SCHIMPL, A. & HUNIG, T. 2008. Naive CD8 T-cells initiate spontaneous autoimmunity to a sequestered model antigen of the central nervous system. *Brain*, 131, 2353-65.
- NA, S. Y., EUJEN, H., GOBEL, K., MEUTH, S. G., MARTENS, K., WIENDL, H. & HUNIG, T. 2009. Antigen-specific blockade of lethal CD8 T-cell mediated autoimmunity in a mouse model of multiple sclerosis. *J Immunol*, 182, 6569-75.
- NEELS, J. G., VAN DEN BERG, B. M., LOOKENE, A., OLIVECRONA, G., PANNEKOEK, H. & VAN ZONNEVELD, A. J. 1999. The second and fourth cluster of class A cysteine-rich repeats of the low density lipoprotein receptor-related protein share ligand-binding properties. *J Biol Chem*, 274, 31305-11.
- NORTON, W. T. & PODUSLO, S. E. 1973. Myelination in rat brain: method of myelin isolation. *J Neurochem*, 21, 749-57.
- OGDEN, C. A., DECATHELINEAU, A., HOFFMANN, P. R., BRATTON, D., GHEBREHIWET, B., FADOK, V. A. & HENSON, P. M. 2001. C1q and mannose binding lectin engagement of cell surface calreticulin and CD91 initiates macropinocytosis and uptake of apoptotic cells. *J Exp Med*, 194, 781-95.
- ORTIZ, F. C., HABERMACHER, C., GRACIARENA, M., HOURY, P. Y., NISHIYAMA, A., NAIT OUMESMAR, B. & ANGULO, M. C. 2019. Neuronal activity in vivo enhances functional myelin repair. *JCI Insight*, 5.
- PATEL, J. & BALABANOV, R. 2012. Molecular mechanisms of oligodendrocyte injury in multiple sclerosis and experimental autoimmune encephalomyelitis. *Int J Mol Sci*, 13, 10647-59.
- POPESCU, B. F., PIRKO, I. & LUCCHINETTI, C. F. 2013. Pathology of multiple sclerosis: where do we stand? *Continuum (Minneapolis)*, 19, 901-21.
- RAASCH, J., ZELLER, N., VAN LOO, G., MERKLER, D., MILDNER, A., ERNY, D., KNOBELOCH, K. P., BETHEA, J. R., WAISMAN, A., KNUST, M., DEL TURCO, D., DELLER, T., BLANK, T., PRILLER, J., BRUCK, W., PASPARAKIS, M. & PRINZ, M. 2011. I κ B kinase 2 determines oligodendrocyte loss by non-cell-autonomous activation of NF- κ B in the central nervous system. *Brain*, 134, 1184-98.

- RAMANUJAM, R., HEDSTROM, A. K., MANOUCHEHRINIA, A., ALFREDSSON, L., OLSSON, T., BOTTAI, M. & HILLERT, J. 2015. Effect of Smoking Cessation on Multiple Sclerosis Prognosis. *JAMA Neurol*, 72, 1117-23.
- RANSOHOFF, R. M. 2012. Animal models of multiple sclerosis: the good, the bad and the bottom line. *Nat Neurosci*, 15, 1074-7.
- RANSOHOFF, R. M., HAFLER, D. A. & LUCCHINETTI, C. F. 2015. Multiple sclerosis-a quiet revolution. *Nat Rev Neurol*, 11, 134-42.
- ROSENER, M., MURARO, P. A., RIETHMULLER, A., KALBUS, M., SAPPLER, G., THOMPSON, R. J., LICHTENFELS, R., SOMMER, N., MCFARLAND, H. F. & MARTIN, R. 1997. 2',3'-cyclic nucleotide 3'-phosphodiesterase: a novel candidate autoantigen in demyelinating diseases. *J Neuroimmunol*, 75, 28-34.
- RUCKH, J. M., ZHAO, J. W., SHADRACH, J. L., VAN WIJNGAARDEN, P., RAO, T. N., WAGERS, A. J. & FRANKLIN, R. J. M. 2012. Rejuvenation of Regeneration in the Aging Central Nervous System. *Cell Stem Cell*, 10, 96-103.
- SACHS, H. H., BERCURY, K. K., POPESCU, D. C., NARAYANAN, S. P. & MACKLIN, W. B. 2014. A new model of cuprizone-mediated demyelination/remyelination. *ASN Neuro*, 6.
- SARGSYAN, S. A., SHEARER, A. J., RITCHIE, A. M., BURGOON, M. P., ANDERSON, S., HEMMER, B., STADELMANN, C., GATTENLOHNER, S., OWENS, G. P., GILDEN, D. & BENNETT, J. L. 2010. Absence of Epstein-Barr virus in the brain and CSF of patients with multiple sclerosis. *Neurology*, 74, 1127-35.
- SAVILL, J. & FADOK, V. 2000. Corpse clearance defines the meaning of cell death. *Nature*, 407, 784-8.
- SAWCER, S., BAN, M., MARANIAN, M., YEO, T. W., COMPSTON, A., KIRBY, A., DALY, M. J., DE JAGER, P. L., WALSH, E., LANDER, E. S., RIOUX, J. D., HAFLER, D. A., IVINSON, A., RIMMLER, J., GREGORY, S. G., SCHMIDT, S., PERICAK-VANCE, M. A., AKESSON, E., HILLERT, J., DATTA, P., OTURAI, A., RYDER, L. P., HARBO, H. F., SPURKLAND, A., MYHR, K. M., LAAKSONEN, M., BOOTH, D., HEARD, R., STEWART, G., LINCOLN, R., BARCELLOS, L. F., HAUSER, S. L., OKSENBERG, J. R., KENEALY, S. J., HAINES, J. L. & INTERNATIONAL MULTIPLE SCLEROSIS GENETICS, C. 2005. A high-density screen for linkage in multiple sclerosis. *Am J Hum Genet*, 77, 454-67.
- SCHINDELIN, J., ARGANDA-CARRERAS, I., FRISE, E., KAYNIG, V., LONGAIR, M., PIETZSCH, T., PREIBISCH, S., RUEDEN, C., SAALFELD, S., SCHMID, B., TINEVEZ, J. Y., WHITE, D. J., HARTENSTEIN, V., ELICEIRI, K., TOMANCAK, P. & CARDONA, A. 2012. Fiji: an open-source platform for biological-image analysis. *Nat Methods*, 9, 676-82.
- SEKI, S. M., STEVENSON, M., ROSEN, A. M., ARANDJELOVIC, S., GEMTA, L., BULLOCK, T. N. J. & GAULTIER, A. 2017. Lineage-Specific Metabolic Properties and Vulnerabilities of T Cells in the Demyelinating Central Nervous System. *J Immunol*, 198, 4607-4617.
- SIEBERT, J. R. & OSTERHOUT, D. J. 2011. The inhibitory effects of chondroitin sulfate proteoglycans on oligodendrocytes. *J Neurochem*, 119, 176-88.
- SKRIPULETZ, T., GUDI, V., HACKSTETTE, D. & STANGEL, M. 2011. De- and remyelination in the CNS white and grey matter induced by cuprizone: the old, the new, and the unexpected. *Histol Histopathol*, 26, 1585-97.

- SONG, H., LI, Y., LEE, J., SCHWARTZ, A. L. & BU, G. 2009. Low-density lipoprotein receptor-related protein 1 promotes cancer cell migration and invasion by inducing the expression of matrix metalloproteinases 2 and 9. *Cancer Res*, 69, 879-86.
- STANGEL, M., KUHLMANN, T., MATTHEWS, P. M. & KILPATRICK, T. J. 2017. Achievements and obstacles of remyelinating therapies in multiple sclerosis. *Nat Rev Neurol*, 13, 742-754.
- STEELMAN, A. J., THOMPSON, J. P. & LI, J. 2012. Demyelination and remyelination in anatomically distinct regions of the corpus callosum following cuprizone intoxication. *Neurosci Res*, 72, 32-42.
- STERN, M., SAVILL, J. & HASLETT, C. 1996. Human monocyte-derived macrophage phagocytosis of senescent eosinophils undergoing apoptosis. Mediation by alpha v beta 3/CD36/thrombospondin recognition mechanism and lack of phlogistic response. *Am J Pathol*, 149, 911-21.
- STILES, T. L., DICKENDESHER, T. L., GAULTIER, A., FERNANDEZ-CASTANEDA, A., MANTUANO, E., GIGER, R. J. & GONIAS, S. L. 2012. LDL Receptor-related Protein-1 is a sialic acid-independent receptor for myelin-associated glycoprotein (MAG) that functions in neurite outgrowth inhibition by MAG and CNS myelin. *J Cell Sci*.
- STRICKLAND, D. K., ASHCOM, J. D., WILLIAMS, S., BURGESS, W. H., MIGLIORINI, M. & ARGRAVES, W. S. 1990. Sequence identity between the alpha 2-macroglobulin receptor and low density lipoprotein receptor-related protein suggests that this molecule is a multifunctional receptor. *J Biol Chem*, 265, 17401-4.
- STROMNES, I. M. & GOVERMAN, J. M. 2006. Active induction of experimental allergic encephalomyelitis. *Nat Protoc*, 1, 1810-9.
- STUDZINSKI, D. M. & BENJAMINS, J. A. 2003. Regulation of CNS glial phenotypes in N20.1 cells. *J Neurosci Res*, 73, 31-41.
- SUBRAMANIAN, M., HAYES, C. D., THOME, J. J., THORP, E., MATSUSHIMA, G. K., HERZ, J., FARBER, D. L., LIU, K., LAKSHMANA, M. & TABAS, I. 2014. An AXL/LRP-1/RANBP9 complex mediates DC efferocytosis and antigen cross-presentation in vivo. *J Clin Invest*, 124, 1296-308.
- SYED, Y. A., BAER, A. S., LUBEC, G., HOEGER, H., WIDHALM, G. & KOTTER, M. R. 2008. Inhibition of oligodendrocyte precursor cell differentiation by myelin-associated proteins. *Neurosurg Focus*, 24, E5.
- TRIPATHI, R. B., RIVERS, L. E., YOUNG, K. M., JAMEN, F. & RICHARDSON, W. D. 2010. NG2 glia generate new oligodendrocytes but few astrocytes in a murine experimental autoimmune encephalomyelitis model of demyelinating disease. *J Neurosci*, 30, 16383-90.
- VOSSENAAR, E. R., ZENDMAN, A. J., VAN VENROOIJ, W. J. & PRUIJN, G. J. 2003. PAD, a growing family of citrullinating enzymes: genes, features and involvement in disease. *Bioessays*, 25, 1106-18.
- WATZLAWIK, J., WARRINGTON, A. E. & RODRIGUEZ, M. 2010. Importance of oligodendrocyte protection, BBB breakdown and inflammation for remyelination. *Expert Rev Neurother*, 10, 441-57.

- WEINER, H. L. 2004. Multiple sclerosis is an inflammatory T-cell-mediated autoimmune disease. *Arch Neurol*, 61, 1613-5.
- WINGERCHUK, D. M. 2012. Smoking: effects on multiple sclerosis susceptibility and disease progression. *Ther Adv Neurol Disord*, 5, 13-22.
- WOOD, D. D., ACKERLEY, C. A., BRAND, B., ZHANG, L., RAIJMAKERS, R., MASTRONARDI, F. G. & MOSCARELLO, M. A. 2008. Myelin localization of peptidylarginine deiminases 2 and 4: comparison of PAD2 and PAD4 activities. *Lab Invest*, 88, 354-64.
- WOOD, D. D., BILBAO, J. M., OCONNORS, P. & MOSCARELLO, M. A. 1996. Acute multiple sclerosis (Marburg type) is associated with developmentally immature myelin basic protein. *Annals of Neurology*, 40, 18-24.
- WOODRUFF, R. H. & FRANKLIN, R. J. 1999. Demyelination and remyelination of the caudal cerebellar peduncle of adult rats following stereotaxic injections of lysolecithin, ethidium bromide, and complement/anti-galactocerebroside: a comparative study. *Glia*, 25, 216-28.
- WUCHERPFENNIG, K. W. & STROMINGER, J. L. 1995. Molecular mimicry in T cell-mediated autoimmunity: viral peptides activate human T cell clones specific for myelin basic protein. *Cell*, 80, 695-705.
- YANG, L., LIU, C. C., ZHENG, H., KANEKIYO, T., ATAGI, Y., JIA, L., WANG, D., N'SONGO, A., CAN, D., XU, H., CHEN, X. F. & BU, G. 2016. LRP1 modulates the microglial immune response via regulation of JNK and NF-kappaB signaling pathways. *J Neuroinflammation*, 13, 304.
- ZHANG, N. & BEVAN, M. J. 2011. CD8(+) T cells: foot soldiers of the immune system. *Immunity*, 35, 161-8.
- ZHANG, Y., CHEN, K., SLOAN, S. A., BENNETT, M. L., SCHOLZE, A. R., O'KEEFFE, S., PHATNANI, H. P., GUARNIERI, P., CANEDA, C., RUDERISCH, N., DENG, S., LIDDELOW, S. A., ZHANG, C., DANEMAN, R., MANIATIS, T., BARRES, B. A. & WU, J. Q. 2014. An RNA-sequencing transcriptome and splicing database of glia, neurons, and vascular cells of the cerebral cortex. *J Neurosci*, 34, 11929-47.
- ZURHOVE, K., NAKAJIMA, C., HERZ, J., BOCK, H. H. & MAY, P. 2008. Gamma-secretase limits the inflammatory response through the processing of LRP1. *Sci Signal*, 1, ra15.